UNIVERSITY COLLEGE LONDON

Optimisation of Chromatography for Downstream Protein Processing

Eleftheria Polykarpou

A thesis submitted in fulfillment for the
degree of Doctor of Philosophy

in the
Department of Biochemical Engineering

November 2011

Declaration of Authorship

I, Eleftheria Polykarpou, declare that this thesis titled, 'Optimisation of Chromatography for Downstream Protein Processing' and the work presented in it are my own. I confirm that:

- This work was done wholly while in candidature for a research degree at University College London.
- Where any part of this thesis has previously been submitted for a degree or any other qualification at this University or any other institution, this has been clearly stated.
- Where I have consulted the published work of others, this is always clearly attributed.
- Where I have quoted from the work of others, the source is always given. With the exception of such quotations, this thesis is entirely my own work.
- I have acknowledged all main sources of help.
- Where the thesis is based on work done by myself jointly with others, I have made clear exactly what was done by others and what I have contributed myself.

Signed: _____

Date: _____

Στη μητέρα μου και τον πατέρα μου

Acknowledgements

I would like to express my deepest gratitude for the help and guidance received by my supervisors Paul A. Dalby and Lazaros G. Papageorgiou, especially acknowledging our regular discussions with Lazaros G. Papageorgiou, without whom this work could not have culminated in such a result.

I am certainly indebted to many people who have helped in various ways throughout; Giovanna for introducing me to PhD life, Melanie for her valuable help in learning to speak LaTeX and Spanish, Sunil Chhatre for his help in understanding the theory of chromatography in depth, Songsong for his expertise in GAMS, Nouri Samsatli for guiding me through using *gPROMS*, and many others who I've collaborated with over the last few years.

Especially those with which I have had the privilege to interact past working constraints and become good friends with, hold a most significant optimising factor of PhD life in London. "Los pinches" Alberto, Miguel and Shane offered amazing times along beer sessions in ULU, and of course Giovanna, Melanie and Chandni made every day so much more than just a working environment. And the later intakes of the PPSE (former CAPE) room Di, Mozhdeh, Ozlem and Shirin, unexpectedly maintained the warmth of having endless discussions about science, life and other diversely interesting issues. Thank you all for being great friends.

Avgoustine, Mitso and Niki, thank you for the many beautiful moments shared together during our time in London (under the same roof or sail at times) and last but not least, Apostoli for sharing and completing yet another experience!

This work was carried out, under the Innovative Manufacturing Research Council and their financial assistance is greatly acknowledged.

On ne peut vivre que le present...

Abstract

Downstream bioprocessing and especially chromatographic steps, commonly used for the purification of multicomponent systems, are significant cost drivers in the production of therapeutic proteins. Lately, there has been an increased interest in the development of systematic methods where operating conditions are defined and chromatographic trains are selected.

Several models have been developed previously, where chromatographic trains were selected under the assumption of 100 % recovery of the desired product. Removing this assumption gives the opportunity not only to select chromatographic trains but also determine the timeline in which the product is selected.

Initially, a mixed integer non-linear (MINLP) programming mathematical model was developed to tackle that problem and was tested using three illustrative examples. Later on, this model was linearised by applying piecewise linear approximation techniques and computational efficiency was improved. Next, an alternative MILP model was developed by discretising the recovery levels of the product and computational efficiency improved even by 100-fold. Finally, the equilibrium dispersive model was used in a simple 4-protein mixture and the MINLP model was validated.

This research represents a significant step towards efficient downstream process operation and synthesis.

Contents

List of Figures

List of Tables

Symbols

Indices	
$p(1, 2, ..., P)$	proteins
$i(1, 2, ..., I)$	chromatographic techniques
dp	desired protein
$j(1, 2, ..., J)$	number of points for PWLA1
$k(1, 2, ..., K)$	number of points for PWLA2
$l(1, 2, ..., L)$	number of points for PWLA3
$ls(1, 2, ..., LS)$	starting recovery level
$lf(1, 2, ..., LS)$	finishing recovery level

Parameters	
KD_{ip}	retention time
P_{ip}	characteristic physicochemical property
Q_{ip}	net charge
MW_{ip}	molecular weight
H_p	hydrophobicity
DF_{ip}	deviation factor
σ_i	peak width
M	big number
mo_p	initial mass of protein p
SP	specified purity
fr	yield fraction
xl_{ip}	abscissa for PWLA1
Al_{ip}	ordinate for PWLA1
α_{ik}	abscissa for PWLA2

β_{ik}	ordinate for PWLA2
γ_l	abscissa for PWLA3
δ_l	ordinate for PWLA3
$CF_{i,p,ls,lf}$	concentration factor
$As_{i,p,ls}$	area related to starting recovery point ls
$Af_{i,p,lf}$	area related to finishing recovery point lf
F	phase ratio
u	inersitial velocity
F_c	eluent flowrate
ϵ_B	bed voidage
D	column diameter
Dax_{ip}	axial dispersion coefficient for protein p at chromatographic bed i and
α_{ip}	adsorption equilibria constant
β_{ip}	adsorption equilibria constant
ϵ_B	particle porosity
ka_{ip}	adsorption rate constant
kd_{ip}	desorption rate constant
Λ_p	adsorption saturation capacity
R_{ip}	recovery
P_{ip}	purity

Continuous Variables

xs_{ip}	operating starting point
xf_{ip}	operating finishing point
CF_{ip}	concentration factor
$x\bar{s}_{ip}$	shifted starting cut-point
$x\bar{f}_{ip}$	shifted finishing cut-point
$\hat{\Delta}s_{ip}$	correction variable when xs_{ip} is before chromatographic peak
$\hat{\Delta}f_{ip}$	correction variable when xf_{ip} is before chromatographic peak

Δs_{ip}	correction variable when xs_{ip} is after chromatographic peak
Δf_{ip}	correction variable when xf_{ip} is after chromatographic peak
m_{ip}	mass of protein p after each chromatographic step i
$m^1_{i-1,p}$	mass of protein p when chromatographic step $i-1$ has been selected
$m^2_{i-1,p}$	mass of protein p when chromatographic step $i-1$ has not been selected
$C\bar{F}_{ip}$	auxiliary variable
$ln\bar{C}F_{ip}$	auxiliary variable
ξ_{ip}	auxiliary variable
As_{ip}	area that lies below xs_{ip}
Af_{ip}	area that lies below xf_{ip}
λs_{ipj}	SOS2 variable
λf_{ipj}	SOS2 variable
μ_{ipk}	SOS2 variable
sl_{ip}	slack variable
ν_{pl}	SOS2 variable
$m^1_{i-1,p,ls,lf}$	mass of protein p when chromatographic step $i-1$ has been selected
$mf^1_{i-1,p,lf}$	mass of protein p that lies below finishing cut point lf when chromatographic step $i-1$ has been selected
$ms^1_{i-1,p,ls}$	mass of protein p that lies below starting cut point ls when chromatographic step $i-1$ has been selected
C_{ip}	mass of protein p in the mobile phase at each chromatographic bed i
Cs_{ip}	mass of protein p in the stationary phase and at each chromatographic bed i
Binary Variables	
E_i	1 if chromatographic step i is selected, 0 otherwise

zs_{ip}	1 if xs_{ip} is after the chromatographic peak, 0 otherwise
zf_{ip}	1 if xf_{ip} is after the chromatographic peak, 0 otherwise
ws_{ip}	1 if xs_{ip} is outside and after the chromatographic peak, 0 otherwise
wf_{ip}	1 if xf_{ip} is outside and after the chromatographic peak, 0 otherwise
ys_{ip}	1 if xs_{ip} is outside and before the chromatographic peak, 0 otherwise
yf_{ip}	1 if xf_{ip} is outside and before the chromatographic peak, 0 otherwise
$\lambda_{i,ls,lf}$	1 if chromatographic step i is selected at starting recovery level ls and finishing recovery level lf, 0 otherwise
$\mu_{i,lf}$	1 if chromatographic step i is selected at finishing recovery level lf, 0 otherwise
$\lambda_{i,ls}$	1 if chromatographic step i is selected at starting recovery level ls, 0 otherwise

Chapter 1

Introduction and theoretical background

1.1 Scope

In the last decade, there has been an increasing pressure in the biopharmaceutical sector for the design of flexible and cost-effective processes. In an attempt to overcome the purification bottleneck, the present work applied optimisation-based techniques on the purification stage of a typical biopharmaceutical process.

Chromatography has been "the work horse" of the purification stage, but still remains the major cost source, hence its optimisation holds a key role in reducing manufacturing cost. Chromatographic purification processes are complex processes and must be well understood for their effective design and optimisation. In this context, a rational approach on modelling and optimisation, as a driving force for enhanced purification processes, was the prime focus of this work.

1.2 Biopharmaceutical industry

Biopharmaceutical industry represents a vibrant industry with the introduction of 13 new products in 2010. In 2009, recombinant therapeutic proteins along with monoclonal antibodies (mAb) based products resulted in a global market value of $99 billion [5], while the global pharmaceutical market is expected to grow 5-7%, in 2011, according to IMS Health [6].

Worldwide pharmaceutical sales increased by more than double between 2000 and 2009, as illustrated in Figure 1.1. Pharmaceutical includes small molecules along with antibodies, peptides, vaccines and therapeutic proteins. The USA alone accounts for 37%, of the market and is still the world's biggest single market with the European Union following in its footsteps. Europe's major five, UK, Germany, France, Spain and Italy, accounted for over 60%, of all European pharmaceutical sales in 2009 [1, 7].

In general, biopharmaceuticals have a few advantages over pharmaceuticals (small molecules). During the last years and given the development in fermentation and methods for discovering new products, biopharmaceuticals have proven to be more profitable than small molecules. More importantly, biopharmaceuticals can achieve a degree of specificity that is impossible for small molecules [8].

Recombinant proteins, which include antibodies, vaccines and therapeutic proteins have a wide range of both diagnostic and therapeutic applications. They have been introduced in a variety of disease therapies including various types of cancer, and chronic diseases such as diabetes. A summary of such products that are isolated by chromatographic techniques is presented in Table 1.1 [4].

The increasing trends of the market, coupled with the fact that chromatography still remains the major bottleneck of the downstream stage

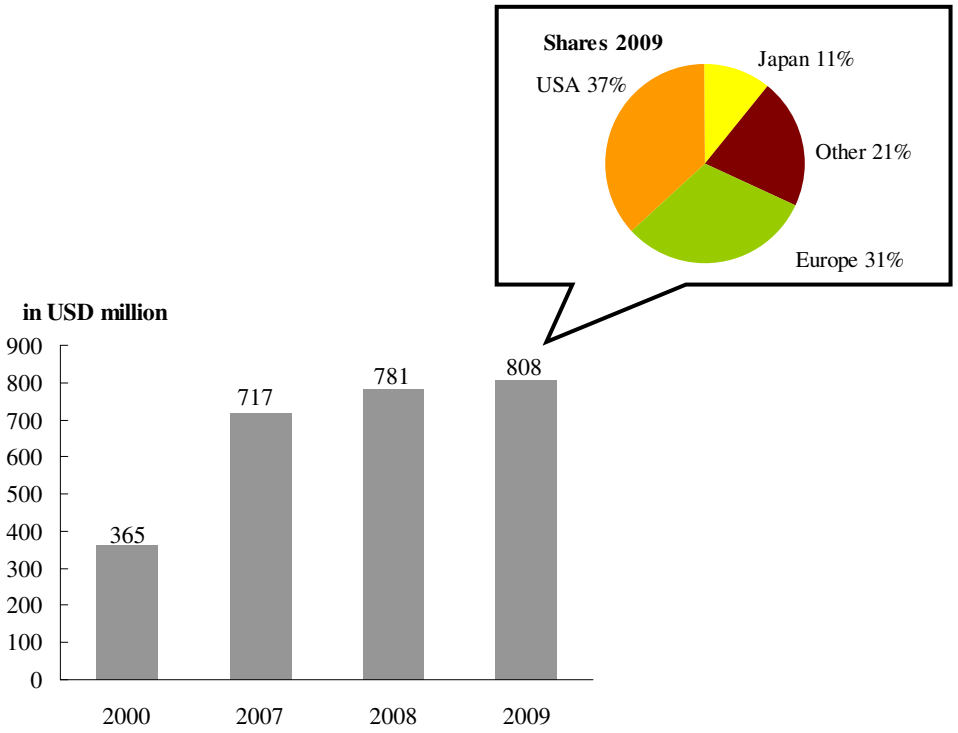

FIGURE 1.1: Global pharmaceutical market statistics as adapted by [1]

TABLE 1.1: Chromatographically purified therapeutics [4]

Product	**Use**
Albumin	plasma substitution
Epidermal growth factor (EGF)	wound healing
Erythropoetin	anemia in dialysis patients
Factor VIII	hemophilia
Human growth hormone	growth disorders
Insulin	diabetes
Interferons, Interleukin-2	cancer treatment
Monoclonal antibodies (mAb)	cancer treatment and diagnosis
Superoxide dismutase (SOD)	myocardial infarction therapy
Tissue plasminogen activator (tPA)	dissolution of blood clots
Tumor necrosis factor (TNF)	cancer treatment and diagnosis

of biopharmaceutical process indicate the need for a better process design and optimisation of the key manufacturing steps.

1.3 Typical flowsheet

As discussed earlier the driving force of this project is enhanced chromatographic purification processes. But where does chromatography stand in the overall process?

A typical biopharmaceutical process would be divided into an upstream and a downstream stage as shown in Figure 1.2. The upstream stage includes bacterial or mammalian cell lines growing in bioreactors, after which the downstream stage follows. This is then divided in two substages; the recovery and the purification. During the recovery step, the initial separation takes place, where the solid impurities are removed through appropriate processes such as centrifugation, filtration etc. Next, the purification stage which consists of several chromatographic steps in series, serves as the target product isolation step. The final step is formulation, where the product gets its final "form", through processes such ultrafiltration or diafiltration.

Chromatography holds a key role in the overall production of biopharmaceuticals. While it has been established as an analytical technique since the 1950s, it is relatively new for large-scale processes. Moreover, the purification of a desired protein is the most complex and costly stage of the overall process, responsible for as much as 60%, of the total manufacturing cost [9]. It is clear that the understanding of the process followed by its efficient design and optimisation is the way to tackle the challenge of downstream process operation and synthesis.

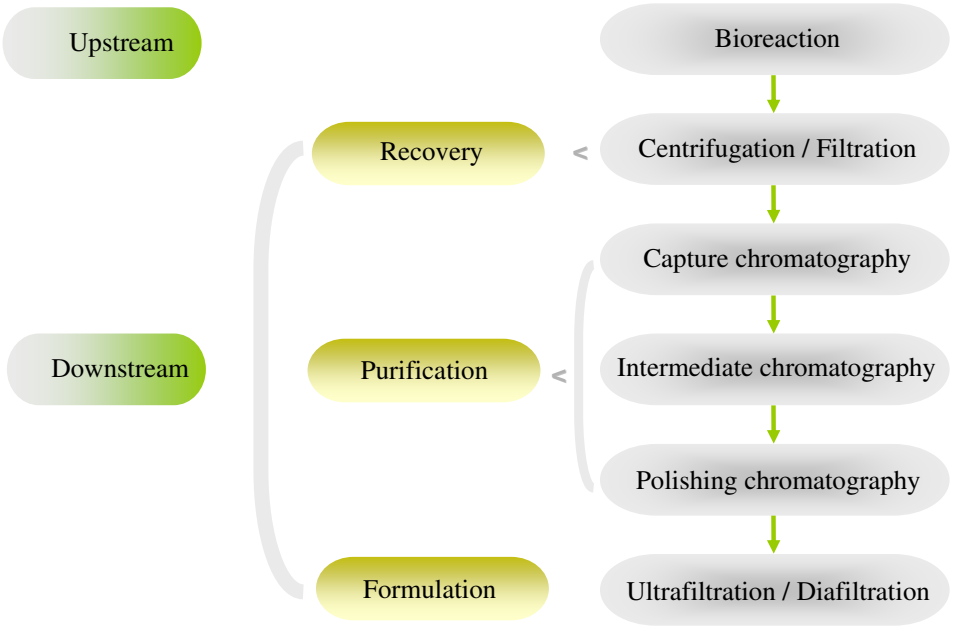

FIGURE 1.2: Flowsheet of a typical biochemical process

1.4 Chromatography

Ettre [10] defines chromatography as *"a physical method of separation in which the components to be separated are distributed between two phases, one of which is stationary (stationary phase) while the other (mobile phase) moves in a definite direction"* .

1.4.1 History of chromatography

The first scientific evidence demonstrating chromatographic phenomena was reported at the end of the 19th century. It was not until 1906, however, that marked the beginning of the era of column chromatography. At that time, Mikhail Tswett, a Russian botanist, published his work on the separation of chloroplast pigments in leaf extracts [11]. Through

his experiments, Tswett identified that adsorption was the mechanism responsible for separation. It was then that the potential of chromatography, as a means of identifying compounds by properties other than their colour was realised. Tswett is considered to be "the father of chromatography", firstly because he coined the term chromatography, coming from the combination of two Greek words "$\chi\rho\acute{\omega}\mu\alpha$", meaning colour, and "$\gamma\rho\acute{\alpha}\phi\epsilon\iota\nu$", meaning to write, and secondly because he was the first one who scientifically described the process [12].

In the 1940s, Martins and Synge proposed liquid-liquid partition chromatography using as a chromatographic stationary phase silica gel loaded with water. Martin suggested the potential use of a gaseous mobile phase [13] but only published this work a decade later [14]. In 1949, Maclean and Hall introduced the first effective form of thin-layer chromatography (TLC) that was later on extensively developed and became an extremely effective separation technique with a wide field of applications [15].

After James and Martin introduced the idea of a gaseous mobile phase, gas-liquid chromatography (GLC) was rapidly developed as it was a simple and inexpensive process. Despite its wide range of application, GLC had several problems, therefore attention was turned to the development of liquid chromatography (LC) [15].

Modern liquid chromatography was introduced in the late 1960s-1970s. Nowadays, liquid chromatography incorporates special column packings and fully automated equipment. High performance liquid chromatography (HPLC) can now achieve faster and sharper separations [16].

1.4.2 How does chromatography work?

As a process of separation, it aims at converting a mixture into its different components, usually by passing it through an adsorbent surface [17]. In Figure 1.3, a schematic of the chromatographic process is

demonstrated. A sample feed is introduced in the inlet and each component in the mixture migrates at a different rate along the column. The components with the lower affinity to the stationary phase will travel faster, therefore elute first from the column. As shown in Figure 1.3, component 2 has a higher affinity for the stationary phase and is adsorbed, while the less adsorbed part of the mixture (component 1) is carried along by the mobile phase, until its elution. Emergence of the outlet is monitored by a detector and the components are collected in sequence producing an output signal; a chromatogram. Eventually, each component leaves the column and passes through the detector. The time between injection and elution, in which each component is retained in the column, is the retention time, a characteristic for each component.

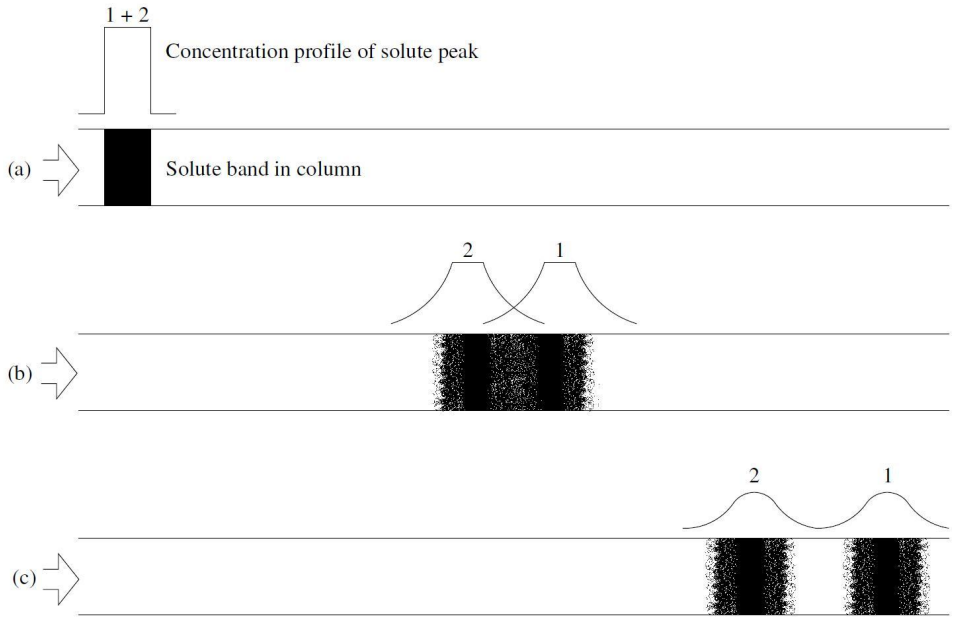

FIGURE 1.3: Chromatographic separation of a two component mixture

1.5 Types of chromatographic separation

There are many different types of chromatography, classified according to the nature of the mobile and stationary phases, the scale of operations and operation modes.

1.5.1 Nature of mobile and stationary phase

There are two main classes of chromatography depending on the nature of the mobile and stationary phases: gas chromatography (GC) and liquid chromatography (LC). In gas chromatography, the mobile phase is commonly a gas. The stationary phase can be a solid or liquid adsorbent distributed over the column's surface. In liquid chromatography, the mobile phase is a liquid and the stationary phase consists of small particles that are usually porous [18]. In this thesis, the focus is on liquid column chromatography, mainly used in biopharmaceutical processes.

1.5.2 Scale of operation

Depending on the scale of operation, liquid chromatography can be divided into ultra scale down, analytical, laboratory scale and process chromatography as summarised in Table 1.2. In ultra scale down the volumes are in the μg-range and can be used early in the process development. In the analytical scale, the volumes are in the μg-range and the aim is to identify the components of the sample. The laboratory scale or preparative chromatography is in the g-scale, used for both analytical and production purposes depending on the process. Finally, in the production or process chromatography, the volumes are in the kg-range and the objective is to purify the target component in order to manufacture a drug.

TABLE 1.2: Definitions of the scale of chromatographic separations

Scale	**Purpose**	**Product quantity**	**Column dimensions (l x d), *mm***
Ultra Scale Down	Information for process synthesis	μg	12 x 4
Analytical	Information for mixture's composition	μg	250 x 4.6
Laboratory	Substance isolation	g	250-300 x 10-100
Process	Preparation of purified material	kg	300 x 1000

1.5.3 Modes of operation

There are three modes in which column chromatography can be operated: elution, displacement and frontal, as defined by Tiselius [19]. There are also some intermediate modes of operation such gradient elution, recycling, simulated moving bed etc. In the following section the three main modes will be discussed along with some intermediate modes that are used in process chromatography.

Elution Chromatography

In elution chromatography the sample is introduced into the column, followed by the mobile phase (see Figure 1.4). The sample components migrate at different rates, hence elute in a series of peaks. As each component in the mixture migrates at a different rate along the column, the mixture separates. The rate of migration of each component of the mixture depends on interactions between the component and both the mobile and stationary phases.

Elution chromatography can be carried out under three different conditions depending on the mobile phase composition as shown in Figure 1.5:

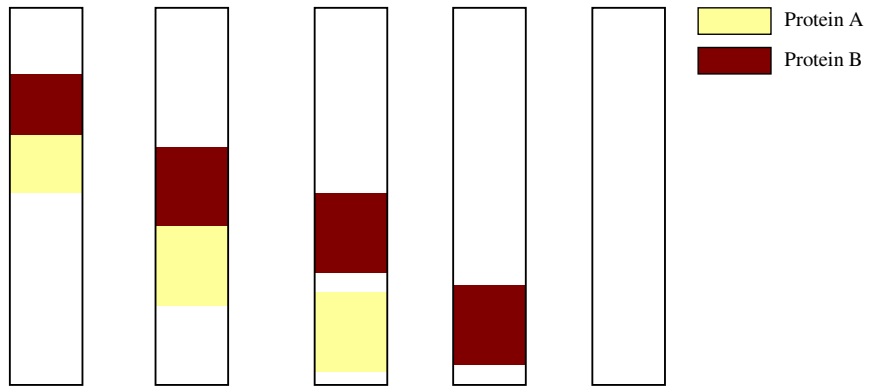

FIGURE 1.4: Elution chromatography

- Isocratic elution: In isocratic elution the mobile composition of the mobile phase is kept constant throughout the elution process 1.5(a).
- Gradient elution: In gradient elution the composition of the mobile phase is increased gradually during the elution process 1.5(b).
- Step elution: The composition of the mobile phase changes periodically 1.5(c).

The most common mode of operation in process chromatography is the gradient elution (linearly increased) [18].

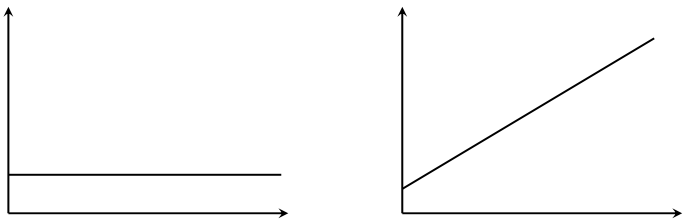

(a) Isocratic elution (b) Gradient elution

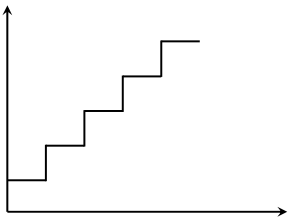

(c) Step elution

FIGURE 1.5: Types of elution chromatography

Displacement Chromatography

In displacement chromatography, the sample mixture is fed into the column and all the compounds in the mixture must compete for the immediately available adsorption sites. The displacer (a substance with high affinity to the stationary phase) first displaces the compound with the strongest adsorption site (protein A in Figure 1.6). Subsequently, this component will now become the displacer for the next one. Each component is displaced progressively by the previous one until they all pass through the column. This mode of operation is not used in analytical and preparative scale chromatography. In process scale, it is rarely used mainly because of the lack of suitable protein displacers [20].

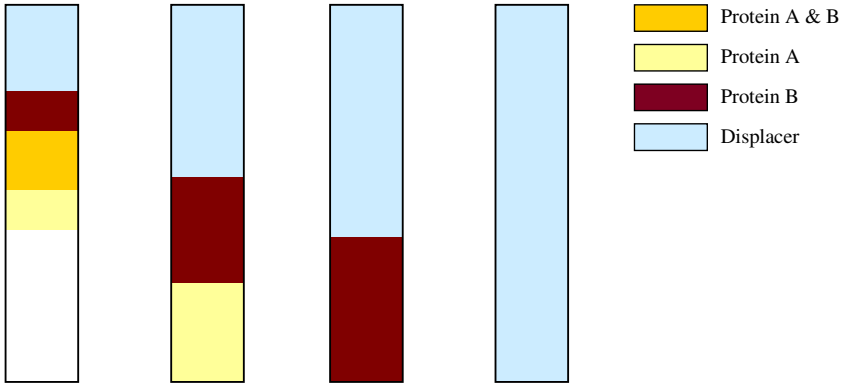

FIGURE 1.6: Displacement chromatography

Frontal Chromatography

In this type of chromatography, the sample is fed continuously into the column. First the mobile phase is collected at the end of the column and subsequently the components are held with a rate of increasing affinity to the stationary phase. As shown in Figure 1.7, protein A is held least strongly in the stationary phase, hence elutes first from the column, followed by protein B. Frontal analysis is not used for analytical applications.

1.6 Principles of separation

In this section, the different principles of separation encountered in chromatographic operations are discussed. Six main categories of such chromatography are described: ion exchange chromatography (IEX), hydrophobic interaction chromatography (HIC), reversed phase chromatography (RPC), affinity chromatography (AC), size exclusion chromatography (SEC) and mixed mode chromatography (MMC). A summary of the different separation principles is presented in Table 1.3.

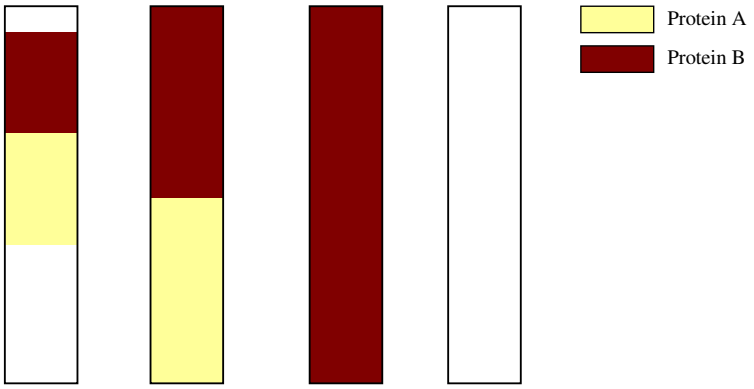

FIGURE 1.7: Frontal chromatography

Table 1.3: Summary of principles of separation

Type of chromatography	**Separation principle**	**Use**
Ion exchange	Surface charge	Removal of charged contaminants Sample concentration
Hydrophobic interaction	Hydrophobicity	Removal of hydrophobic contaminants Sample concentration
Reversed-phase	Hydrophobicity	Sample concentration and desalting of peptides Removal of hydrophobic contaminants Separation of complex peptide samples
Affinity	Biological function	One step purification of target molecules from complex samples Purification of tagged recombinant proteins Group separations Removal of specific contaminants
Size exclusion	Molecular size and shape	Sample conditioning (desalting, buffer exchange) Removal of low Mr or high Mr contaminants Separation of complex samples
Mixed mode	Depends on the type	Separation of enzymes, human serum proteins and plant proteins Vaccine purification processes

Ion Exchange Chromatography (IEC): A reversible adsorption process takes place, in which exchange of ions occurs between the aqueous mobile phase and the charged surface of the stationary phase, as shown in Figure 1.8.

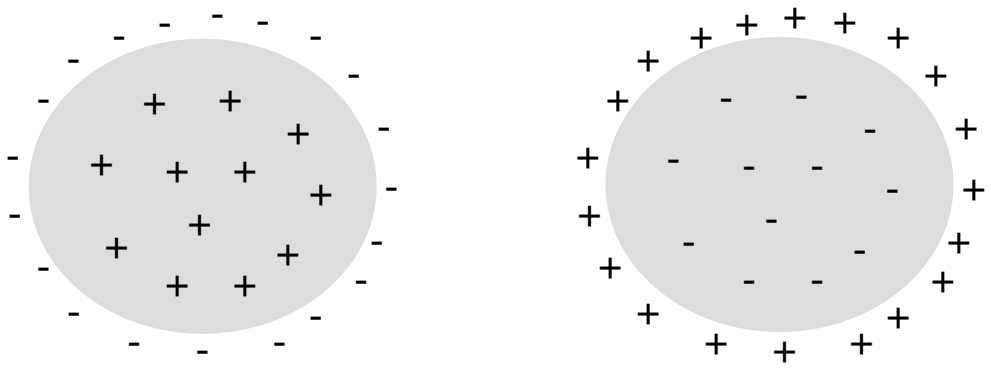

FIGURE 1.8: Mechanism of ion exchange chromatography
(a) Anion exchange (b) Cation exchange

The stationary phase is usually an insoluble polymeric matrix that is permeable to ionic solutes. The mechanism responsible for separation is ion-exchange of solute ions X and mobile phase ions Y with the charged groups R of the stationary phase [18].

$$X^- + R^+Y^- = Y^- + R^+X^- \qquad \text{(anion exchange)} \qquad (1.1)$$

$$X^+ + R^-Y^+ = Y^+ + R^-X^+ \qquad \text{(cation exchange)} \qquad (1.2)$$

The stronger the component ion X interacts with the exchanger ion, the stronger it is retained in the column. For cation exchange chromatography positively charged ions are separated, while for anion exchange chromatography negatively charged ions are separated. As ion exchange

chromatography can be carried out with a mobile phase close to physiological conditions, it is a very important technique used for protein separation.

Hydrophobic Interaction Chromatography (HIC): The interaction between the hydrophobic regions of the solutes' surface and the non-polar ligands of the stationary phase is the driving force in this type of chromatography. As shown in Figure 1.9, the compound with prominent hydrophobic site binds stronger while the one of low hydrophobicity does not bind.

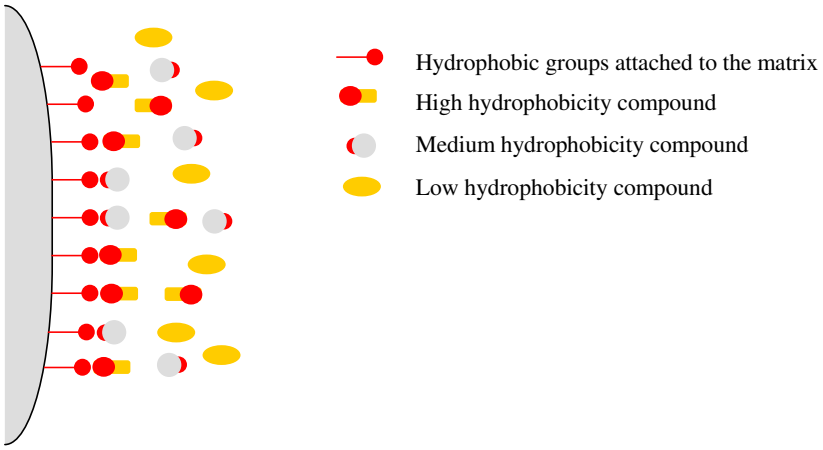

FIGURE 1.9: Mechanism of hydrophobic interaction and reversed-phase chromatography

The basic principle of HIC is similar to that of the reverse phase chromatography (RPC), only the conditions are milder, hence it is a technique appropriate for protein purification. Hydrophobic interaction chromatography can be very selective. This technique can be used for the separation of components with similar size and charge, since small differences in surface hydrophobicities between the solutes can be used as an efficient means of separation.

Reverse-phase Chromatography (RPC): Reverse-phase chromatography involves a hydrophobic stationary phase and the separation principle is similar to the one of HIC as shown in Figure 1.9. The difference between HIC and RPC is that in RPC, the medium is highly substituted with hydrocarbon chains. This makes the RPC very hydrophobic, hence the proteins can adsorb even when diluted in water, while in HIC the need of salt is necessary in order to achieve adsorption. The adsorption in RPC is so strong that requires eluents to achieve desorption [21]. These eluents can affect the protein stability, hence this technique is not preferred for protein purification where biological activity is important.

Size exclusion chromatography (SEC):

In size exclusion chromatography or gel filtration, the bed is packed with a porous gel which separates the compounds of a mixture depending on their difference in molecular mass and shape. The larger compounds elute first since they can not enter the pores. Smaller molecules permeate the pores and move through the column slowly.

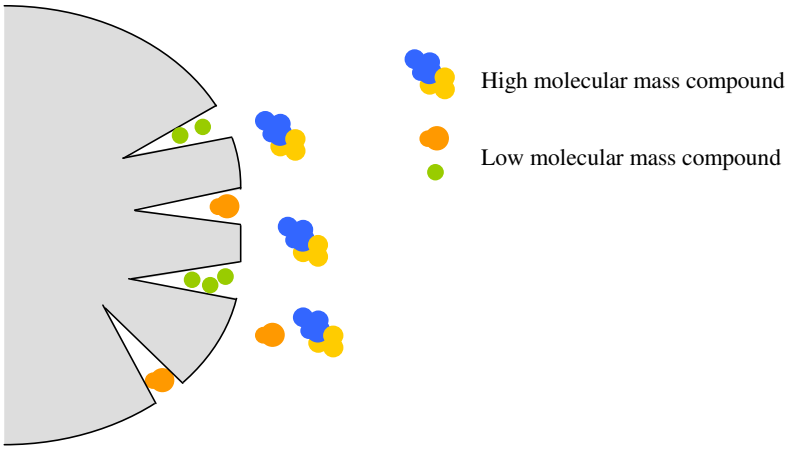

FIGURE 1.10: Mechanism of size exclusion chromatography

Affinity Chromatography (AC):

In affinity chromatography, the matrix is coupled with a ligand which has the ability to bind the target molecule as shown in Figure 1.11. The adsorption mechanism is the result of molecular recognition. For example, an enzyme might preferentially bind to ligand sites on the matrix that mimic the natural substrate of the enzyme. Solutes that do not have substrate-binding sites that are structurally related to the matrix ligand sites will be poorly bound, if at all, on to the matrix. The unbound molecules flow through the column while the components that bind are subsequently eluted.

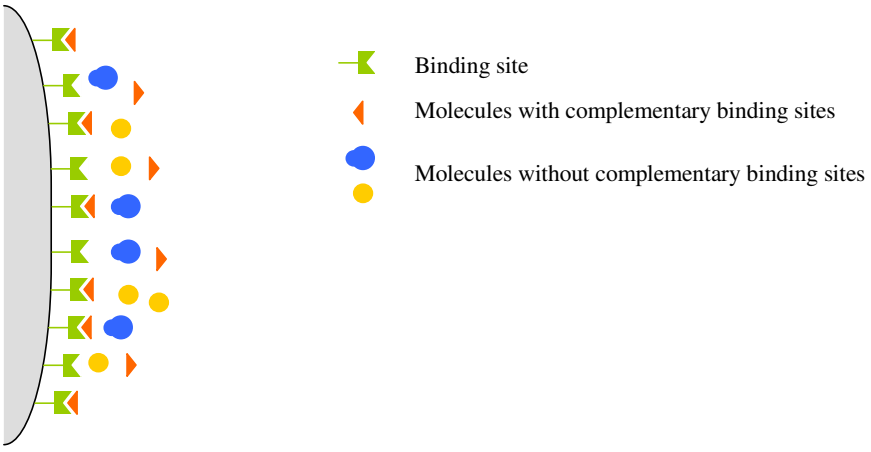

FIGURE 1.11: Mechanism of affinity chromatography

Mixed Mode Chromatography (MMC):

In this type of chromatography, different separation principles are applied in order to resolve a mixture to its components. Some examples of mixed mode chromatography are hydrophobic charge interaction chromatography (HCIC) and hydroxyapatite chromatography (HC). In HCIC, adsorption is based on mild hydrophobic interaction and is

achieved without addition of salts but by reduction of pH. In HC, negatively charged carboxyl groups and positively charged amino groups of the mobile phase interact with the stationary phase involving positively charged calcium ions and negatively charged phosphate ions respectively, hence HC can be considered as mixed-mode ion exchange chromatography. HCIC is usually applied to mixtures where the components have very similar isoelectric points and HC is commonly used for viral removal [22].

1.7 Aims and objectives

Albeit chromatography has been used for the last five decades, more efficient operation and design remain within the current scope of improvement. Chromatography has always been of significant interest for industry because of its complexity and high capital and operating costs involved [23]. It still accounts for up to 60 % of the total manufacturing cost of the final product [24]. Further development of chromatographic operations represents one of the most significant challenges for the biopharmaceutical industry.

Motivated by the necessity of enhanced chromatographic processes, the aim of this work was *to develop models based on mathematical programming techniques in order to enhance downstream processing.*

1.8 Outline of the thesis

The rest of the thesis is divided in five chapters. Chapter 2 discusses the literature in downstream process operation and synthesis. An overview of the different methods, models and techniques are analysed.

Chapter 3 addresses the problem of synthesis of downstream protein processing that incorporates product losses. The problem is formulated as a mixed integer non-linear programming (MINLP) framework and integrates the selection of optimum number of chromatographic techniques along with the timeline when the product is collected.

Chapter 4 describes the development of a mixed integer linear programming (MILP) model for tackling the same problem as that described in Chapter 3, by modifying the MINLP model through piecewise linear approximations of the non-linear functions, in order to improve computational efficiency.

An alternative MILP model using discrete recovery levels is introduced in Chapter 5. The methodology for all the developed models is illustrated through their application on three examples containing up to 21 candidate alternative steps and 13 proteins.

In Chapter 6, a model based on first principles was developed in order to validate the optimisation models described in the previous chapters. The example used was a four-protein mixture in a purification flowsheet containing two chromatographic columns.

Finally, Chapter 7 summarises the main contributions of the thesis and provides suggestions for future work.

Chapter 2

Literature Review

2.1 Drivers for change

Process chromatography has been a prime tool of industry for the last decades. Its development within the last 20 years resulted into a large rise of revenues for the major healthcare companies [25]. Although alternative bioseperation technologies are making their way into the market, process chromatography will remain a high resolution process for industry in the years to come [26].

Advances in cell cultures that have resulted in increased titers along with the strict requirements for purification of today's therapeutics have shifted most of the burden to downstream processing [27–29]. As a result, manufacturers are exploring multiple ways for achieving more systematic purification processes [30, 31].

This emphasises the need for new tools and strategies that can provide solutions for the challenges faced in downstream processing design [32]. This is also encouraged by the Food and Drug Administration (FDA) [33]. To overcome the bottleneck of downstream processes in a multiproduct biopharmaceutical facility, different decisions need to be taken at different levels. The first level of decision is related to design

and operation, where process alternatives are evaluated and operating conditions are determined. The second level is related to scheduling where sequence and timing of the selected unit operations are decided. Simultaneously describing process conditions, process alternatives and plant scheduling would be the ideal strategy. Although there have been efforts for the simultaneous process synthesis, operation and scheduling of a biopharmaceutical process, as it will be described in section 2.4, to date, there are no adequate methodologies for efficient protein purification process design and synthesis.

This work focuses on the first level of decisions and more specifically on process synthesis and operating conditions. Below, a brief literature review on recent work determining both operating conditions and chromatographic trains will be discussed.

2.2 Operation of chromatographic processes

In traditional methods for operating chromatographic techniques, the focus has been to deal with each step individually. Investigating the performance and robustness of a chromatographic column has been a significant part of research. As discussed in Chapter 1, many different modes of operation and principles of separation exist, therefore there was a large spectrum of possibilities to investigate. An overview of alternative approaches is presented below.

Depending on the chromatographic technique applied, different parameters affect its performance. The size of the column (diameter and length) as well as the packing parameters (particle size and porosity) can produce significant changes in the separation achieved. In terms of the mobile phase, the pH of the buffer (ionic strength) along with the flowrate and the collecting timeline are quite crucial. A summary of the key variables defining the performance of chromatography is illustrated in Figure 2.1.

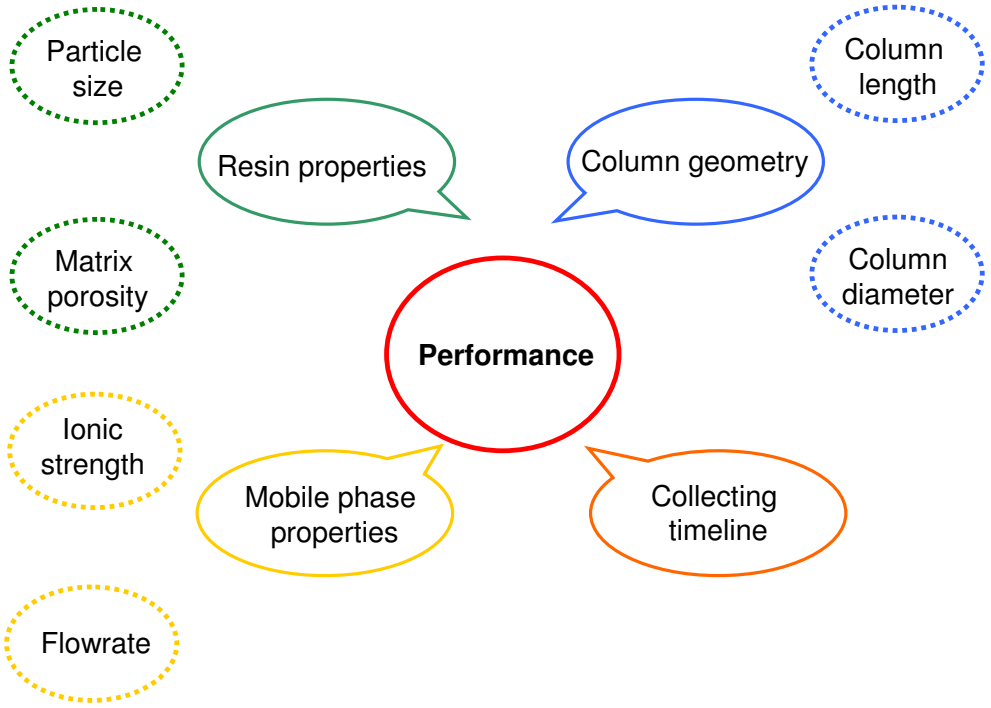

FIGURE 2.1: Key performance parameters

Apart from the parameters mentioned above, depending on the principle of separation applied, there are some specific key parameters affecting the column performance. For example, in ion exchange chromatography some of the key design variables are: the pH and the charge strength [34]. For hydrophobic interaction chromatography, the polar solvent and the type of hydrophobic ligand can have a significant impact in the column performance [35]. Since, ion exchange chromatography and hydrophobic interaction are two of the most widely used chromatographic techniques for protein purification in the biopharmaceutical industry [36, 37], a great part of the research has focused in these two techniques.

Different approaches have been used, in order to evaluate the performance and robustness of a chromatographic process within a single

column. These approaches can be divided into the following categories: protein structure approaches, mechanistic approaches, graphical approaches and black box approaches.

2.2.1 Protein structure approaches

In these approaches, the 3-D structure of the protein is taken into account as well as its orientation when in contact with a a binding surface. Hubbuch and coworkers [38] initially focused on understanding the binding mechanism between protein and resin and then studied the effect of ionic strength and mobile phase pH on the binding orientation of lysozyme in different IEX resins [39].

Later, they used experimental data on adsorption of lysozyme in different ion exchange resins and developed a more detailed model that proved how significant is the effect of the ligand density in the adsoprtion behavior of lysozyme [40].

2.2.2 Mechanistic approaches

In mechanistic approaches, the phenomena that take place in the column are taken into account. Mass transfer through diffusion and convection have been mathematically described by many researchers. Modelling chromatographic processes has been a complex task, largely due to the complexity of the process itself and the interactions between the compounds to be separated. Significant research work focused on tackling this challenge. Initially, modelling chromatography has resulted in improved understanding of the physical phenomena that take place in the column. Enhanced understanding resulted in the prediction of the system behaviour and the better design configuration and operation of the process.

The selection of the appropriate model is an important issue and many research groups have worked in developing new models and evaluating

existing ones. There are several mathematical models based on first principles that have widely been studied in the literature. The most common ones are: plate model and rate models (ideal model, equilibrium dispersive model, general rate model). These models are discussed and analysed in detail in Chapter 6.

Many research groups have evaluated different modelling approaches, applying them to both ion exchange and hydrophobic interaction chromatography [41–44]. Although plate model has worked fine in some cases [45] and has even been used for an industrial practical application [46], it is still not the preferred one mainly because of the lack of flexibility for complex mixtures where protein interactions have a significant role.

On the contrary, the rate model takes into account adsorption kinetics therefore is capable of describing these interactions but is computationally demanding. Rate models have been extensively used in the literature [44, 47, 48], with the equilibrium dispersive model being the common choice, mainly because it provides a good enough description of the phenomena taking place in the column without *a priori* requirements of many parameters and is relatively easier to implement and solve computationally than the general rate model.

In most cases, the developed models were used in order to predict the best operating conditions of a single chromatographic column. This was achieved by changing some of the crucial parameters such as flowrate or ionic strength gradient for *IEX*, followed by some sort of qualitative or quantitative evaluation of the separation achieved.

Karlsson et al [41], used the general rate model to simulate a three protein mixture in an ion-exchange chromatography step and investigate the impact of loading time and gradient in the elution. Orellana et al [48] also used the general rate model to simulate a three protein mixture in IEX. They were interested in the effect of flowrate and the initial protein concentration on the retention time.

Degerman and coworkers [49], used the general rate model and evaluated the critical process parameters by using the worst case scenario method where purity was lowest possible for the purification of immunoglobulinG through ion exchange chromatography. The worst case approach was also used by Jakobsson et al [50], where they tried to evaluate the robustness of an ion exchange chromatography step for a two-protein mixture.

2.2.3 Graphical approaches

The output of a chromatographic process is a chromatogram. However, it is not easy to extract the sensitivity of a chromatogram under different operating conditions [51]. For this reason, several graphical approaches have been developed by various research groups in order to describe the reaction of a chromatographic stage when changing the operating conditions.

Ngiam et al [51] calculated chromatographic performance by using fractionation diagrams to represent recovery trade-offs for a three-component mixture in size exclusion chromatography.

Multivariate statistical analysis is another graphical approach used by Tichener-Hooker and co-workers, where a small set of experimental separations can be enough to investigate a wide range of separation characteristics and variables affecting chromatographic performance [52].

The necessity to look at chromatographic techniques as a whole and produce an optimal set of operating conditions led Tichener-Hooker and coworkers [23] to apply some graphical approaches for a three-protein mixture by three consecutive chromatographic techniques. Later, from the same group the tie-line method was used to decrease the window of operation for a three protein mixture through two consecutive chromatographic techniques, in order to quantify the trade-offs between purity and recovery [53].

2.2.4 Black-box approaches

In this type of approaches, there is no need to take into account the physical phenomena that take place in the column. Such typical methods include partial least squares (PLS), artificial neural networks (ANN) and support vector regression (SVR). Cramer and his group have done a lot of research in this field on both IEX and HIC where they used structural descriptors along with statistical evaluation of experiments to predict protein retention behaviour [54–56] and HIC [57–59].

A disadvantage of all the methods described above is that the system configuration is known *a priori*, hence only the operating conditions are being evaluated, although the determination of the number of steps is a major challenge for the biopharmaceutical industry.

2.3 Synthesis of chromatographic processes

A typical biochemical process usually involves several chromatographic steps so as to achieve a final product according to confined specifications. However, biopharmaceutical companies usually operate in suboptimal conditions and for this reason, many efforts have focused on developing systematic methods, for the efficient design of process chromatography.

Some of the strategies are based on high throughput experimentation, knowledge-based approaches and algorithmic or optimisation-based techniques as discussed below.

2.3.1 High-throughput experimentation

In this strategy, conventional or high-throughput screening is conducted, where some of the key design variables are investigated in order to get

the optimal values [60, 61]. This requires a large number of measurements, nevertheless there is no guarantee that the final solution will be the best one. Trial and error methods were quite common even in the industrial scale [43]. In order to create some rational tools for process design, researchers started looking for more systematic methodologies [62].

2.3.2 Heuristics or knowledge-based approaches

First efforts started in the late 80s and employed heuristics (rules of thumb) in designing purification processes [36, 63–70]. These methods were based on insights and available knowledge [71]. The aim has always been to produce a product with the highest possible purity and yield using the minimal resources (cost). In order to rationalise the methodology researchers employed sets of rational rules that would ensure the required specifications. An example of these rules was presented by Asenjo and coworkers [69], reproduced below.

- Rule 1: Decide on separation process based on different physicochemical properties.
- Rule 2: First remove the impurities in abundance.
- Rule 3: Choose those processes that will exploit the differences in the physicochemical properties of the product and impurities in the most efficient manner.
- Rule 4: Use a high-resolution step as early as possible.
- Rule 5: Do the most arduous step last.

Further efforts employed expert knowledge and systematic approaches to select unit operations in order to synthesise economically favourable processes, based on the ability of chromatographic techniques to exploit differences in physicochemical properties of the compounds within the

mixture [71–75]. These methods inherently hold the drawback of being qualitative and cannot guarantee that the proposed solution is the best due to the size of the design space. Nonetheless they hold the advantage of reducing the search space to a level where quantitative analysis can be employed.

2.3.3 Optimisation-based approaches

In recent years, advances in mathematical programming techniques, solvers and computer power laid the foundation for the use of algorithmic and optimisation based techniques.

Early efforts were based on physicochemical properties to screen purification unit operations together with a mixed-integer non-linear programming (MINLP) problem for the final process synthesis [76, 77]. Later on, several authors reported mathematical models based on mixed-integer linear programming (MILP). In [2, 78], two MILP models were developed, utilising physicochemical properties of all the components in the mixture, in order to synthesise the optimal flowsheet for a specified purity and recovery.

In addition, these have been combined with the physicochemical properties of amino acids to predict the behaviour and design of peptide-fusion tags that alter the purification of proteins [79–82]. Such optimisation methods can be very powerful when combined with systematic approaches to obtain the necessary input parameters, as they significantly reduce the design search space [32, 83].

Under the assumption of complete product recovery, several optimisation models have been developed [78, 80]. However, the flexibility of also selecting the times of product collection (peak cut-points) provides the opportunity to capture the trade-offs between product quality (purity) and quantity. Previous work partially tackled this challenge allowing discrete percentage levels of product collection [84, 85].

2.4 Simultaneous process operation and synthesis

One important challenge in chromatography is to simultaneously describe process conditions, process alternatives and plant scheduling. Samsatli et al [86–88] proposed a two-stage approach, where the first stage was related to the conditions of the unit operations of a multi-product plant and the second to the scheduling of the process. The only structural decisions made in the first stage are related to the number of fermentors working in parallel while the purification process was predetermined.

Later, Asenjo and coworkers [89–91] tried tackling the same problem for a plant aiming to produce four recombinant proteins including human insulin, hepatitis B vaccine, chymosin and cryophilic protease. In this approach, time and size factors were used to evaluate the different design configurations. Decisions involved the number of fermentors and chromatographic columns working in parallel as well as storage tanks.

More recently, Asenjo and coworkers [92] proposed a methodology where a two stage approach was used; in the first stage the sequence of chromatographic steps is determined and then the operating conditions (flowrate, ionic strength gradient) are optimised.

2.5 Summary

As seen in the pages above, chromatography has been and still remains a focus of many researchers around the world. Running chromatographic steps in the best possible way in order to achieve optimal separation is a challenge to be tackled. Different approaches were used in order to achieve the same target; optimal separation. For defining the operating conditions, the approaches vary from detailed and analytical to black-box methods. For chromatographic process synthesis, methods

were proposed starting from experience and rules of thumb to algorithmic and optimisation-based approaches. In this work, we will focus on optimisation-based methods in order to tackle the challenge of chromatographic synthesis and operation.

This work extends a work done by Pinto and coworkers [78], where chromatographic trains were synthesised with the assumption of complete recovery of the product. This work removes the assumption of complete recovery and apart from process synthesis, it also encompasses on selecting the timeline at which the product is collected, hence this work essentially incorporates simultaneous process operation and synthesis.

Chapter 3

An MINLP formulation for purification process synthesis

In this chapter, a novel approach based on mathematical programming is proposed and a mathematical model for the design of protein purification processes is presented, along with the fundamental basics of our model and the solution approach utilised for the specific chromatographic separation problem.

3.1 Introduction

As mentioned in Chapter 1 enhanced downstream process synthesis holds a key in reducing the manufacturing cost. To achieve that there are a few suggested strategies such as decreasing the number of steps, avoiding complex steps and reducing raw material costs. As shown in [93], many companies adopt molecule specific approaches based on a particular impurity challenge and can select from a set of candidate chromatographic steps. Many criteria have to be met for cost effectiveness, while always meeting stringent purity specifications. Particularly challenging in this context is the optimum selection of a process sequence from the available chromatographic steps.

3.2 Problem statement

The overall problem for the synthesis of the purification processing can be stated as follows.

Given:

- a mixture of proteins (p: 1,...,P) with known physicochemical properties (charge and hydrophobicity);
- a set of available chromatographic techniques (i: 1,...,I), each performing a separation by exploiting a specific physicochemical property;
- specifications for the desired protein (dp) in terms of minimum purity and recovery levels.

Determine:

- the flowsheet of the purification process
- operating starting and finishing cut-points ($xs_{i,dp}$, $xf_{i,dp}$)

So as to optimise the overall number of chromatographic steps taking into account product losses.

The model is based solely on the approximation of the chromatographic peaks by isosceles triangles and uses as inputs the physicochemical properties of the proteins in the complex mixture as shown in [2], [78]. The main features and basis of the chromatographic operations are explained in the following section.

3.3 Basis for the chromatographic separation model

Each chromatographic peak is approximated by an isosceles triangle. The physicochemical property data of all proteins in the mixture are also required [2]. The chromatographic behaviour of each protein is determined by the retention time. Each chromatographic technique performs separation by exploiting a different physicochemical property of the protein such as charge, hydrophobicity, molecular weight, etc. The dimensionless retention time, KD_{ip}, is a function of a characteristic physicochemical property, P_{ip}, and is defined by:

$$KD_{ip} = f(P_{ip}) = \frac{t_r - t_0}{t_f - t_0} \qquad \forall i, p \tag{3.1}$$

where t_r corresponds to the retention time, t_0 to the time in which the salt gradient is initiated and t_f to the time in which the salt gradient is terminated.

The methodology presented in [72] is used to estimate the dimensionless retention time for both ion exchange and hydrophobic interaction chromatography. It was observed that the dimensionless retention time for ion exchange chromatography could be successfully described as a function of the charge densities [2] as shown below.

- Anion Exchange Chromatography

$$KD_{ip} = \frac{8826 \cdot |Q_{ip}/MW_p|}{1 + 18875 \cdot |Q_{ip}/MW_p|} \quad if \quad Q_{ip} < 0 \quad \forall i \in AE, p \in P \tag{3.2}$$

$$KD_{ip} = 0 \quad if \quad Q_{ip} \geq 0 \quad \forall i \in AE, p \in P \tag{3.3}$$

- Cation Exchange Chromatography

$$KD_{ip} = 0 \quad if \quad Q_{ip} \leq 0 \quad \forall i \in CE, p \in P \tag{3.4}$$

$$KD_{ip} = \frac{7424 \cdot |Q_{ip}/MW_p|}{1 + 20231 \cdot |Q_{ip}/MW_p|} \quad if \quad Q_{ip} > 0 \quad \forall i \in CE, p \in P \tag{3.5}$$

For hydrophobic interaction chromatography, the dimensionless retention time was given through a quadratic function of hydrophobicity [94]:

$$KD_{ip} = -12.14 \cdot H_p^2 + 12.07 \cdot H_p - 1.74 \qquad \forall i \in HI, p \in P \tag{3.6}$$

Concentration factors, CF_{ip}, indicate the efficiency of each chromatographic technique and is a function of the deviation factor, DF_{ip}, the peak width, σ_i, which will be explained below. CF_{ip} for the various chromatographic steps are calculated based on the distance between the chromatographic peaks of the desired product and that of the contaminant [2]. Deviation factors, DF_{ip}, are defined as the distance between two peaks (see Figure 3.1), one of them being that of the target protein.

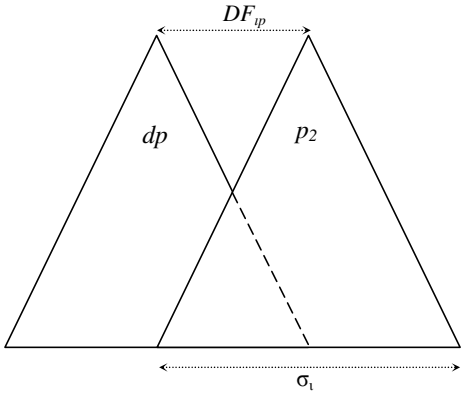

FIGURE 3.1: Graphical representation of deviation factor DF_{ip}

$$DF_{ip} = KD_{ip} - KD_{i,dp} \qquad \forall i, p \tag{3.7}$$

As mentioned before, product losses along the purification process are possible, thus the assumption of 100 % recovery of the product is removed. In order to achieve that, starting $xs_{i,dp}$ and finishing $xf_{i,dp}$ cut-points are applied. A graphical explanation of how the cut-points behave depending on the recovery is presented in Figure 3.2.

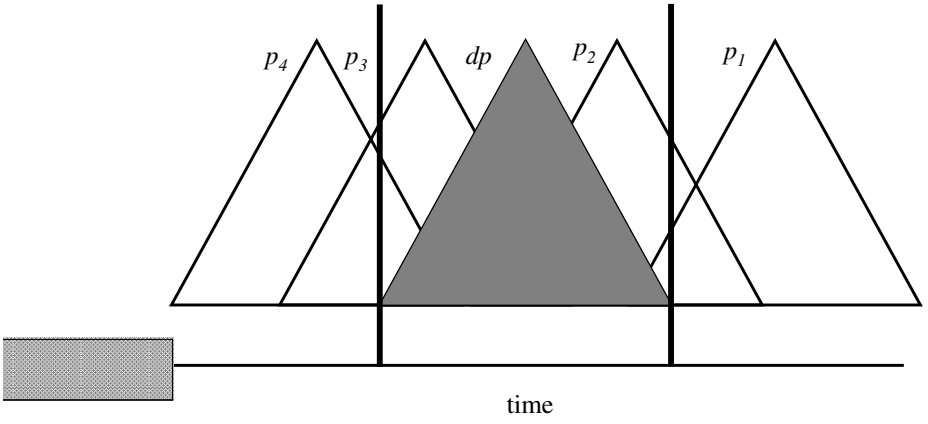

(a) 100%, recovery of the target protein

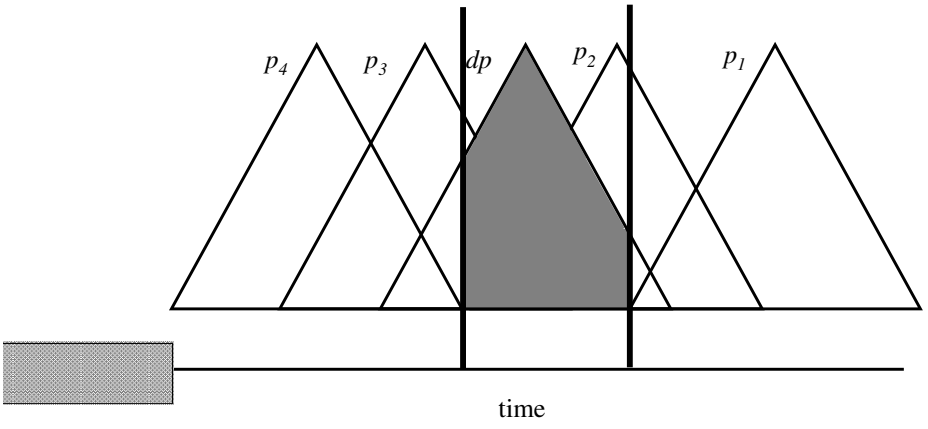

(b) <100%, recovery of the target protein

FIGURE 3.2: Graphical explanation of cut-points

In Figure 3.2(a), the cut points are located at the borders of the peak width, while in Figure 3.2(b), the cut-points can be located across the peak width line depending on the required recovery.

A brief breakdown of the different cases that may arise depending on the position of these cut-points is described below. In Figure 3.3, the triangles refer to the target protein and the shaded areas represent the remaining amount of the target protein within the mixture after the chromatographic technique has been applied.

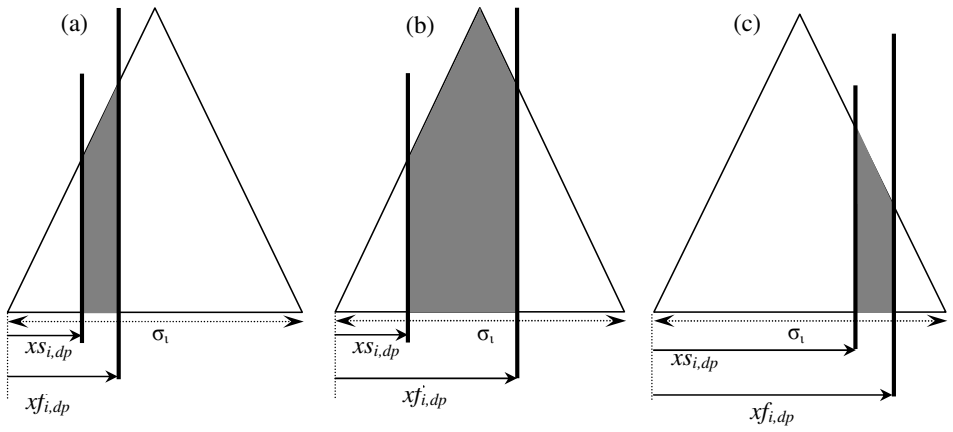

FIGURE 3.3: Representation of chromatographic peaks for the target protein

The mathematical expressions presented below represent the three cases presented in Figure 3.3. The chromatograms are approximated by isosceles triangles assuming constant shapes. Furthermore, the peak width has been averaged for each chromatographic technique. The peak width parameter σ_i only depends on the type of chromatographic operation and was calculated by averaging over several proteins. For ion exchange, the value for the peak width is σ_i=0.15 and for hydrophobic interaction σ_i=0.22 [2]. Note that both KD_{ip} and σ_i are both dimensionless or have units of time.

- $xs_{i,dp}$, $xf_{i,dp} < \frac{\sigma_i}{2}$

$$CF_{i,dp} = \frac{2 \cdot \left(xf_{i,dp}^2 - xs_{i,dp}^2\right)}{\sigma_i^2} \tag{3.8}$$

- $xs_{i,dp} < \frac{\sigma_i}{2}$, $xf_{i,dp} > \frac{\sigma_i}{2}$

$$CF_{i,dp} = 1 - \frac{2 \cdot \left[(xs_{i,dp})^2 + (\sigma_i - xf_{i,dp})^2\right]}{\sigma_i^2} \tag{3.9}$$

- $xs_{i,dp}$, $xf_{i,dp} > \frac{\sigma_i}{2}$

$$CF_{i,dp} = \frac{2 \cdot \left[(\sigma_i - xs_{i,dp})^2 - (\sigma_i - xf_{i,dp})^2\right]}{\sigma_i^2} \tag{3.10}$$

It is important to note that three different cases may arise depending on the relative positions of the cut-points. In the first case, Figure (3.3a) both cut-points are applied before the chromatogram has reached its peak and the other extreme case Figure (3.3c) is valid when both cut-points are applied after the chromatogram has reached its peak. Finally, the remaining case shown in Figure (3.3b) is when the starting point is applied before the chromatogram reaches its peak and the finishing point is applied after the chromatogram reaches its peak.

For the contaminants, the concentration factor is calculated similarly, but in this case the concentration factor is also a function of the deviation factor. Many different cases may arise depending on the relative positions of the triangles and the cut-points as well.

Below, we can see a graphical representation of how the different chromatograms can be allocated depending on their peak distance. Retention time data available in [2] were used to create the actual chromatograms. In Figure 3.4, we can see a visual representation of how the different proteins elute in different times and how this results in a typical separation problem. In all figures, the solid line triangle refers to the target protein and the rest are considered as contaminants. As

shown, in some cases, peaks of target protein and contaminants can almost completely overlap (difficult to separate) Figures (3.4(a), 3.4(f)) or in other cases the two peaks are far from each other (easy to separate) Figures (3.4(c), 3.4(d)).

3.4 Mathematical model

The mathematical model for the optimisation of the selection of the chromatographic steps for the purification of proteins is described next.

Objective Function

An objective function that selects the minimum number of chromatographic steps is defined as follows:

$$Minimise \quad S = \sum_{i} E_i \tag{3.11}$$

where E_i is a binary variable, activated when a chromatographic technique i is selected.

Target Protein Constraints

This set of constraints determines the concentration factors for the target protein. Binary variables, zs_{ip} and zf_{ip}, are introduced for starting and finishing cut-points, respectively. In Figure 3.5, a graphical representation of how these variables are activated is presented. Each binary variable indicates whether the relevant cut-point is located before or after the chromatogram peak.

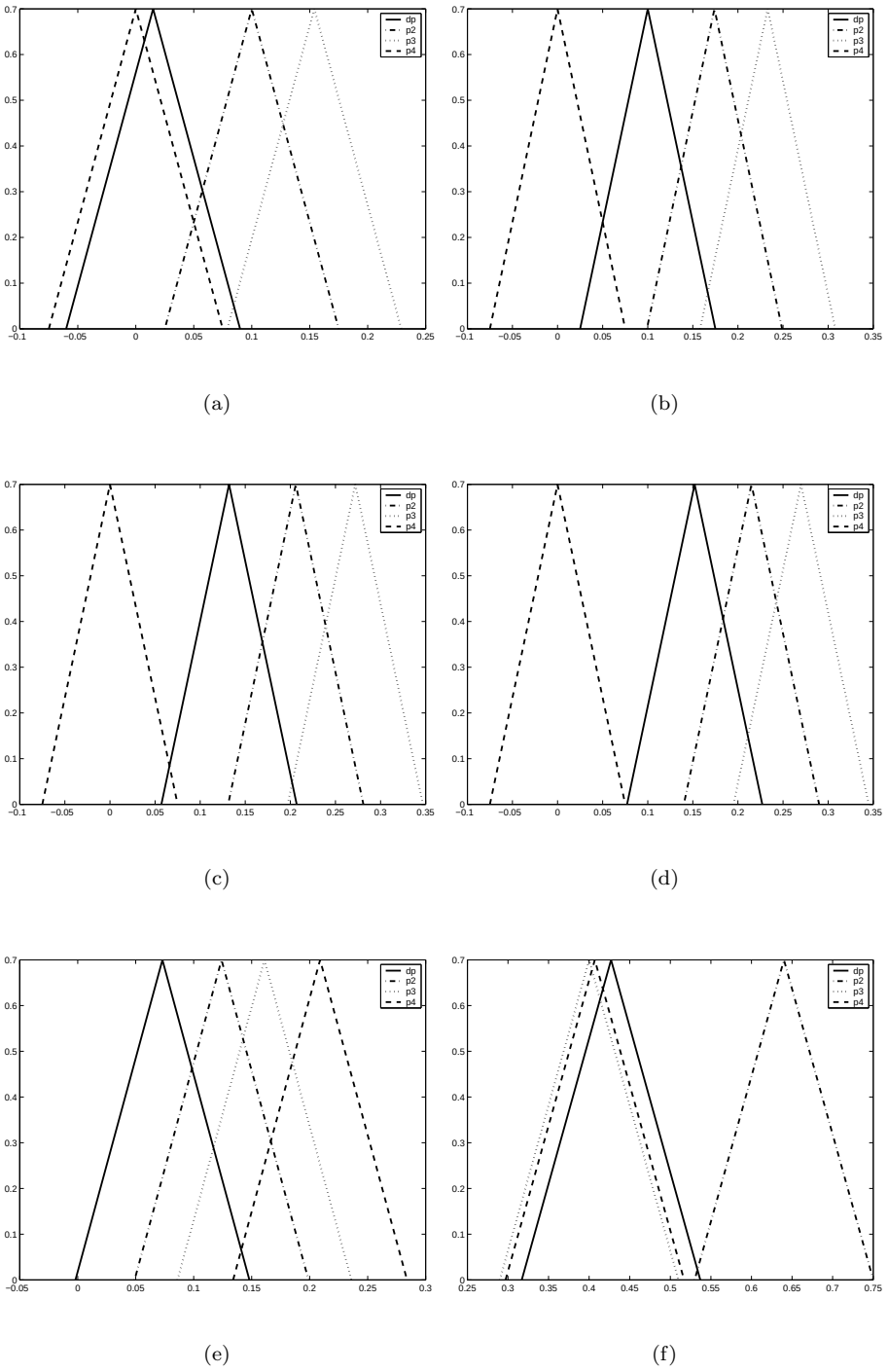

FIGURE 3.4: Typical protein elution problem using data from [2]

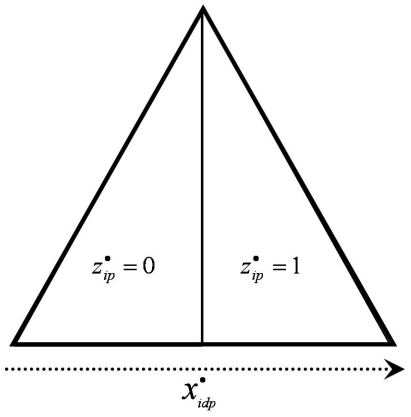

FIGURE 3.5: Representation of binary variables for the target protein indicated by Equation 3.12

Depending on the values of these binary variables, Equation 3.12 can cover all possible cases that were demonstrated in Figure 3.3.

$$CF_{ip} = 2 \cdot \frac{(xf_{ip})^2}{\sigma_i^2} \cdot (1 - zf_{ip}) + \left[1 - \frac{2 \cdot (\sigma_i - xf_{ip})^2}{\sigma_i^2}\right] \cdot zf_{ip} \\ -2 \cdot \frac{(xs_{ip})^2}{\sigma_i^2} \cdot (1 - zs_{ip}) - \left[1 - \frac{2 \cdot (\sigma_i - xs_{ip})^2}{\sigma_i^2}\right] \cdot zs_{ip} \qquad \forall i, p = dp \tag{3.12}$$

Equations 3.13 and 3.14 determine the position within the target protein's range for both xs_{ip} and xf_{ip}. If the cut-point is after the chromatogram's peak ($> \sigma_i/2$), the corresponding binary variable is equal to one otherwise ($< \sigma_i/2$) is forced to zero.

$$\frac{\sigma_i}{2} \cdot zs_{ip} \leq xs_{ip} \leq \frac{\sigma_i}{2} + M \cdot zs_{ip} \qquad \forall i, p = dp \tag{3.13}$$

$$\frac{\sigma_i}{2} \cdot zf_{ip} \leq xf_{ip} \leq \frac{\sigma_i}{2} + M \cdot zf_{ip} \qquad \forall i, p = dp \tag{3.14}$$

Finally, Constraint 3.15 is a logical constraint that indicates that the starting cut-point, xs_{ip}, should always be before the finishing cut-point, xf_{ip}.

$$xs_{ip} \leq xf_{ip} \qquad \forall i, p = dp \tag{3.15}$$

Contaminant Protein Constraints

Similarly to the target protein, a set of constraints also applies for determining concentration factors, CF_{ip}, for all contaminants in the mixture.

All possible cases that may arise depending on the relative position of the triangles can be calculated by using shifted starting and finishing cut-points as shown in Equations 3.16 and 3.17. For the shifted cut-points, the concentration factors of the contaminants CF_{ip} also depend on the deviation factors DF_{ip}.

$$\bar{x}s_{ip} = xs_{i,dp} - DF_{ip} \qquad \forall i, p \neq dp \tag{3.16}$$

$$\bar{x}f_{ip} = xf_{i,dp} - DF_{ip} \qquad \forall i, p \neq dp \tag{3.17}$$

If the shifted cut-point is after the chromatogram's peak ($> \sigma_i/2$), the corresponding binary variable zs_{ip} or zf_{ip} is equal to one otherwise ($< \sigma_i/2$) is forced to zero by constraints 3.18 and 3.19.

$$\frac{\sigma_i}{2} - M \cdot (1 - zs_{ip}) \leq \bar{x}s_{ip} \leq \frac{\sigma_i}{2} + M \cdot zs_{ip} \qquad \forall i, p \neq dp \tag{3.18}$$

$$\frac{\sigma_i}{2} - M \cdot (1 - zf_{ip}) \leq \bar{x}f_{ip} \leq \frac{\sigma_i}{2} + M \cdot zf_{ip} \qquad \forall i, p \neq dp \tag{3.19}$$

Correction variables $\hat{\Delta}s_{ip}$, $\hat{\Delta}f_{ip}$, Δs_{ip}, Δf_{ip} defined in Equations 3.20 - 3.23, along with additional binary variables ys_{ip}, yf_{ip}, ws_{ip}, wf_{ip} are introduced for the shifted starting and finishing cut-points, $\bar{x}s_{ip}$ and $\bar{x}f_{ip}$, respectively. These variables are introduced as in many cases the shifted cut-points are outside the contaminant's peak width.

$$\hat{\Delta}s_{ip} \equiv max \qquad (\bar{x}s_{ip}, 0) \qquad \forall i, p \neq dp \tag{3.20}$$

$$\hat{\Delta}f_{ip} \equiv max \qquad (\bar{x}f_{ip}, 0) \qquad \forall i, p \neq dp \tag{3.21}$$

$$\Delta s_{ip} \equiv min \qquad (\bar{x}s_{ip}, \sigma_i) \qquad \forall i, p \neq dp \tag{3.22}$$

$$\Delta f_{ip} \equiv min \qquad (\bar{x}f_{ip}, \sigma_i) \qquad \forall i, p \neq dp \tag{3.23}$$

If the shifted cut-point is before the contaminant's chromatogram (<0), then constraints 3.24, 3.25 are activated and binary variable ys_{ip} or yf_{ip} is equal to one otherwise is forced to zero.

$$-M \cdot ys_{ip} \leq \bar{x}s_{ip} \leq M \cdot (1 - ys_{ip}) \qquad \forall i, p \neq dp \tag{3.24}$$

$$-M \cdot yf_{ip} \leq \bar{x}f_{ip} \leq M \cdot (1 - yf_{ip}) \qquad \forall i, p \neq dp \tag{3.25}$$

When ys_{ip} or yf_{ip} is equal to one then from constraints 3.26 or 3.27, $\hat{\Delta}s_{ip}$ or $\hat{\Delta}f_{ip}$ is forced to zero otherwise the original values of $\bar{x}s_{ip}$ or $\bar{x}f_{ip}$, are kept.

$$\hat{\Delta s_{ip}} = \bar{x}s_{ip} \cdot (1 - ys_{ip}) \qquad \forall i, p \neq dp \tag{3.26}$$

$$\hat{\Delta f_{ip}} = \bar{x}f_{ip} \cdot (1 - yf_{ip}) \qquad \forall i, p \neq dp \tag{3.27}$$

If the shifted cut-point is after the contaminant's chromatogram ($> \sigma_i$), constraints 3.28, 3.29 are activated and binary variable ws_{ip} or wf_{ip} is equal to one otherwise is forced to zero.

$$\sigma_i - M \cdot (1 - ws_{ip}) \leq \bar{x}s_{ip} \leq \sigma_i + M \cdot ws_{ip} \qquad \forall i, p \neq dp \tag{3.28}$$

$$\sigma_i - M \cdot (1 - wf_{ip}) \leq \bar{x}f_{ip} \leq \sigma_i + M \cdot wf_{ip} \qquad \forall i, p \neq dp \tag{3.29}$$

When ws_{ip} or wf_{ip} is equal to one then from Equations 3.30 or 3.31, Δs_{ip} or Δf_{ip} is forced to σ_i, otherwise the original values ($\bar{x}s_{ip}$ or $\bar{x}f_{ip}$) are kept.

$$\Delta s_{ip} = \bar{x}s_{ip} + (\sigma_i - \bar{x}s_{ip}) \cdot ws_{ip} \qquad \forall i, p \neq dp \tag{3.30}$$

$$\Delta f_{ip} = \bar{x}f_{ip} + (\sigma_i - \bar{x}f_{ip}) \cdot wf_{ip} \qquad \forall i, p \neq dp \tag{3.31}$$

In Equation 3.32, the concentration factor for each contaminant is calculated by:

$$CF_{ip} = 2 \cdot \frac{(\hat{\Delta} f_{ip})^2}{\sigma_i^2} \cdot (1 - zf_{ip}) + \left[1 - \frac{2 \cdot (\sigma_i - \Delta f_{ip})^2}{\sigma_i^2}\right] \cdot zf_{ip}$$
$$-2 \cdot \frac{(\hat{\Delta} s_{ip})^2}{\sigma_i^2} \cdot (1 - zs_{ip}) - \left[1 - \frac{2 \cdot (\sigma_i - \Delta s_{ip})^2}{\sigma_i^2}\right] \cdot zs_{ip} \qquad \forall i, p \neq dp \tag{3.32}$$

A graphical representation of how the new binary variables are activated is shown in Figure 3.6.

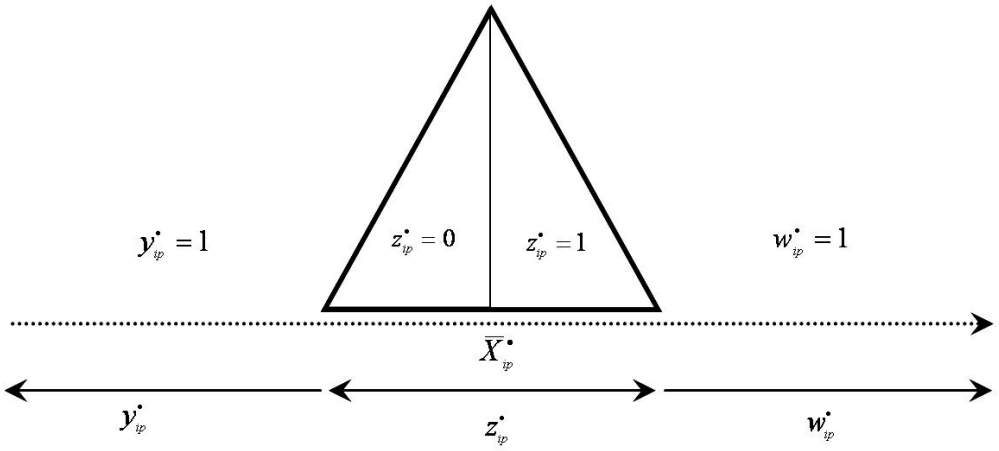

FIGURE 3.6: Representation of binary variables for the contaminants

Process Synthesis Constraints

The following set of constraints enforces the mass of each protein, m_{ip}, in the mixture t be reduced when the chromatographic technique i has been selected [2]. Constraint 3.33 indicates the mass of each protein after the first chromatographic step has been applied, where mo_p is the initial mass of each protein. If chromatographic step i is selected (E_i=1)then the mass of all the proteins in the mixture is forced to be reduced, otherwise it remains the same. Constraints 3.34 - 3.37 are active for all

chromatographic steps except the first one and when Constraint 3.36 is active, Constraint 3.37 holds.

$$m_{ip} = CF_{ip} \cdot mo_p \cdot E_i + mo_p \cdot (1 - E_i) \qquad \forall i = 1, p \qquad (3.33)$$

$$m_{ip} = CF_{ip} \cdot m^1_{i-1,p} + m^2_{i-1,p} \qquad \forall i \geq 2, p \qquad (3.34)$$

$$m_{i-1,p} = m^1_{i-1,p} + m^2_{i-1,p} \qquad \forall i \geq 2, p \qquad (3.35)$$

$$m^1_{i-1,p} \leq mo_p \cdot E_i \qquad \forall i \geq 2, p \qquad (3.36)$$

$$m^2_{i-1,p} \leq mo_p \cdot (1 - E_i) \qquad \forall i \geq 2, p \qquad (3.37)$$

Specification Constraints

This set of constraints enforces purity, *SP*, and recovery, *fr*, specifications.

$$m_{i,dp} \geq SP \cdot \sum_{p'} m_{ip'} \qquad \forall i = I \qquad (3.38)$$

$$m_{i,dp} \geq fr \cdot mo_{dp} \qquad \forall i = I \qquad (3.39)$$

Model Summary

Below, a summary of the proposed model is provided. The objective is to minimise the overall number of chromatographic steps.

$$Minimise \quad S = \sum_i E_i$$

subject to:

target protein Constraints 3.12 - 3.15;

contaminant Constraints 3.32 - 3.19, 3.24 - 3.31;

process synthesis Constraints 3.33 - 3.37;

specification Constraints 3.38, 3.39;

domain Constraints: E_i, zs_{ip}, zf_{ip}, ws_{ip}, wf_{ip}, ys_{ip}, $yf_{ip} \in \{0, 1\}$
m_{ip}, m^1_{ip}, $m^2_{ip} \geq 0 \qquad \forall i, p$

3.5 Solution approach

The overall problem is formulated as mixed integer non-linear programming (MINLP) model. The resulting optimisation model is non-convex and the nonlinearities arise in:

- Equations 3.12 and 3.32, for the calculation of the concentration factors for both the target protein and the contaminants,
- Equations 3.26 - 3.27 and 3.30 - 3.31 for the estimation of the correction variables,
- Equations 3.33 - 3.34 for the calculation of the mass of all the proteins in in the mixture.

Trying to solve the monolithic MINLP resulted in many of the cases in no solution or into very large CPU times, therefore a two-stage solution is proposed to identify the optimal flowsheet of the purification process.

Stage 1: Solve screening MILP [78] that does not take into account product losses, to determine candidate chromatographic steps.

Stage 2: Solve proposed MINLP with losses over the reduced set of alternatives determined by stage 1.

Note that the screening MILP model is used over the full set of candidate chromatographic steps. Its result is a reduced set of candidates, but not the minimum number of chromatographic steps to achieve product specifications. The minimum number of chromatographic steps is only determined after stage 2 of the solution procedure, where product losses are taken into account.

3.6 Results and discussion

The methodology was tested with three examples modelled in GAMS 22.8 [95]. Solutions were obtained using different MINLP solvers on a Dell Desktop Core Duo 3.25 GB RAM 3.16z,GHz machine.

3.6.1 Example 1

This first example is based on experimental data taken from [2] involving serum from bovine albumin which is the desired product (dp), ovalbumin (p_2), soybean trypsin inhibitor (p_3) and thaumatin (p_4). The physicochemical properties as well as the initial protein concentration of the mixture are given in Table 3.1. In summary, there are 11 candidate chromatographic steps: anion exchange chromatography (AE) at $pH4$, AE at $pH5$, AE at $pH6$, AE at $pH7$, AE at $pH8$, cation exchange chromatography (CE) at $pH4$, CE at $pH5$, CE at $pH6$, CE at $pH7$, CE at $pH8$ and hydrophobic interaction (HI). In Tables A.1 and A.2 in Appendix A, the calculated dimensionless retention times, KD_{ip} and deviation factors, DF_{ip} are presented.

TABLE 3.1: Physicochemical properties of protein mixture in example 1

				Q_{ip} (C/molecule) $\times 10^{-17}$				
Protein	mo_p (mg/ml)	MW_p (Da)	H_p	$pH4$	$pH5$	$pH6$	$pH7$	$pH8$
dp	2	67000	0.86	1.03	-0.14	-1.16	-1.68	-2.05
p1	2	43800	0.54	1.40	-0.76	-1.65	-2.20	-2.36
p2	2	24500	0.90	1.22	-0.76	-1.54	-2.17	-2.13
p3	2	22200	0.89	1.94	1.90	1.98	-1.87	0.91

Initially, the screening MILP was solved for 98 % purity and no losses, resulting in a reduced set of 3 candidates ($AE7$, $AE8$, HI). Then, the MINLP model was solved for both purity and recovery set to 98 %. The optimal solution, shown in Figure 3.7, achieves a purity of 98.1 % and

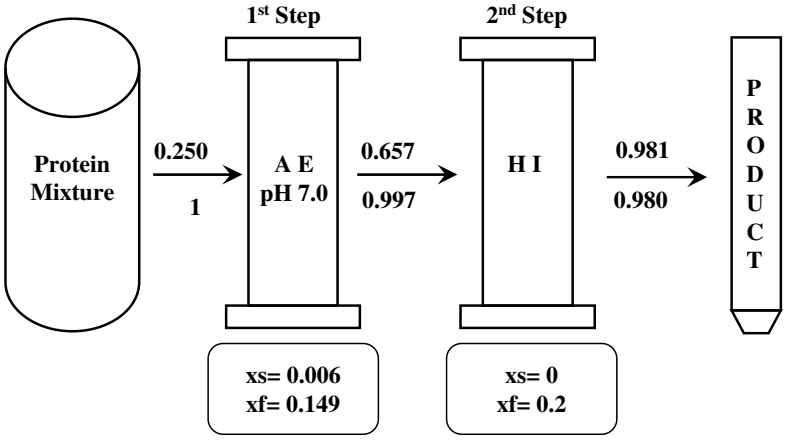

FIGURE 3.7: Optimal flowsheet for purification of protein mixture in example 1

98 % recovery, involving two chromatographic steps: *AE* at *pH7* and *HI*. In all flowsheets, the number above the arrow refers to purity and the one below to recovery.

3.6.2 Example 2

This example utilises data available in [2]. The mixture includes target protein $\beta - 1,3$ glucanase from *Bacillus Subtilis* and 8 contaminants. Physicochemical properties along with initial concentrations of the protein mixture are available in Table 3.2. Overall, we have 21 candidate chromatographic steps. Besides the ones presented in example 1, we have additional steps: anion exchange chromatography (*AE*) at *pH4.5*, *AE* at *pH5.5*, *AE* at *pH6.5*, *AE* at *pH7.5*, *AE* at *pH8.5*, cation exchange chromatography (*CE*) at *pH4*, *CE* at *pH5*, *CE* at *pH6.5*, *CE* at *pH7.5*, *CE* at *pH8.5*. In Tables A.3 and A.4 in Appendix A, the calculated dimensionless retention times, KD_{ip}, and deviation factors, DF_{ip}, are given.

TABLE 3.2: Physicochemical properties of protein mixture in example 2

Protein	mo_p (mg/ml)	MW_p (Da)	H_p	Q_{ip} (C/molecule) $\times 10^{-17}$									
				pH4	*pH4.5*	*pH5*	*pH5.5*	*pH6*	*pH6.5*	*pH7*	*pH7.5*	*pH8*	*pH8.5*
dp	0.62	31000	0	1.46	0.09	-0.62	-0.66	-1.02	-1.82	-2.33	-2.52	-2.52	-3.51
p1	0.42	62500	0	1.46	0.09	-1.06	-0.98	1.17	-1.71	-2.79	-3.52	-3.32	-3.32
p2	0.25	40600	0	1.46	0.09	-0.55	-0.22	-0.22	-0.26	-0.73	-1.26	-1.82	-3.51
p3	0.25	69600	0	1.46	0.09	-0.55	-0.22	-0.22	-0.26	-0.73	-1.26	-1.82	-3.51
p4	0.09	40600	0	1.46	3.14	1.46	0.28	-0.47	-0.89	-1.06	-1.08	-1.04	-1.01
p5	0.09	69600	0	1.46	3.14	1.46	0.28	-0.47	-0.89	-1.06	-1.08	-1.04	-1.01
p6	2.74	41000	1.5	1.46	0.93	0.26	-0.35	-0.87	-1.31	-1.65	-1.9	-2.04	-2.06
p7	2.74	32900	1.5	1.46	0.09	0	-1.7	-2.7	-2.9	-3.51	-3.51	-3.51	-3.51
p8	0.25	35500	0.2	1.46	0.09	-0.55	-0.22	-0.22	-0.26	-1.26	-1.82	-1.82	-3.51

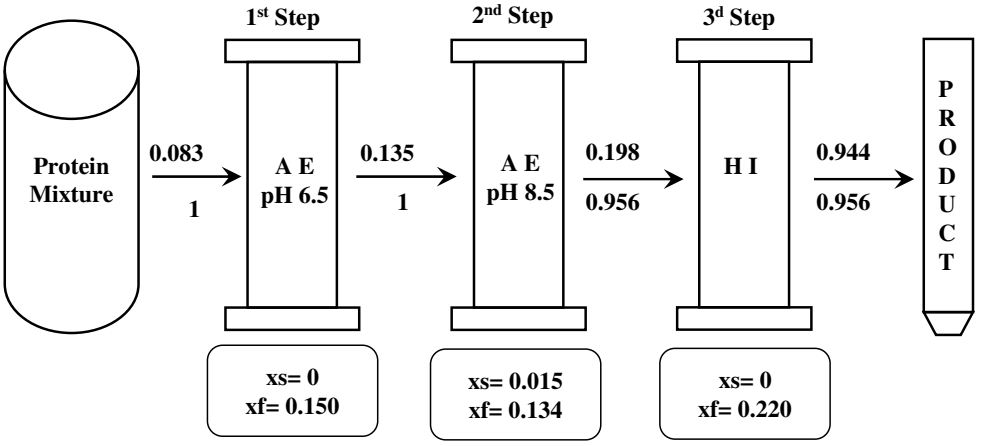

FIGURE 3.8: Optimal flowsheet for purification of protein mixture in example 2

After the solution of the screening MILP for 94 % purity and no losses, the set of candidates was reduced from 21 candidate steps to 6 (*AE6*, *AE6.5*, *AE7*, *AE7.5*, *AE8.5*, *HI*). Next, the MINLP model was solved for both purity and recovery set to 94 %. Figure 3.8 shows the optimal flowsheet. For this mixture, the model identified a solution that achieves a purity of 94.4 % and 95.6 % recovery, for which three chromatographic steps are necessary: *AE* at *pH6.5*, *AE* at *pH8.5* and *HI*.

3.6.3 Example 3

For our final example, we used experimental data taken from [79]. This specific example is the largest one of the three and the most complex in terms of separation potential, mainly because of the overlapping of elution profiles between the target protein and the contaminants. It involves 13 proteins and all the necessary information are presented in Table 3.3. There are 11 candidate chromatographic steps as presented in the first example. In Tables A.5 and A.6, the calculated dimensionless retention times, KD_{ip}, and deviation factors, DF_{ip}, are presented.

TABLE 3.3: Physicochemical properties of protein mixture in example 3

Protein	mo_p (mg/ml)	MW_p (Da)	H_p	Q_{ip} (C/molecule) $\times 10^{-17}$				
				pH4	*pH5*	*pH6*	*pH7*	*pH8*
dp	2	77000	0.28	2.04	1.06	-0.37	-0.81	-1.13
p1	2	22000	0.27	1.60	1.57	1.56	1.55	0.75
p2	2	23600	0.31	2.15	1.46	1.17	0.78	0.38
p3	2	13500	0.23	1.83	0.65	0.26	-0.20	-0.33
p4	2	43800	0.28	1.16	-0.63	-1.36	-1.82	-1.95
p5	2	15900	0.27	2.89	2.81	2.8	2.64	2.07
p6	2	14400	0.32	-0.46	-0.47	-0.63	-1.21	-1.25
p7	2	17500	0.21	0.45	-0.62	-0.79	-1.26	-1.7
p8	2	50000	0.27	-0.12	-0.32	-0.76	-0.91	-1.04
p9	2	12100	0.18	1.46	0.62	-1.02	-1.33	-1.52
p10	2	25500	0.30	1.01	-0.63	-1.27	-1.59	-1.76
p11	2	26000	0.28	2.96	1.26	0.92	0.54	0.01
p12	2	19900	0.25	0.93	0.33	-0.12	-0.34	-0.5

The screening MILP was solved for 93 % purity and no losses, resulting to a reduced set of 5 candidates (*AE6*, *AE7*, *CE4*, *CE5*, *HI*). Then the MINLP model was solved for a purity of 93 % and a recovery of 90 %. The optimal solution is presented in Figure 3.9. Three chromatographic steps are required: *AE* at *pH7*, *CE* at *pH4* and *HI* to achieve a purity of 93 % and 90 % recovery.

Table 3.4 presents computational statistics for the three examples studied using the proposed MINLP model and applying the two-stage solution approach described earlier.

TABLE 3.4: Summary of Computational Statistics

Example	Constraints	Discrete/Continuous Variables	CPU time (s)
1	237	63/101	3.1
2	1188	306/499	277
3	1454	375/605	505

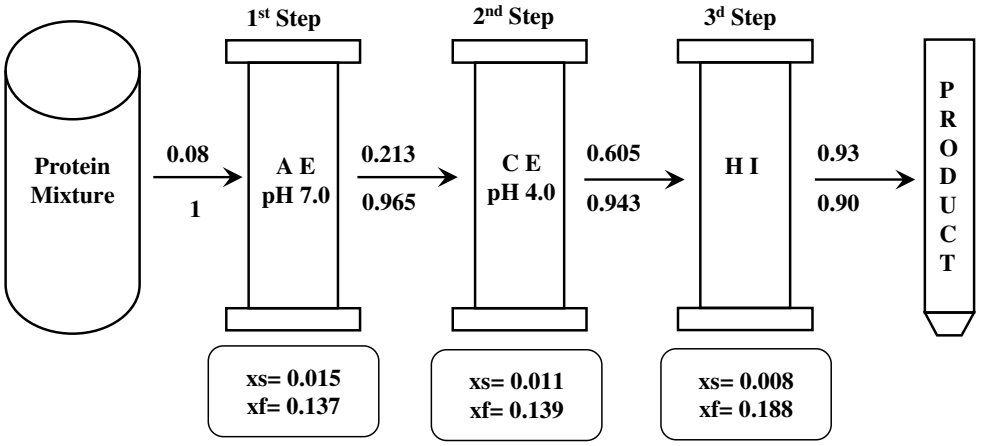

FIGURE 3.9: Optimal flowsheet for purification of protein mixture in example 3

3.6.4 Comparative results

Several MINLP solvers were tested for all three examples. Default settings were used for all solvers tested. As presented in Table 3.5, BARON appeared to be the most appropriate solver for the proposed MINLP model. Although LindoGlobal obtained a solution for all three examples, the CPU time was significantly higher while worse solution was provided for example 2. BARON took only 505 seconds to solve example 3, while LindoGlobal was able to find the same solution in 2595 sec. Moreover, SBB was not able to provide any solution for examples 2 and 3. Finally, CoinBonmin produced no result for the last two example and took more than 500 seconds to solve the second one, while DICOPT could not obtain a solution for any of them.

TABLE 3.5: Comparative results using different MINLP solvers

Solver	CPU time (s)	Number of Steps	Final Purity (%)	Final Recovery (%)
		Example 1		
BARON	3.1	2	98.1	98
CoinBonmin	118.5	2	98.3	98.2
DICOPT		Solver Failure (Iteration Limit)		
LindoGlobal	1.58	2	98	98
SBB	3.1	2	99.1	98
		Example 2		
BARON	277	3	94.8	94.8
CoinBonmin		No Solution Returned		
DICOPT		Solver Failure (Iteration limit)		
LindoGlobal	2595	4	94	94
SBB		Solver Failure (Node limit)		
		Example 3		
BARON	505	3	93	90
CoinBonmin		No Solution Returned		
DICOPT		Solver Failure (Iteration limit)		
LindoGlobal	1177	3	93	90
SBB		Solver Failure (Node limit)		

3.7 Conclusions

In this Chapter, an optimisation framework was presented for the synthesis of chromatographic steps for the purification of protein mixtures. The effect of product losses was explicitly accounted for, which consists a novel feature of the work. The overall problem was formulated as an MINLP model and a two-stage solution approach was proposed. Three examples of protein mixtures were tested to demonstrate the efficiency of the proposed methodology.

Solution robustness and computational requirements are still issues that require further attention. Along these line, the next two Chapters attempt to address these issues by investigating alternative frameworks base on MILP models.

Chapter 4

An MILP formulation for the synthesis of protein purification processes

In this chapter, the mathematical model described in Chapter 3 is linearised in an effort to improve computational efficiency. First, we present the model for chromatographic separation, followed by the optimisation model where all the constraints are explained in detail. Finally, the model is tested by using the same examples presented in Chapter 3 and the results are compared with the ones of the MINLP model

4.1 Introduction

In the previous Chapters, the importance of synthesising and operating chromatographic processes in the best possible way was highlighted . In an effort to tackle that challenge, we developed a model based on mathematical programming. Trying to solve the monolithic MINLP model resulted in no solution and this is why a two-stage solution was developed.

After that the model was solved over a reduced set of candidate steps but still resulted in large CPU times, especially for the larger examples. For this reason, a new model is proposed in this Chapter. Using piecewise linear approximations, the non-linear functions that are present in the model described in Chapter 3 were approximated as necessary without compromising the quality of the solution. In the following section, we present the mathematical model developed.

4.2 Mathematical model

In this section, an MILP model is proposed that is based on the MINLP model introduced in Chapter 3. The model comprises two parts. Initially, the chromatographic separation model is presented along with the methodology and the actual equations that are the background for the optimisation model. Finally, the material balances for the selection of the optimum flowsheet are defined.

The objective function is to minimise the overall number of steps from a set of alternatives.

Objective Function:

$$Min \qquad S = \sum_{i} E_i \tag{4.1}$$

Binary variable E_i is activated when the chromatographic step i is selected.

4.2.1 Chromatographic separation model

As shown in the previous Chapter, the chromatographic peaks are usually approximated by the use of isosceles triangles[2, 74]. The first parameter defined is the dimensionless retention time, KD_{ip}, which was

experimentally determined to be a function of a characteristic physicochemical property, P_{ip}. The dimensionless retention time is characteristic for each protein p and each chromatographic technique i. The methodology presented in [72] was used to estimate the dimensionless retention time for both ion exchange (*IEX*) and hydrophobic interaction chromatography (*HIC*). It was observed that the dimensionless retention time for *IEX* could successfully be described as a function of the charge densities (Q_{ip}/MW_p) for the operating conditions considered, as presented in Equations 3.2 - 3.5.

For *HIC*, the dimensionless retention time can be described through a quadratic function of hydrophobicity based on the methodology proposed by [94] as shown in equation 3.6.

Although each protein p needs a different amount of time to elute from a different column/technique i, this information alone is not enough to quantify the efficiency of each chromatographic step. To do that the distance between peaks has to be considered. Deviation factors, DF_{ip}, are defined as the distance between two peaks as shown in figure 3.1, one of them being the target protein's peak as shown in [2].

As mentioned earlier the chromatograms are approximated by isosceles triangles. The peak width parameter, σ_i, is assumed to be dependant on the type of chromatographic operation and was calculated by averaging over several proteins [2], [73]. For ion exchange, the value for the peak width is σ_i=0.15 and for hydrophobic interaction σ_i=0.22 [2].

Finally, the efficiency of each chromatographic technique can be quantified by the concentration factor, CF_{ip}. The concentration factor is practically the ratio of the mass before and after each chromatographic technique i. As described in [78] the concentration factor, CF_{ip}, is usually a function of DF_{ip} and σ_i. For this model though, some percentage of product losses is allowed. For this to be quantified, two extra variables are introduced. Starting cut-point, $xs_{i,dp}$, is the starting time for collecting the product and finishing cut-point, $xf_{i,dp}$, is the ending time

for collecting our product (target protein). In order to calculate CF_{ip}, both $xs_{i,dp}$ and $xf_{i,dp}$ have to be determined first.

The mathematical expressions presented below represent the $CF_{i,dp}$ calculations for the target protein. A graphical representation is illustrated in Figure 3.3 where the triangles refer to the target protein and the shaded areas represent the remaining amount of the target protein within the mixture after chromatographic technique i has been applied. It is important to note that three different cases may arise depending on the relative positions of the cut-points.

For the contaminants, depending on $xs_{i,dp}$, $xf_{i,dp}$ and DF_{ip}, new variables called shifted cut-points are introduced and defined below. The concentration factor is calculated based on the methodology shown in Equations 3.8 - 3.10, but in this case CF_{ip} is also a function of DF_{ip} because of the shifted cut-points defined in Equations 4.2, 4.3.

$$\bar{xs}_{ip} = xs_{i,dp} - DF_{ip} \qquad \forall i, p \neq dp \tag{4.2}$$

$$\bar{xf}_{ip} = xf_{i,dp} - DF_{ip} \qquad \forall i, p \neq dp \tag{4.3}$$

Next, the material balances for each protein in the mixture are necessary. m_{ip} is the mass of each protein p after each chromatographic technique i and is calculated in the following set of constraints where mo_{ip} is the initial mass of each protein p in the mixture and m^1_{ip}, m^2_{ip} denote the masses after selection and no-selection of technique i [79], [3].

$$\begin{aligned}
m_{ip} &= CF_{ip} \cdot mo_p \cdot E_i + mo_p \cdot (1 - E_i) && \forall i = 1, p \\
m_{ip} &= CF_{ip} \cdot m^1_{i-1,p} + m^2_{i-1,p} && \forall i \geq 2, p \\
m_{i-1,p} &= m^1_{i-1,p} + m^2_{i-1,p} && \forall i \geq 2, p \\
m^1_{i-1,p} &\leq mo_p \cdot E_i && \forall i \geq 2, p \\
m^2_{i-1,p} &\leq mo_p \cdot (1 - E_i) && \forall i \geq 2, p
\end{aligned} \tag{4.4}$$

Finally, the purity and recovery specifications are enforced by Constraints 4.5 and 4.6.

$$m_{i,dp} \geq sp \cdot \sum_{p'} m_{ip'} \qquad \forall i = I \tag{4.5}$$

$$m_{i,dp} \geq fr \cdot mo_{dp} \qquad \forall i = I \tag{4.6}$$

4.2.2 Material balance transformation

The material balances shown in equation 4.4 use nonlinear terms given that the concentration factors are variables and depend on the selection of cut-points, $xs_{i,dp}$, $xf_{i,dp}$. In order to linearise this set of constraints, a strategy similar to that proposed by [81] is followed. The final concentration for each protein in the mixture is given by the following relationship.

$$m_{Ip} = mo_p \cdot \prod_i \overline{CF_{ip}} \qquad \forall p \tag{4.7}$$

where $\overline{CF_{ip}}$ is a new auxiliary variable defined by:

$$\begin{aligned} \overline{CF_{ip}} &= CF_{ip} \quad if \quad E_i = 1 \quad \forall i, p \\ \overline{CF_{ip}} &= 1 \quad if \quad E_i = 0 \quad \forall i, p \end{aligned} \tag{4.8}$$

Thus, variable $\overline{CF_{ip}}$ can be expressed as an exponential form:

$$\overline{CF_{ip}} = e^{(lnCF_{ip}) \cdot E_i} \qquad \forall i, p \tag{4.9}$$

Therefore, by combining Equations 4.7 and 4.9, the mass of each protein p at the last chromatographic step I can be calculated as shown in

equation 4.10.

$$m_{Ip} = mo_p \cdot e^{\sum_i lnCF_{ip} \cdot E_i} \qquad \forall p \qquad (4.10)$$

Adopting that,

$$\overline{lnCF_{ip}} \equiv lnCF_{ip} \cdot E_i \qquad \forall i, p \qquad (4.11)$$

the final mass balance is given by equation 4.12.

$$m_{Ip} = mo_p \cdot \xi_p, \qquad where \qquad \xi_p = e^{\sum_i \overline{lnCF_{ip}}} \qquad \forall p \qquad (4.12)$$

This is still a nonlinear equation, but now all the nonlinear terms are present in a single term, hence can be linearly approximated. In the next section, various piecewise linear approximations are described in order to remove all nonlinear terms in the model, to represent CF_{ip}, $lnCF_{ip}$ and ξ_p.

4.2.2.1 Piecewise linear approximations

There are three non-linear parts in the model as it is now. The first one is relating the cut-points $xs_{i,dp}$, $xf_{i,dp}$ with the areas that lie below them, hence concentration factors calculations. The second one relates CF_{ip} with $lnCF_{ip}$ and the last one $\overline{lnCF_{ip}}$ with ξ_p. In total, three piecewise linear approximations are required.

For all required linearisations, the approach presented in [96] was employed in order to obtain the optimal points that approximate the relevant non-linear functions. A summary of the procedure is provided in Appendix B, where a set of points within the non-linear function is given, so that the resulting piecewise linear function is composed of all linear segments between the selected points.

Moving on to the first linearisation, cut-points $xs_{i,dp}$, $xf_{i,dp}$ are related with the areas that lie below them and represent the mass of the protein collected at that specific cut-point. The relevant constraints are shown below.

$$xs_{ip} = \sum_j xl_{ij} \cdot \lambda s_{ipj} \qquad \forall i, p \qquad (4.13)$$

$$As_{ip} = \sum_j Al_{ij} \cdot \lambda s_{ipj} \qquad \forall i, p \qquad (4.14)$$

$$\sum_j \lambda s_{ipj} = 1 \qquad \forall i, p \qquad (4.15)$$

$$xf_{ip} = \sum_j xl_{ij} \cdot \lambda f_{ipj} \qquad \forall i, p \qquad (4.16)$$

$$Af_{ip} = \sum_j Al_{ij} \cdot \lambda f_{ipj} \qquad \forall i, p \qquad (4.17)$$

$$\sum_j \lambda f_{ipj} = 1 \qquad \forall i, p \qquad (4.18)$$

In Equations 4.13 - 4.15 and 4.16 - 4.18, the starting and finishing cut-points are calculated along with the areas that lie below them. Parameters xl_{ij} and Al_{ij} define the piecewise linear points used, with xl_{ij} being the abscissa and Al_{ij} the ordinate. Variables λs_{ip}, λf_{ip} are of SOS2 type, so that at most two adjacent of them can be non-zero at the same time.

A representation of that function for *IEX* is shown in Figure 4.1. For *HIC* the only difference is due to the fact that σ_i is equal to 0.22. The actual non-linear function is shown with the solid line, while the piecewise linear approximation is denoted by dotted line connecting diamond points.

Having calculated the cut-points and the areas that lie below them, the concentration factor has to also be calculated as well. But as described above for the mass balances, we need $\overline{lnCF_{ip}}$. The function

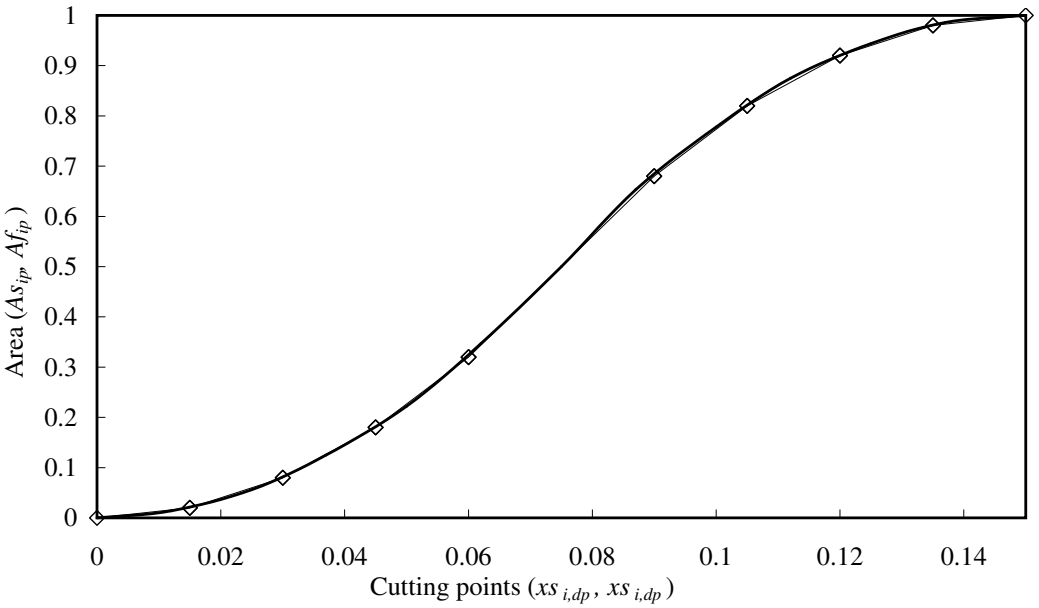

FIGURE 4.1: Linearisation 1: Areas As_{ip}, Af_{ip} vs. Cutting points $xs_{i,dp}$, $xf_{i,dp}$ for *IEX*

relating CF_{ip} and $lnCF_{ip}$ is graphically shown in Figure 4.2 and the mathematical expression is described by Equations 4.19 - 4.23.

$$\overline{lnCF_{ip}} = \sum_k \beta_{ik} \cdot \mu_{ipk} + sl_{ip} \qquad \forall i, p \tag{4.19}$$

$$\sum_j Al_{ij} \cdot \lambda f_{ipj} - \sum_j Al_{ij} \cdot \lambda s_{ipj} = \sum_k \alpha_{ik} \cdot \mu_{ipk} \qquad \forall i, p \tag{4.20}$$

$$\sum_k \mu_{ipk} = 1 \qquad \forall i, p \tag{4.21}$$

$$sl_{ip} \leq -ln(D) \cdot (1 - E_i) \qquad \forall i, p \tag{4.22}$$

$$-ln(D) \cdot E_i \geq \overline{lnCF_{ip}} \geq ln(D) \cdot E_i \qquad \forall i, p \tag{4.23}$$

where D is a small number.

Parameters β_{ik} and α_{ik} define the piecewise linear approximations used, with α_{ik} being the abscissa and β_{ik} the ordinate. Variables μ_{ipk} are of a SOS2 type. In Equation 4.20, the first term refers to the area that lies

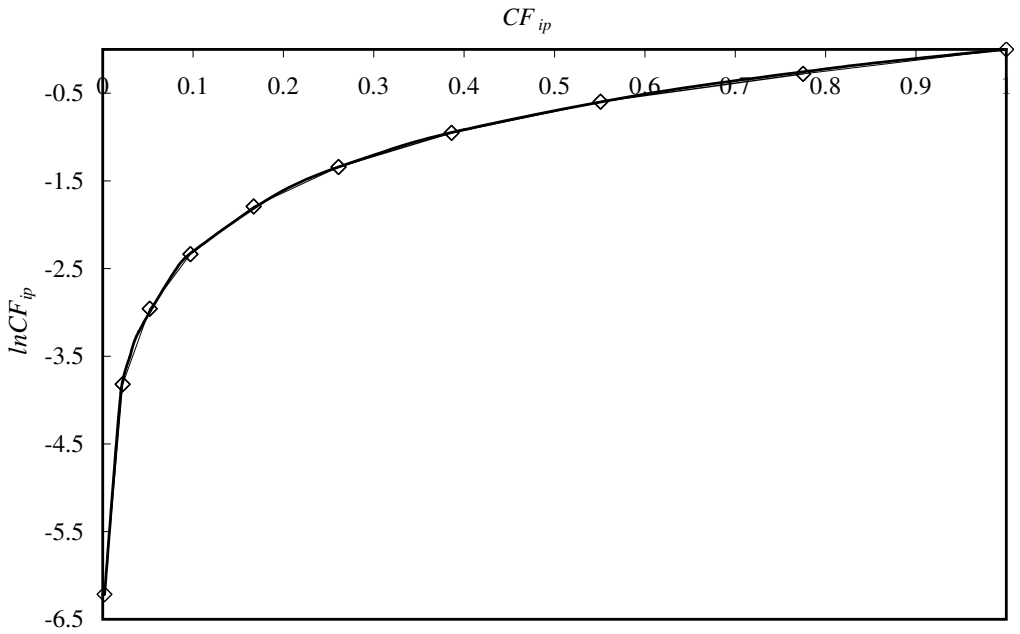

FIGURE 4.2: Linearisation 2: $lnCF_{ip}$ vs. Concentration factor CF_{ip}

below the finishing cut-point, the second term to the area that lies below the starting cut-point and the difference is concentration factor, CF_{ip}. Finally, slack variables, sl_{ip}, are imposed so that $\overline{lnCF_{ip}}$ is equal to zero when no separation takes place (i.e. $E_i = 0$) through Constraints 4.22 and 4.23.

From equation 4.12, the final concentrations of all proteins in the mixture are calculated. This nonlinear equation can be linearised in a similar way as described above. Parameters γ_l and δ_l are the values of the ordinate and abscissa, respectively, and along with SOS2 variables, ν_{pl}, define the exponential piecewise linear approximation (see figure 4.3) described by:

$$\sum_i \overline{lnCF_{ip}} = \sum_l \gamma_l \cdot \nu_{pl} \qquad \forall p \tag{4.24}$$

$$\xi_p = \sum_l \delta_l \cdot \nu_{pl} \qquad \forall p \tag{4.25}$$

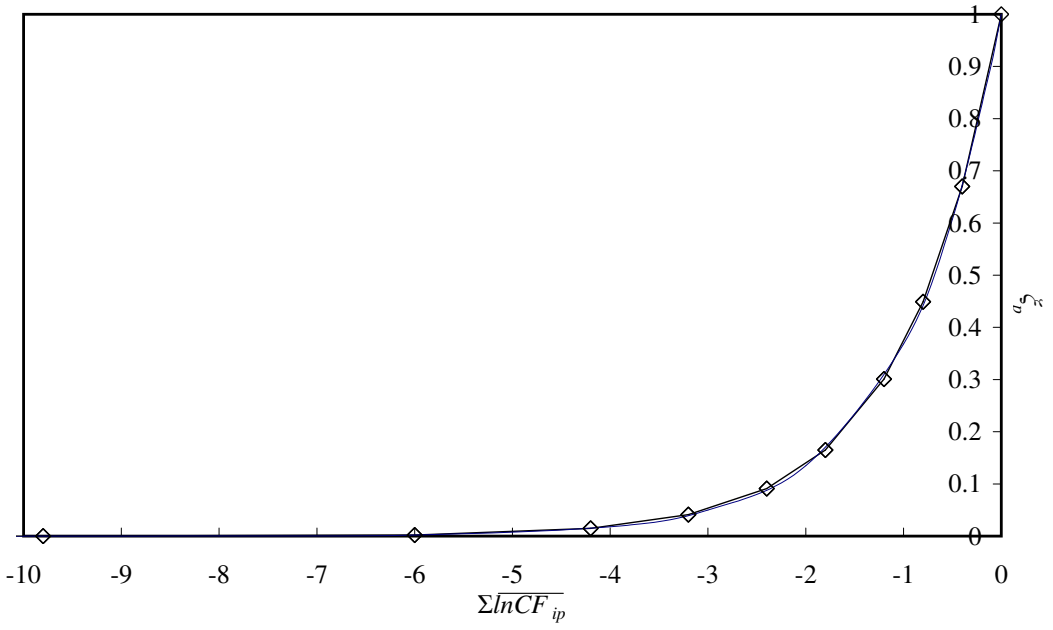

FIGURE 4.3: Linearisation 3: ξ_p vs. $\sum_i \overline{lnCF_{ip}}$

$$\sum_l \nu_{pl} = 1 \qquad \forall p \tag{4.26}$$

4.3 System definition

Below, a summary of the mathematical proposed model is presented. The objective is to minimise the overall number of chromatographic steps.

$$Min \qquad S = \sum_i E_i$$

subject to:

- Equations 4.2 - 4.3 for the calculation of the shifted cut-points
- Equations 4.13 - 4.18, where cut-points $xs_{i,dp}$, $xf_{i,dp}$ along with the areas As_{ip}, Af_{ip} are calculated.

- Equations 4.19 - 4.23, where CF_{ip} against $\overline{lnCF_{ip}}$ is approximated.
- Equations 4.24 - 4.26, where ξ_p is calculated.
- Equation 4.12, where the mass balance is described.
- Equations 4.5 and 4.6, where the purity and recovery specifications are enforced.

The overall problem is formulated as a mixed integer linear programming (MILP) model. Trying to solve the full examples resulted in no solutions for the two large examples and an optimal solution in a relatively small CPU time (35s) for the first example. Although we were able to obtain a solution for the first example, we still need to apply the two-stage solution approach as presented in the Chapter 3, where first a screening MILP [78] is solved, in order to determine candidate chromatographic steps, followed by the proposed MILP over the reduced set of alternatives (determined by the first stage).

4.4 Results and discussion

In this section, the solutions of the proposed model are analysed. The methodology was tested with three examples modelled in the GAMS 22.8 [95]. Solutions for the MILP and MINLP models were obtained using the CPLEX (optcr 1 %) and BARON solvers respectively, on a Dell Desktop Core Duo 3.25GB RAM 3.16GHz machine.

4.4.1 Example 1

This first example is based on experimental as shown in Section 3.6.1. The resulting mathematical model involves 661 constraints, 521 continuous variables, and 427 binary variables and was solved in 0.3 s. The optimal solution is presented in Figure 4.4, where the value above the

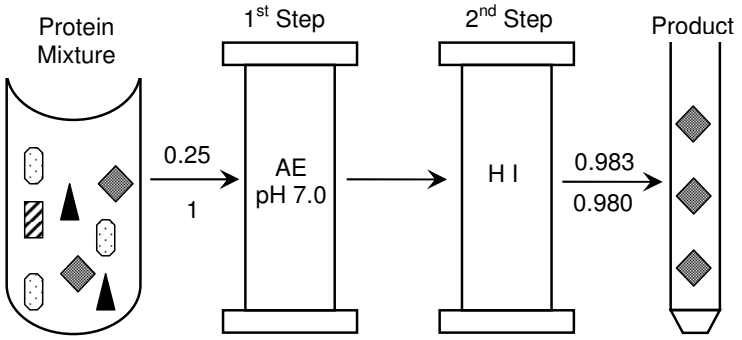

FIGURE 4.4: Optimal flowsheet for purification of protein mixture (example 1)

arrow denotes the purity, and below refers to the recovery achieved. The model was able to identify a solution that achieves purity $sp = 0.983$ and recovery $fr = 0.98$ for the target protein, for which two steps are required: *AE7*, *HI*. The cut-points for $AE7$ were: $xs_{AE7,dp} = 0.004$ and $xf_{AE7,dp} = 0.143$ and for HI: $xs_{HI,dp} = 0.002$ and $xf_{HI,dp} = 0.220$. In Figure 4.5, the actual cut-points selected from the model are presented on the chromatograms.

4.4.2 Example 2

This example utilises data available on [2] as shown in Section 3.6.2.

This example involves 2835 constraints, 2224 continuous variables, and 1824 binary variables and was solved in 4.2 s. The optimal solution is presented in Figure 4.6, where a purity of $sp = 0.951$ and a recovery of $fr = 0.94$ is achieved after three steps: *AE6.5*, *AE8.5*, *HI*. The cut-points for $AE6.5$ were: $xs_{AE6.5,dp} = 0.012$ and $xf_{AE6.5,dp} = 0.147$, for $AE8.5$ were: $xs_{AE8.5,dp} = 0.013$ and $xf_{AE8.5,dp} = 0.150$ and for HI: $xs_{HI,dp} = 0$ and $xf_{HI,dp} = 0.198$.

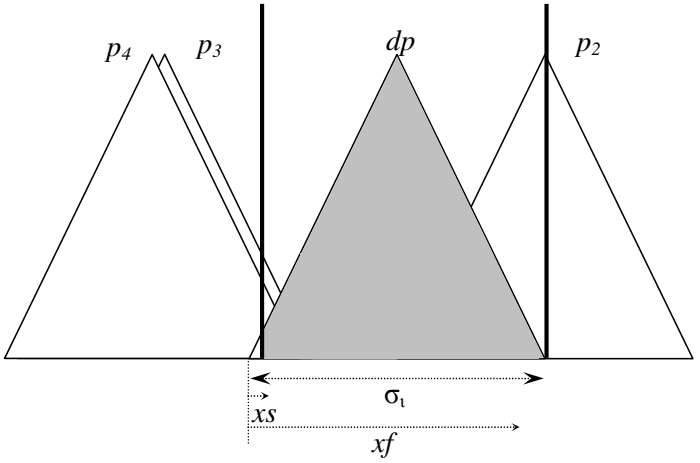

(a) *AE7*

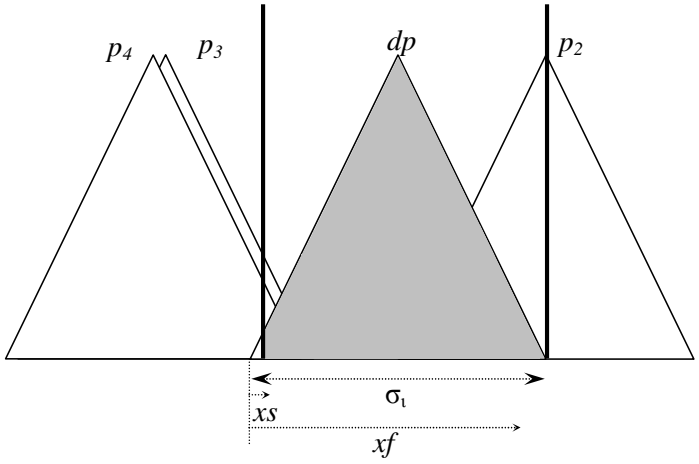

(b) *HI*

FIGURE 4.5: Solution of example 1

4.4.3 Example 3

For our final example, data taken from [79] was used as presented in Section 3.6.3. This example is the largest one of the three and the more complex in terms of separation potential. It involves 13 proteins and all the necessary information are presented in Table 3.3. There are 11 candidate chromatographic steps as presented in example 1.

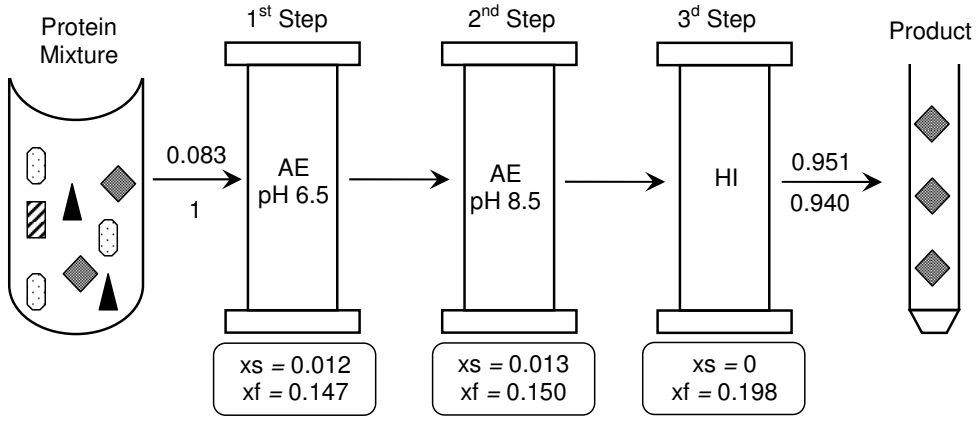

FIGURE 4.6: Optimal flowsheet for purification of protein mixture (example 2)

It takes 7.3 s to obtain the optimal solution and includes 3451 constraints, 2215 continuous variables, and 2705 binary variables. The optimal solution achieved, is presented in Figure 4.7. Two steps are required: *AE7*, *CE4*, *HI* in order to achieve a purity of $sp = 0.937$ and a recovery of $fr = 0.903$ for the target protein. The cut-points for $AE7$ were: $xs_{AE7,dp} = 0.013$ and $xf_{AE7,dp} = 0.134$, for $CE4$ were: $xs_{CE4,dp} = 0.007$ and $xf_{CE4,dp} = 0.133$ and for HI: $xs_{HI,dp} = 0.013$ and $xf_{HI,dp} = 0.212$.

4.4.4 Comparative results

In an effort to demonstrate the benefits of the proposed model, a comparison with the MINLP approach introduced in Chapter 3 is undertaken. The MILP model was solved for five, ten and fifteen internal knots for the piecewise linear approximation. All computational results are summarised in Table 4.1, For all examples, ten internal knots were sufficient to obtain the optimal solutions which was the same as the ones determined by the MINLP described in Chapter 3. Using five

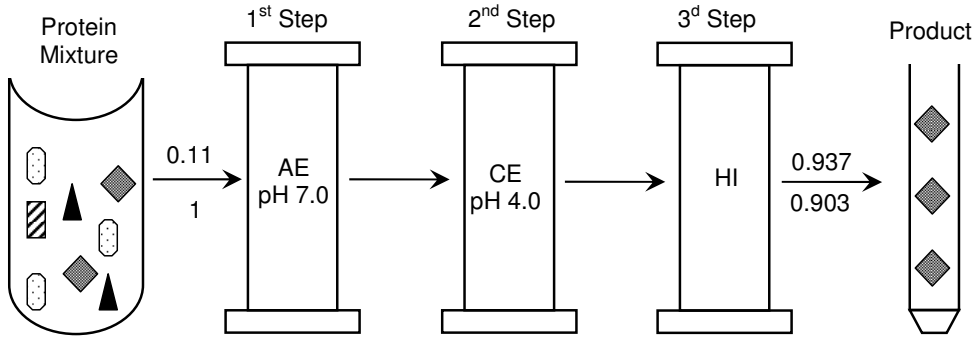

FIGURE 4.7: Optimal flowsheet for purification of protein mixture (example 3)

knots was not adequate for the first two examples, since it resulted in sub-optimal solutions.

Moreover, in terms of CPU savings the MILP model was able to solve all examples in less than 10 seconds as shown in Figure 4.8. It is quite interesting, that although the MINLP model has fewer constraints and has even six times fewer binary variables, it is even seventy times less efficient than the proposed MILP.

4.5 Conclusions

In this Chapter, a novel MILP model formulation has been presented for tackling the problem of downstream protein processing synthesis. This model simultaneously optimises the process flowsheet composed of distinct chromatographic steps and determines the specific cut-points for product collection by allowing product losses. Further comparisons with previously published models underlined the efficiency of the proposed formulation, which was able to obtain the optimal solutions with significantly less computational time required.

TABLE 4.1: Computational statistics

example	model	NoC[a]	NoCV/NoBV [b]	CPU (s)	obj. value
1	MINLP[c]	237	101/63	2.7	2
	MILP[d]	461	321/227	0.1	3
	MILP[e]	661	521/427	0.3	2
	MILP[f]	861	721/627	0.5	2
2	MINLP[c]	1188	499/306	249	3
	MILP[d]	1980	1369/969	0.9	5
	MILP[e]	2835	2224/1824	4.2	3
	MILP[f]	3690	3079/2679	5.2	3
3	MINLP[c]	1454	605/375	501	3
	MILP[d]	2411	1665/1175	2.7	4
	MILP[e]	3451	2705/2215	7.3	3
	MILP[f]	4491	3745/3255	117	3

[a] No of Constraints
[b] No of Continuous Variables/ No of Binary Variables
[c] Chapter 3
[d/e/f] 5 knots/10 knots/15 knots

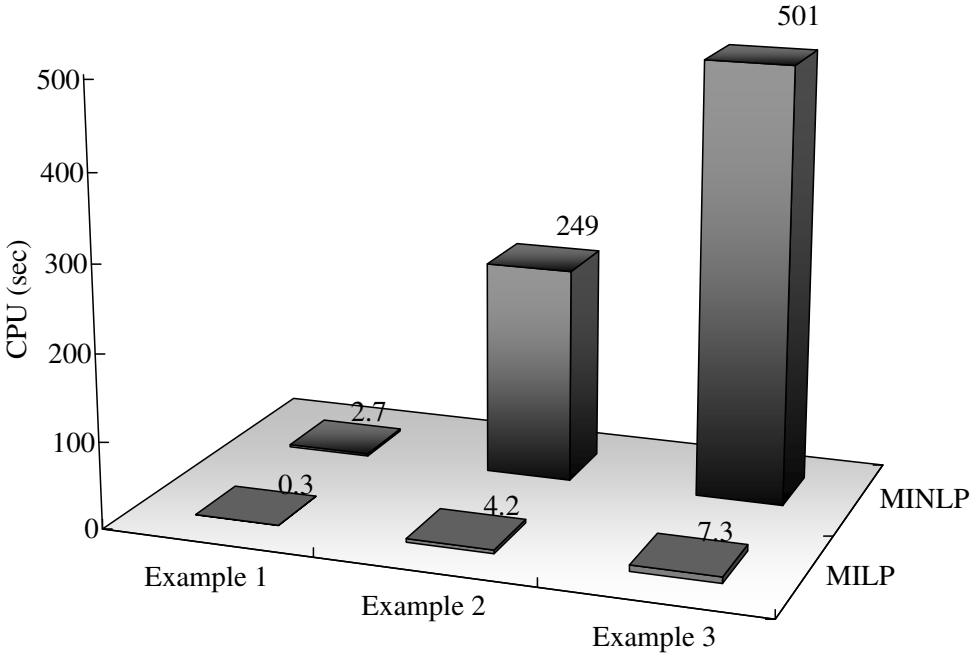

FIGURE 4.8: Comparison between MINLP presented in Chapter 3 and proposed MILP

Even though there has been a significant improvement in computational efficiency, still the model can not cope with the large examples that include up to 13 protein and 21 candidate steps. In the next Chapter an alternative approach is used in order to improve solution robustness and avoid the two-stage solution approcah that was used here.

Chapter 5

An alternative MILP formulation for the synthesis of protein purification processes

In this Chapter, we present an alternative MILP model for downstream process synthesis. Instead of using piecewise linear approximation as in the previous Chapter, we now use discrete recovery levels for the product.

5.1 Introduction

In the previous Chapter we approximated the non-linearities that were present in the model and although the efficiency of the model improved significantly, the two-stage solution was not avoided for the larger examples. The objective was to be able to apply the developed models in large mixtures that contain up to 20 contaminants.

The use of discrete recovery levels gives us the opportunity to take advantage of the simplicity of the resulting linear models presented below and obtain the optimal flowsheet in very small CPU times.

The basic assumption of the model is that each chromatographic peak can be represented by an isosceles triangle. Again, the only necessary input for this model are the mathematical correlations that relate the retention time with the relevant physicochemical properties, responsible for separation. The core for the modelling of chromatographic separations remains the same as described in detail in Chapter 3.

5.2 Mathematical Models

In this section two alternative models will be described for solving the problem of downstream protein processing.

5.2.1 Model 1

The objective function is to minimise the total number of steps from a set of alternatives. Binary variable, Ei, is activated when a chromatographic step i is selected.

Objective Function:

$$Min \qquad S = \sum_{i} E_i \tag{5.1}$$

The mass of each protein that remains after the first step is indicated by equation 5.2. If the first technique is selected at starting recovery level, *ls*, and finishing recovery level, *lf*, then the mass of protein p is reduced, otherwise it is equal to the initial mass. Calculation of concentration factors, CF_{ip}, is shown in Appendix C.

$$m_{1p} = \sum_{ls} \sum_{lf} CF_{1,p,ls,lf} \cdot \lambda_{1,ls,lf} \cdot mo_p + (1 - \sum_{ls} \sum_{lf} \lambda_{1,ls,lf}) \cdot mo_p \qquad \forall p \tag{5.2}$$

Similarly, in the following constraints, the mass of each protein for $i \geq 2$ is calculated. If step i is selected at starting recovery level ls and finishing recovery level lf, the mass of protein p is calculated by equation 5.3.

$$m_{ip} = \sum_{ls} \sum_{lf} CF_{i,p,ls,lf} \cdot m^1_{i-1,p,ls,lf} + m^2_{i-1,p} \qquad \forall p, i \geq 2 \tag{5.3}$$

If step i is selected, $m^1_{i-1,p,ls,lf}$ is activated, otherwise $m^2_{i-1,p}$ is valid.

$$m_{i-1,p} = \sum_{ls} \sum_{lf} m^1_{i-1,p,ls,lf} + m^2_{i-1,p} \qquad \forall p, i \geq 2 \tag{5.4}$$

$$m^1_{i-1,p,ls,lf} \leq mo_p \cdot \lambda_{i,ls,lf} \qquad \forall p, i \geq 2 \tag{5.5}$$

$$m^2_{i-1,p} \leq mo_p \cdot (1 - \sum_{ls} \sum_{lf} \lambda_{i,ls,lf}) \qquad \forall p, i \geq 2 \tag{5.6}$$

The following constraint ensures that for each i only one starting recovery level ls and one finishing recovery level lf are activated, if step i is selected.

$$\sum_{ls} \sum_{lf} \lambda_{i,ls,lf} \leq E_i \qquad \forall i \tag{5.7}$$

In the two final constraints, purity, sp, and recovery, fr, specifications are enforced.

$$m_{i,dp} \geq sp \cdot \sum_{p'} m_{ip'} \qquad \forall i = I \tag{5.8}$$

$$m_{i,dp} \geq fr \cdot mo_{dp} \qquad \forall i = I \tag{5.9}$$

5.2.2 Model 2

The objective function is to minimise the overall number of steps from a set of alternatives. Binary variable E_i is activated when a chromatographic step i is selected.

Objective Function:

$$Min \qquad S = \sum_{i} E_i \tag{5.10}$$

The mass of each protein that remains after the first step is indicated by equation 5.11. If the first technique is selected at starting recovery level *ls* and finishing recovery level *lf*, then the mass of protein p is reduced, otherwise it is equal to initial mass. $As_{1,p,ls}$ is the area that lies below the starting cut point and $Af_{1,p,lf}$ is the area that lies below the finishing cut point.

An example case on how the areas are related with the concentration factors is shown in Figure 5.1. The first triangle considers the case where only starting cut-point is considered and the shaded are represents the amount of contaminant remaining after the chromatographic technique has been applied ($As_{i,p,ls}$). The second triangle represents the case that only finishing cut-point is considered ($Af_{i,p,lf}$) and the final case is where their difference is taken into account ($Af_{i,p,lf} - As_{i,p,ls}$). Calculation of $As_{i,p,ls}$, $Af_{i,p,lf}$ along with concentration factors CF_{ip} is shown in Appendix C.

$$m_{1p} = \left[\sum_{lf} Af_{1,p,lf} \cdot \mu_{1,lf} - \sum_{ls} As_{1,p,ls} \cdot \lambda_{1,ls}\right] \cdot mo_p + (1 - E_i) \cdot mo_p \qquad \forall p \tag{5.11}$$

In the following constraint, the mass of each protein for $i \geq 2$ is calculated. If step i is selected at starting recovery level *ls* and finishing

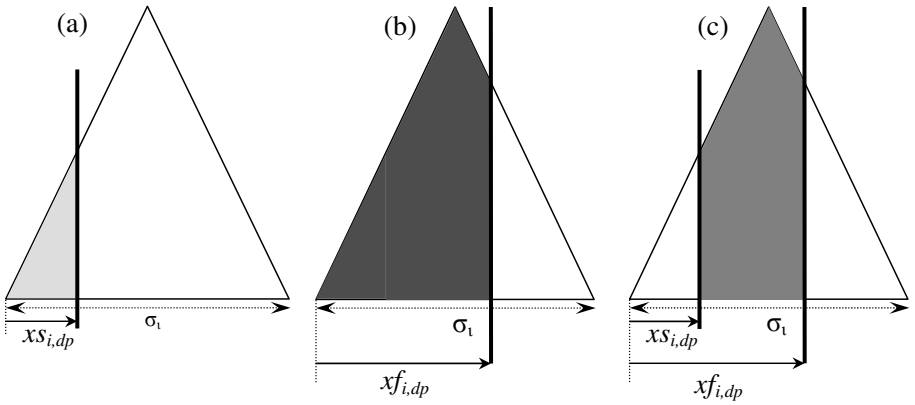

FIGURE 5.1: Representation of areas

recovery level *lf*, the mass of protein p is calculated by Equation 5.12 where the first and second term of Equation 5.12 are active. These two terms are similar to first term of Equation 5.3. The third term represents the case in which chromatographic step i has not been chosen, hence protein is not reduced.

$$m_{ip} = \sum_{lf} Af_{i,p,lf} \cdot mf^1_{i-1,p,lf} - \sum_{ls} As_{i,p,ls} \cdot ms^1_{i-1,p,ls} + m^2_{i-1,p} \qquad \forall p, i \geq 2 \tag{5.12}$$

Similarly, in Equation 5.13 the mass of each protein p is calculated at step *i-1*.

$$m_{i-1,p} = \sum_{lf} mf^1_{i-1,p,lf} - \sum_{ls} ms^1_{i-1,p,ls} + m^2_{i-1,p} \qquad \forall p, i \geq 2 \tag{5.13}$$

In equations 5.14 - 5.16, we have the calculation of terms $mf^1_{i-1,p,lf}$, $ms^1_{i-1,p,ls}$, $m^2_{i-1,p,lf}$ which are activated depending on the selection of chromatographic step *i*.

$$mf^{1}_{i-1,p,lf} \leq mo_p \cdot \mu_{i,lf} \qquad \forall p, i \geq 2 \qquad (5.14)$$

$$ms^{1}_{i-1,p,ls} \leq mo_p \cdot \lambda_{i,ls} \qquad \forall p, i \geq 2 \qquad (5.15)$$

$$m^{2}_{i-1,p} \leq mo_p \cdot (1 - E_i) \qquad \forall p, i \geq 2 \qquad (5.16)$$

The following two constraints ensure that binary variables $\mu_{i,lf}$ and $\lambda_{i,ls}$ are active only when a chromatographic step i is selected ($E_i = 1$).

$$\sum_{lf} \mu_{i,lf} \leq E_i \qquad \forall i \qquad (5.17)$$

$$\sum_{ls} \lambda_{i,ls} \leq E_i \qquad \forall i \qquad (5.18)$$

In the two final constraints, purity, *sp*, and recovery, *fr*, specifications are enforced.

$$m_{i,dp} \geq fp \cdot \sum_{p'} m_{ip'} \qquad \forall i = I \qquad (5.19)$$

$$m_{i,dp} \geq fr \cdot mo_p \qquad \forall i = I \qquad (5.20)$$

5.2.3 Discretisation method

As mentioned above the important item for these models is the discrete recovery levels. In Figure 5.2, a chromatogram is represented by an isosceles triangle and the peak width is discretised in a number of levels. Given the recovery level selected the relevant concentration factor will be calculated as presented in Appendix C.

In an effort to decide how many discrete levels should be provided in advance, for both cut points $xs_{i,dp}$, $xf_{i,dp}$ 5 and 10 recovery levels were considered. ($xs_{i,dp}$ can vary from 0 to $\sigma_i/10$ and ($xf_{i,dp}$ can vary from $\sigma_i/2$ to σ_i. The values used for the discretisation of both starting and finishing cut-points are presented in Appendix C.

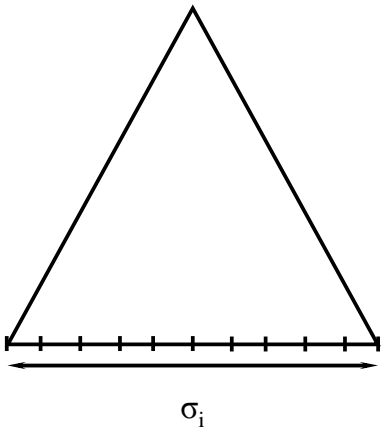

FIGURE 5.2: Representation of a chromatogram with discrete recovery levels

5.3 Results and discussion

In this section, we analyse the solutions of the proposed models. The problem is solved for two scenarios; one having $xs_{i,dp} = 0$ and the other one having $xs_{i,dp} = free$. For scenario 1, only $xf_{i,dp}$ is considered and for scenario 2 both $xs_{i,dp}$ and $xf_{i,dp}$ will be optimised.

Later, the solutions of the two models are compared with the solutions from the MINLP model proposed by our group [3]. The methodology is tested with three examples modeled in GAMS 22.8 [95]. Solutions are obtained using CPLEX solver for the MILP model and Baron Solver [97] for the MINLP model, on a Dell Desktop Core Duo 3.25GB RAM 3.16GHz machine.

5.3.1 Examples

For all the examples, the physicochemical properties as well as the initial protein concentration of the mixture are given in Appendix A.

All examples are based on literature data and they are the same ones presented in the previous two chapters.

5.3.2 Scenario 1: $xs_{i,dp} = 0$

In Table 5.1 the solutions from all examples and for xs_{ip}=*0* are presented. First, the MINLP model described in Chapter 3 is presented followed by the two MILP models proposed here. Both MILP models were solved using 5 and 10 discrete points.

For example 1 and 2, solution obtained from the MINLP model agreed with the ones from the MILP models. An interesting observation from Table 5.1 is that for some cases, models 1 and 2 do not select the same steps and this can happen because there is more than one solution that can achieve the purity and recovery levels required (degeneracy).

For example 3, the MINLP selects 3 steps to achieve the requirements while none of the MILP models can do that. To further investigate this, example 3 was solved using 15, 20 and 25 discrete points for both $xs_{i,dp}$ and $xf_{i,dp}$. For 25 discrete points, 3 steps (*AE8, CE4, HI*) were necessary to achieve a purity of $fr = 0.931$ and a recovery of $fr = 0.90$.

5.3.3 Scenario 1: $xs_{i,dp} = free$

For this scenario, starting cut-point xs_{ip} is not fixed, but is a decision variable. As expected, the purification flowsheet is improved with fewer steps required as clearly presented in Table 5.2.

The most significant result was reported in example 2, where the number of steps is reduced from five to two. For this case, just 5 discrete points were enough to achieve the same solutions as these obtained from the MINLP.

5.3.4 Comparative results and computational statistics

In this section, the proposed models are compared with the MINLP model presented in Chapter 3 in terms of size and CPU time. In Table 5.3, CPU times are presented for all examples using the two proposed MILPs for the scenarios described above and the MINLP.

In Figure 5.3, the CPU times along with computational statistics are presented. For the MILP models the full size example is solved, while for the MINLP the reduced problem is solved and yet the MINLP requires the most of CPU time to obtain the solution. Moreover, the MINLP has less binary and continuous variables but still takes more CPU time to determine the optimal solution. Comparing the first MILP with second, it is obvious that the second one is more efficient in computational time. Binary and continuous variables along with the number of constraints decrease significantly in the second MILP model proposed, hence CPU time decreases as well.

TABLE 5.1: Solutions for all models and for $xs_{i,dp} = 0$

Example	Model	S	*lf*	sp	fr
1	MINLP	3 (*AE7, AE8, HI*)	N/A	99.9	99.8
	MILP1[a]	3 (*AE5, AE8, HI*)	5, 5, 5	99.9	100
	MILP1[b]	3 (*AE6, AE8, HI*)	9, 9, 10	99.9	98.8
	MILP2[a]	3 (*AE6, AE8, HI*)	5, 5, 5	99.7	100
	MILP2[b]	3 (*AE5, AE8, HI*)	9, 9, 9	99.9	98.2
2	MINLP	5 (*AE6, AE6.5, AE7.5, AE8.5, HI*)	N/A	94.1	94.6
	MILP1[a]	5 (*AE6, AE6.5, AE7, AE8.5, HI*)	5, 5, 5, 5, 5	95.3	100
	MILP1[b]	5 (*AE6.5, AE7, AE8.5, CE4, HI*)	7, 10, 10, 10, 10	95.3	94.5
	MILP2[a]	5 (*AE6.5, AE7, AE8, AE8.5, HI*)	5, 5, 5, 5, 4	95.1	96.9
	MILP2[b]	5 (*AE6, AE6.5, AE8.5, CE4, HI*)	9, 8, 10, 10, 10	94.9	96.9
3	MINLP	3 (*AE7, CE4, HI*)	N/A	93.1	90
	MILP1[a]	4 (*AE8,CE4, CE6, HI*)	4, 4, 5, 4	93.4	90.9
	MILP1[b]	4 (*AE6,AE8, CE4, HI*)	10, 10, 6, 10	95.9	90.1
	MILP2[a]	4 (*AE8,CE4, CE6, HI*)	4, 4, 5, 5	93.5	93.9
	MILP2[b]	4 (*AE6,AE8, CE4, HI*)	10, 6, 10, 10	93.6	90.1

[a] 5 discrete points
[b] 10 discrete points

TABLE 5.2: Solutions for all models and for $xs_{i,dp} = free$

Example	Model	S	*ls*	*lf*	sp	fr
1	MINLP	2 (*AE7, HI*)	N/A	N/A	98.9	98
	MILP1[a]	2 (*AE7, HI*)	3, 1	5, 5	98.1	99.5
	MILP1[b]	2 (*AE7, HI*)	3, 1	9, 10	98	99.3
	MILP2[a]	2 (*AE7, HI*)	3, 3	5, 5	98.1	99
	MILP2[b]	2 (*AE7, HI*)	3, 2	9, 10	98.1	99.3
2	MINLP	3 (*AE6.5, AE8.5, HI*)	N/A	N/A	94.4	94.6
	MILP1[a]	3 (*AE6.5, AE8.5, HI*)	5, 3, 1	4, 5, 5	95.4	94.3
	MILP1[b]	3 (*AE6.5, AE8.5, HI*)	8, 10, 10	8, 10, 10	96	94.3
	MILP2[a]	3 (*AE6.5, AE8.5, HI*)	1, 5, 6	9, 10, 11	94.3	94.3
	MILP2[b]	3 (*AE6.5, AE8.5, HI*)	1, 5, 6	9, 10, 11	94.3	94.3
3	MINLP	3 (*AE8, CE4, HI*)	N/A	N/A	93.1	90
	MILP1[a]	3 (*AE8, CE4, HI*)	2, 3, 2	4, 4, 5	93.2	93.2
	MILP1[b]	3 (*AE8, CE4, HI*)	5, 4, 5	7, 8, 9	94.6	90.6
	MILP2[a]	3 (*AE7, CE4, HI*)	5, 5, 1	4, 4, 5	93.2	90
	MILP2[b]	3 (*AE8, CE4, HI*)	2, 4, 8	8, 7, 10	93.1	90.1

[a] 5 discrete points
[b] 10 discrete points

TABLE 5.3: Comparative results for all models for both $xs_{i,dp} = 0$ and $xs_{i,dp} = free$

		$xs_{i,dp} = 0$		$xs_{i,dp} = free$		
Example	Model	S	CPU (s)	S	CPU (s)	NoBV/NoCV/NoC[a]
	MINLP	3	9	2	3.1	63/101/237
1	MILP1[b]	3	0.2	2	0.5	286/1074/1138
	MILP1[c]	3	1.7	2	1.2	1111/4074/4138
	MILP2[b]	3	0.2	2	0.1	121/485/600
	MILP2[c]	3	1.1	2	0.7	231/885/989
	MINLP	5	233	3	277	306/499/1188
2	MILP1[b]	5	2.3	3	16	536/4859/5073
	MILP1[c]	5	10.3	3	661	2111/18370/18573
	MILP2[b]	5	3.9	3	14.2	231/2170/2574
	MILP2[c]	5	15.2	3	2.2	441/3970/4374
	MINLP	3	285	3	505	375/605/1454
3	MILP1[b]	4	0.5	3	5.4	1437/4286/3513
	MILP1[c]	4	7.4	3	201	1111/13263/3667
	MILP2[b]	4	0.5	3	1.6	121/1574/1858
	MILP2[c]	4	1.7	3	3.7	231/2874/3169

[a] Number of binary variables/ continuous variables/ constraints
[b] 5 discrete points
[c] 10 discrete points

5.4 Conclusions

In this Chapter, two novel novel MILP model formulations have been presented for tackling the problem of downstream protein processing synthesis. This model simultaneously optimises the process flowsheet composed of distinct chromatographic steps and determines the specific cut-points for product collection by allowing product losses. Further comparisons with previously published models underlined the efficiency of the proposed formulation, which was able to obtain the optimal solutions with significantly less computational time required.

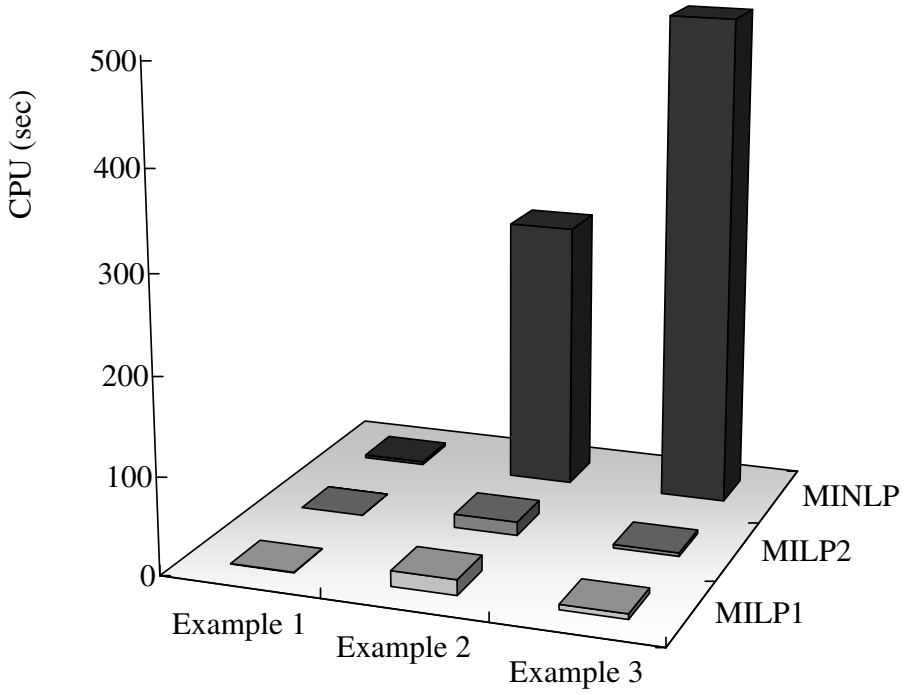

FIGURE 5.3: Comparison between MINLP [3] and proposed MILPs

Chapter 6

Computational experimentation using *gPROMS*

In this Chapter, the main mechanistic methodologies for chromatographic processes will be discussed, followed by the specific model implemented in *gPROMS*, along with the results obtained in an effort to validate findings obtained in previous Chapters.

6.1 Introduction

As already mentioned, chromatography is a powerful separation method that has been used for decades, initially as an analytical method and later on as a purification method for complex mixtures. It is evidents from Chapter 2 that a significant amount of research has been done in an effort to synthesise and operate chromatographic steps in the best possible way.

To do that, many researchers focused on mechanistic methods, where the phenomena that take place into the column are considered. This

has not been a simple task since the process itself is quite complex, but mainly because of the interactions between proteins within the mixture. Several mathematical models are available in the literature and are generally classified into two categories: plate models and rate models. These models can be very powerful given that the necessary parameters are known. In the next section, the main types of plate and rate models are reviewed.

6.1.1 Plate model

This is the simplest model for chromatography and is based in the assumption that the column is divided into a number of separate layers, called theoretical plates. The concept of theoretical plates was first used in distillation processes but was soon adapted by Martin and Synge [13]. Later on, other researchers [62, 98] used this type of model to optimise ion exchange chromatography. The limitations of the plate model are that it does not take into account adsorption kinetics, therefore can not describe a multicomponent mixture where protein interactions are significant.

6.1.2 Rate models

Rate models consider non-equilibrium conditions in the column and take into account the contributions of mass transfer mechanisms. There are many variations of the rate model such as the ideal model, the equilibrium dispersive model, the transport dispersive model, the lumped kinetic and the general rate model [99]. In the next section, some of these models are discussed in detail.

6.1.2.1 Ideal model

The ideal model is the simplest model, where the chromatographic column is considered as one dimensional, hence the bed is considered radially homogeneous. Moreover, the mobile and stationary phase are always in equilibrium [100]. The mass balance for each component p in each bed i is described in Equation 6.1.

$$\frac{\partial C_{ip}}{\partial t} + F \cdot \frac{\partial C s_{ip}}{\partial t} + u \cdot \frac{\partial C_{ip}}{\partial x} = 0 \quad \forall i, p \tag{6.1}$$

where the first term is the rate of accumulation of component p in step i within the particle, the second term is the rate of accumulation of component p in step i in the mobile phase, the third is the rate transport through convection, F is the phase ratio, u is the intersitial velocity, calculated by the following equation.

$$u = \frac{4 \cdot F_c}{\epsilon_B \cdot D^2} \tag{6.2}$$

where F_c is the eluent flowrate, ϵ_B is the bed voidage and D is the column diameter.

This model is still used but mainly for single columns or binary mixtures, mainly because it can accommodate protein interactions in complex mixtures [42, 101].

6.1.2.2 Equilibrium-dispersive model

In this case, the mass transfer is fast but not infinitely fast, therefore contributions due to non-linear equilibrium can be described by an apparent axial dispersion coefficient term Dax_{ip} [100]. The mass balance for each component p in each bed i is described in Equation 6.3.

Moreover the equilibrium dispersive model is based on the following assumptions:

- Packed bed is assumed to be isothermal and uniformly packed.
- Radial velocity is negligible.
- Concentration profiles are assumed to be one-dimensional.
- Diffusion coefficients of solutes in both mobile and stationary phase are considered.
- Adsorption equilibrium is supposed to be instantaneous and can be described by the axial dispersion term [100].

$$\frac{\partial C_{ip}}{\partial t} + F \cdot \frac{\partial Cs_{ip}}{\partial t} + u \cdot \frac{\partial C_{ip}}{\partial x} = Dax_{ip} \cdot \frac{\partial^2 C_{ip}}{\partial x^2} \quad \forall i, p \tag{6.3}$$

where last term is the rate of transport by axial dispersion and Dax_{ip} is the axial dispersion coefficient.

The equilibrium dispersive model is widely used in literature [47, 102, 103]. Teoh et al. [47], applied this model for a high performance liquid chromatography of an aromatic mixture of four components. Vaquez-Alvarez et al. [102], employed the same model for an ion exchange chromatography of a four protein mixture and Marcus et al. [103] for the separation of protein monomers from dimers.

Adsorption equilibria

The adsorption mechanism that describes the phenomena present inside the chromatographic column is mathematically expressed by an isotherm relationship. In the following paragraphs, some examples of isotherms are discussed.

Linear adsorption isotherm

This is the simplest theoretical isotherm used in the modelling of liquid chromatography. In this type of isotherm, the components in the mixture behave independently of each other. The solute concentration in the stationary phase, Cs_{ip}, is related to the one of the mobile phase, C_{ip}, with a constant, α_{ip}. The mathematical form for this isotherm is presented in Equation 6.4.

$$Cs_{ip} = a_{ip} \cdot C_{ip} \quad \forall i, p \tag{6.4}$$

Langmuir isotherm

This is the most widely used theoretical isotherm employed for modelling of chromatographic processes. The components are assumed to be adsorbed on fixed number of sites and each site may accept only one compound. There is no interaction between adsorbed compounds and a local equilibrium is assumed between the stationary and the mobile phase [100, 104].

The mathematical form for this isotherm is presented in Equation 6.5.

$$Cs_{ip} = \frac{a_{ip} \cdot C_{ip}}{1 + b_{ip} \cdot C_{ip}} \quad \forall i, p \tag{6.5}$$

where a_{ip} and b_{ip} are coefficient for each component p and each bed i.

Competitive Langmuir isotherm

When there is a multicomponent mixture, the amount of each component adsorbed at equilibrium is smaller than if that component was alone. The mathematical form for this isotherm is presented in Equation 6.6.

$$Cs_{ip} = \frac{a_{ip} \cdot C_{ip}}{1 + \sum_{p'} b_{ip'} \cdot C_{ip'}} \quad \forall i, p \tag{6.6}$$

6.1.2.3 General rate model

The general rate model is the most complex one because it takes into account all the phenomena that may influence the column such axial dispersion, external mass transfer, intraparticle diffusion and the adsorption kinetics. It is the most comprehensive model in literature, however it requires the determination of many parameters *a priori*. It consists of two partial differential equations. The first one is Equation 6.3 and the second one is the following equations where the mass balance for each component p in the pore phase is given.

$$\epsilon_p \cdot \frac{\partial Cp_{ip}}{\partial t} + (1-\epsilon_p) \cdot \frac{\partial Cs_{ip}}{\partial t} = \epsilon_p \cdot Dax_{ip} \cdot \left[\frac{1}{r^2} \frac{\partial}{\partial r} \left(r^2 \cdot \frac{\partial Cp_{ip}}{\partial r} \right) \right] \quad \forall i,p \tag{6.7}$$

where the first term is the rate of accumulation in the pore liquid, the second the rate of accumulation on the solid surface and the right hand side is related to the rate of radial diffusion. ϵ_p is the particle porosity.

For the second term of Equation 6.7 we need to calculate the rate of adsorption and this is why we need the following equation.

$$\frac{\partial Cps_{ip}}{\partial t} = ka_p \cdot (\Lambda_p - \sum_p Cps_{ip}) \cdot Cp_{ip} - kd_p \cdot Cps_{ip} \quad \forall i,p \tag{6.8}$$

where ka_p and kd_p are the adsorption and desorption rate constants for each component p, $\Lambda_p - \sum_p Cps_{ip}$ are the available free sites, where Λ_p is the adsorption saturation capacity for each component p.

6.1.3 Comparing chromatographic models

Plate and rate models were described in detail in the sections above. The plate model is able to predict elution profiles and was popular

when computational efficiency was limited. However, even at that time it was clear that the plate model had limited capabilities because of its simplicity. On the contrary rate models are very comprehensive models that can thoroughly describe the phenomena taking place in the column. In the two extremes, we have the ideal model and general rate model with the first one being simplistic and the last one being to detailed and difficult to accommodate because of the requirements in input parameters. The equilibrium dispersive model will be employed because it provides a sufficient understanding of the process and does not require so many parameters.

6.2 Model selection

After reviewing the several available mathematical models the decision was to use the equilibrium dispersive model. It has been proven to be efficient and less demanding in terms of necessary input parameters [44]. This type of model has been widely used in literature [47], [102] and was first described by Bellot and Condoret in 1991 [105].

The first equation is the material balance (Equation 6.3) as described earlier, along with the Langmuir isotherm as described in Equation 6.5. The initial and boundary conditions are given from Equations 6.9 - 6.11.

Initial Condition

$$C_{ip}|_{t_0,x} = 0 \quad \forall i, p, x \in (0, L) \tag{6.9}$$

Boundary Conditions

$$\frac{\partial C_{ip}}{\partial x}\Big|_{x=L} = 0 \quad \forall i, p \tag{6.10}$$

$$C_{ip}|_{x=0} = C_{ip}^{in} \quad \forall i \tag{6.11}$$

where for the first chromatographic step *i=1* $C_{ip}^{in} = Cfeed$ and $C_i^{in} = Cout(i-1) \quad \forall \quad i > 1$.

Since the system we are considering is a multicolumn one, the output of each chromatographic step becomes the input of the next. A graphical explanation of that is presented in Figure 6.1.

FIGURE 6.1: Mass flow in the multicolumn system

A shown in Figure 6.1 a new variable is introduced, C_{ip}^{out}, which is the amount of protein that is collected at the specific integral and is defined by Equation 6.12.

$$C_{ip}^{out} = \int_{tstart}^{tfinish} C_{ip}|_{x=L} dt \tag{6.12}$$

In Figure 6.2, the necessary intervals are presented. T_1 is the interval where the column is fed with the mixture, followed by T_2 in which no action takes place, but at its end the starting cut-point presented in Chapter 3 occurs and finally T_3 which is the collection interval and at its end is where finishing cut-point occurs.

Finally, the purity and recovery are calculated by Equations 6.13 and 6.14.

Calculation of purity

$$R_{ip} = \frac{C_{ip}^{out}}{C_{ip}^{in}} \forall i, p = dp \tag{6.13}$$

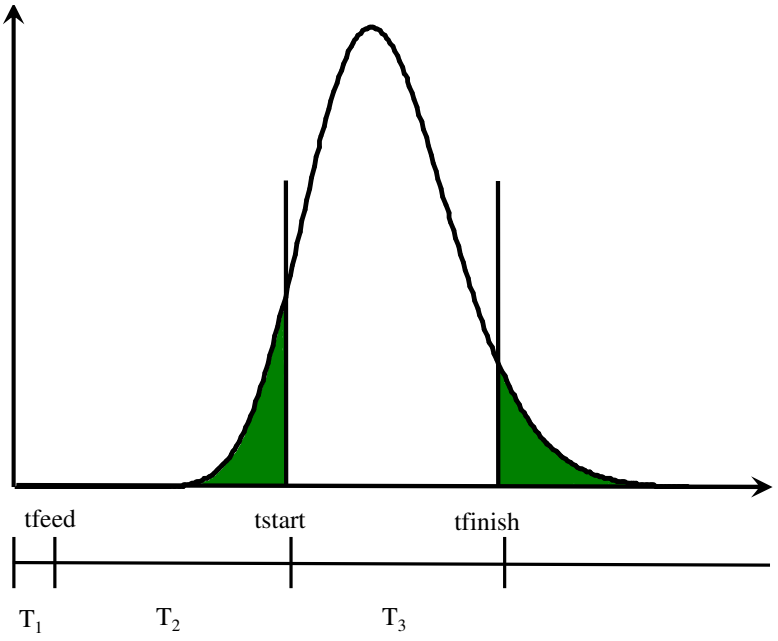

FIGURE 6.2: Graphical representation of a chromatogram and time integrals

Calculation of recovery

$$P_{ip} = \frac{C_{i,p}^{out}}{\sum_{p'} C_{ip'}^{out}} \forall i \tag{6.14}$$

6.3 Case study and numerical simulation

The case study considered is four-protein mixture and four candidate chromatographic steps. The data used for this model are shown in Tables 6.1 and 6.2. In the first table the data related to the column are presented. The values are the same as the ones from Teoh's paper [47].In Table 6.2 the Langmuir parameters, α_{ip}, β_{ip}, and the axial dispersion coefficients, Dax_{ip} are presented.

The system of equations described above was implemented using *gPROMS* [106]. The axial domain was discretized using 3rd order orthogonal collocation with 200 uniform elements (OCFEM). After running the simulation for each chromatographic step individually, the retention times

TABLE 6.1: Column parameters used for the simulation

Column Length	0.25 m
Phase ratio	0.38
Inertial velocity	0.027 m/s

TABLE 6.2: Langmuir parameters used for the simulation

	α_{ip}	β_{ip}	Dax_{ip}	α_{ip}	β_{ip}	Dax_{ip}
		Bed 1			Bed 2	
target protein	1100	0.09	5.1E-5	700	0.08	5.2E-5
contaminant 1	700	0.1	5.0E-5	1000	0.07	4.8E-5
contaminant 2	1300	0.08	5.2E-5	1350	0.09	4.9E-5
contaminant 3	1400	0.07	5.3E-5	1400	0.1	5.0E-5
		Bed 3			Bed 4	
target protein	850	0.07	9.0E-5	950	0.09	9.0E-5
contaminant 1	750	0.1	8.0E-5	1050	0.08	8.0E-5
contaminant 2	950	0.08	6.0E-5	850	0.1	6.0E-5
contaminant 3	1050	0.1	5.0E-5	1150	0.08	5.0E-5

for each component p as well as the relative peak width, σ_i, were calculated and the values are given in Table 6.3. Moreover, the output of *gPROMS* simulation for the individual columns are presented in Appendix D. In all four Figures, the chromatogram in red is the target protein and the ones in black, green and blue are considered to be the contaminants.

TABLE 6.3: Parameters used in GAMS

	tr_{ip}	σ_{ip}	tr_{ip}	σ_{ip}
	Bed 1		Bed 2	
target protein	3760	2910	2390	1970
contaminant 1	2390	1930	3420	2620
contaminant 2	4440	3420	4620	3440
contaminant 3	4780	3670	4780	3590
	Bed 3		Bed 4	
target protein	2840	2970	3170	3270
contaminant 1	2514	2530	3530	3620
contaminant 2	3230	2750	2890	2500
contaminant 3	3590	2780	3930	3010

Using the data presented above, we were able to run the MINLP and MILP models presented in Chapter 3, 4 and 5. Purity and recovery requirements are set to 99 % and 97 % respectively.

6.4 Results and Discussion

6.4.1 GAMS

The MINLP model described in Chapter 3 along with the MILP models described in Chapters 4 and 5 were implemented in GAMS and solved, for a purity of $sp = 0.99$ and a recovery of $fr = 0.97$. For all models the chromatographic steps selected were: $Bed1$ and $Bed2$. The cut-points for all the models are presented in table 6.4.

Table 6.4: Cut-points resulting from GAMS models

	Bed 1		Bed 2	
	$xs_{Bed1,dp}$	$xf_{Bed1,dp}$	$xs_{Bed2,dp}$	$xf_{Bed2,dp}$
MINLP Section 3.4	230	2855	0	1788
MILP1 Section 4.2	291	2910	0	1879
MILP2 Section 5.2.2	290	2910	0	1880

These cut-points were used as part of schedule in *gPROMS* simulation for validation.

6.4.2 gPROMS

After implementing these scheduling times in *gPROMS*, the purity and the recovery achieved are presented in table 6.5.

The output of *gPROMS* is presented in Figure 6.3 but only for the MINLP model, where the first graph shows the first bed. As expected, there are all four proteins in the mixture and after the cut-points are applied then in the second bed, only the target protein and one of

TABLE 6.5: Purities and recoveries achieved by gPROMS

	Purity	Recovery
MINLP Section 3.4	99.5 %	96 %
MILP1 Section 4.2	99 %	97 %
MILP2 Section 5.2.2	99 %	97 %

the contaminants are left, because the other two contaminants were discarded during the first step.

Below, the final two figures present how does purity and recovery change during time. In Figure 6.4, the black line represents the first bed and the red line the second bed. Initially the purity is very high and gradually decreases until it reaches 33 %. This happens because at the beginning as it is shown in Figure 6.3, only the target protein is collected, therefore the purity is high, but then the contaminants start occuring and the purity drops. In the second bed, the purity again starts from a high values because the target protein is the first protein to elute from the column and remains high because the contaminant still in the mixture is never collected. Similarly, in Figure 6.5, we have a gradual increase of the recovery of the target protein until it reaches the final 96 %.

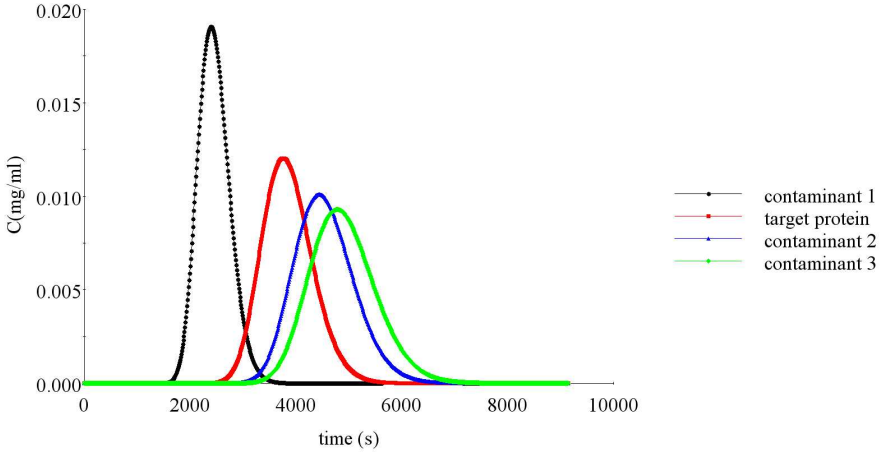

(a) Bed 1

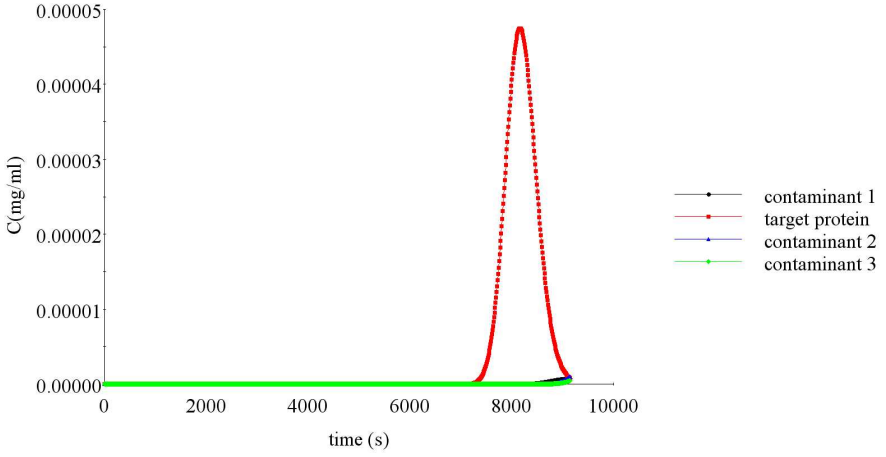

(b) Bed 2

FIGURE 6.3: *gPROMS* output for two-step simulation

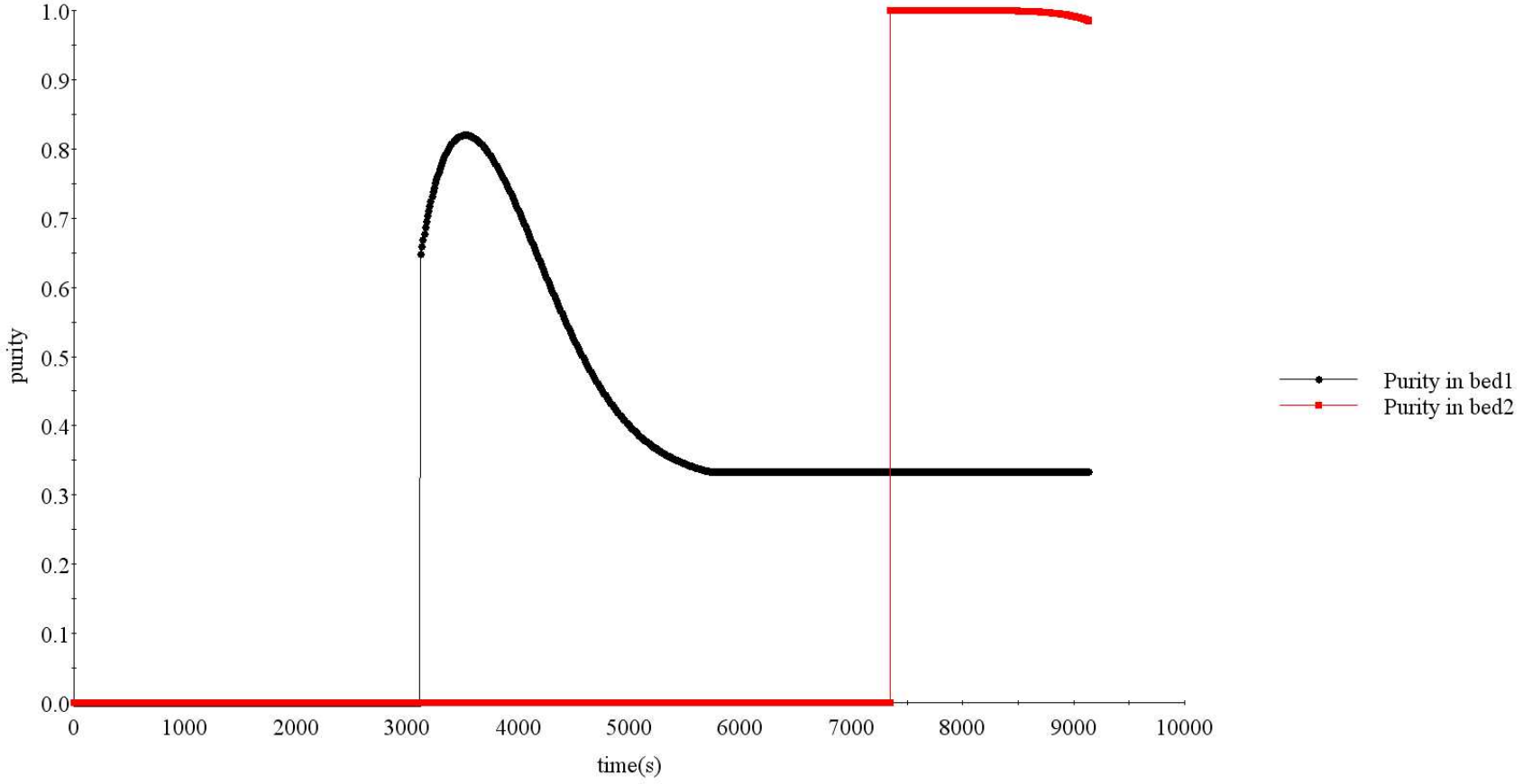

FIGURE 6.4: *gPROMS* output on purity

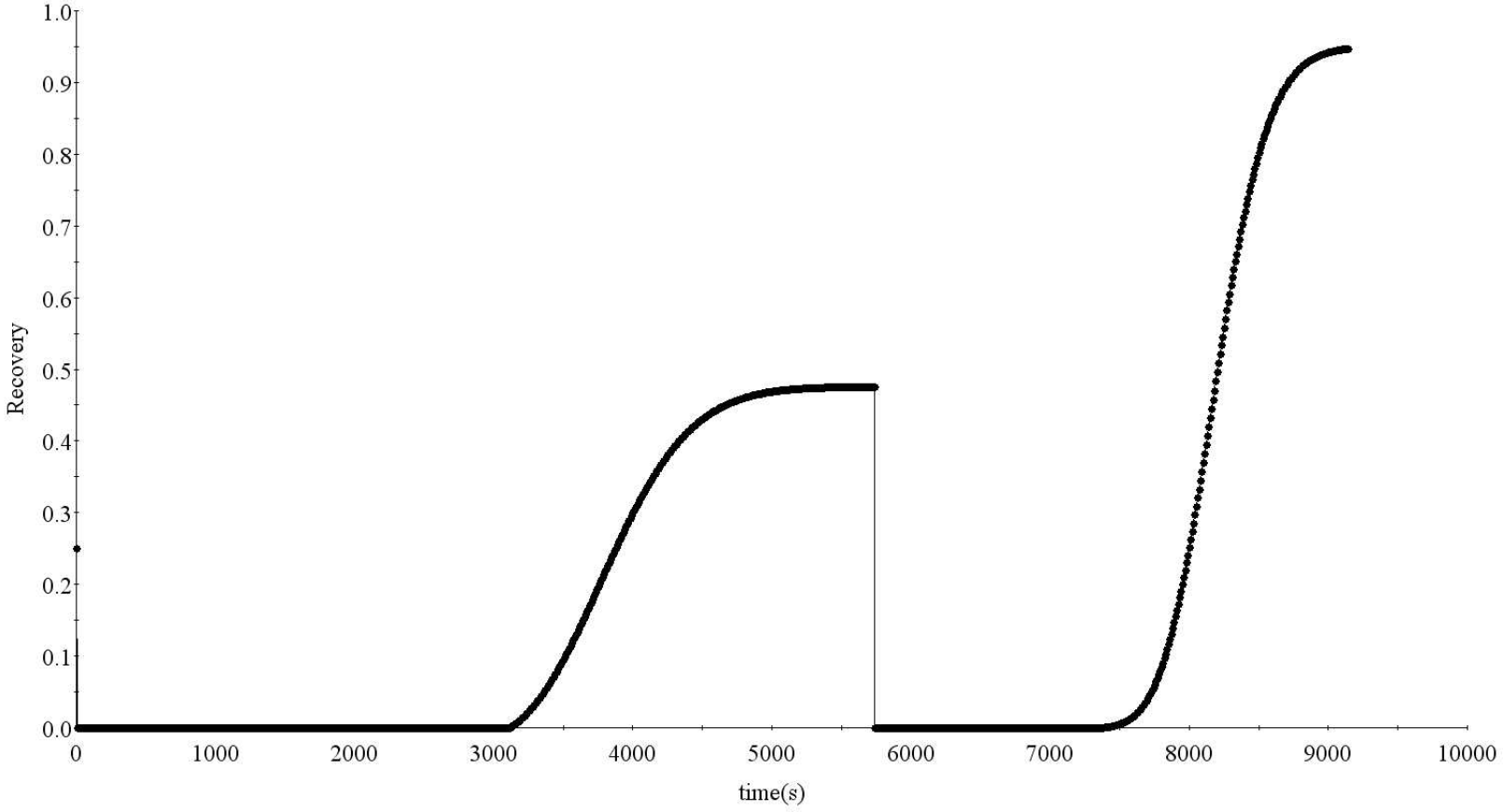

FIGURE 6.5: *gPROMS* output on recovery

6.5 Conclusions

In this Chapter, the main mechanistic models available in literature were reviewed and the equilibrium dispersive model was selected for the validation process of the models described in Chapter 3, 4, 5. After, the selected model was used to implement a case study in *gPROMS* and the results were used as the input in all developed models described in Chapter 3, 4, 5. After the selected steps and the respective cut-points were determined from GAMS, the models were simulated in *gPROMS* and the purity and recovery were calculated and validated. Values of both purity and recovery have a maximum error of 1 %.

Chapter 7

Conclusions and future directions

The aim of this thesis was to investigate different methodologies in order to enhance operation and synthesis of chromatographic purification processes. Towards that goal, a number of mathematical models were developed and their results were presented in the previous chapters. In the following section, the main contributions of the thesis are summarised followed by new directions for future work.

7.1 Contributions of the thesis

This thesis focused on the optimisation of downstream processes in biopharmaceutical plants. In Chapter 1, some basic background information were presented for the biopharmaceutical industry in today's market, followed by the description of a typical flowsheet. Chromatography was targeted as the bottleneck of downstream processing and the main source of cost and was the focus of this work. Next, a brief history of how chromatography has evolved in the last decades from an analytical process to a full scale industrial process, followed.

In Chapter 2, current approaches in the area of of downstream process synthesis and operation were highlighted. Based on some previsously developed work [78, 79] for the synthesis of purification processes, we then presented an MINLP approach that can take into account product losses and minimises the number of chromatographic steps in the purification process. This framework not only optimises the flowsheet but also selects the timeline in which the product is selected, therefore operating conditions can also be manipulated for the benefit of the process. This MINLP model was solved using a two-stage process and tested through three illustrative examples.

Next, in Chapter 4, and by applying piecewise linear approximation, the MINLP model was linearised in order to improve computational efficiency. With this new model, we were able to avoid the two-stage procedure for the first example, but not for the two larger examples. Nevertheless, quality of the solution was indicative of a successful approximation.

Later on, in Chapter 5, two models were developed using discrete recovery levels for the target protein. These models were also tested with the same three examples and they were able to cope with the full problem size up to 21 candidate steps and 13-protein mixtures. Finally, in Chapter 6, models based on first principles were reviewed and the equilibrium dispersive model was implemented in the simulation platform *gPROMS* [106]. Purities and recoveries were compared with the ones from the mathematical models from GAMS and the error did not exceed 1%.

7.2 Recommendations for future work

There are a number of possible future directions related to the synthesis and operation of chromatographic processes:

7.2.1 Additional chromatographic processes

One obvious direction would be the addition of more chromatographic steps. In Chapter 1, we spoke about the different principles of separation. Apart from ion-exchange chromatography (*IEX*) and hydrophobic interaction (*HIC*) which are used in this thesis, size exclusion (*SE*), affinity chromatography (*AC*) and mixed mode (*MMC*)could be considered. The only constraint for this suggestion is the lack of experimental data and the relevant mathematical correlations. For *IEX*, we have the mathematical correlation relating retention time with charge and molecular weight. For *AC* and *MMC*, these correlations are quite a challenge mainly because in the first case the adsorption mechanism is the result of molecular recognition which is not easy to be quantified and for the second case because one of the two separation principles will be more significant than the other and again this needs to be somehow quantified.

7.2.2 Model enhancement

Another direction would be to extend the model itself. As mentioned in Chapter 2, the overall aim is to model the whole biopharmaceutical process in order to predict operating conditions, different configurations and scheduling. Taking small steps, we could try and incorporate some operating parameters that affect chromatographic performance, such as flowrate or ionic strength. Again the constraint is that there are no direct correlations that relate retention time with flowrate.

Since the focus of this project was downstream processes, an idea would be to include processes such as of filtration, centrifugation as part of the flowsheet and try to optimise the flowsheet by minimising the number of units.

7.2.3 Economic evaluation

This can be incorporated either in the objective function by just adding an approximate cost of each purification step, but it can be also done in great detail using cost of goods (COG) strategies, where resin cost, buffer cost, column cost and resin lifetime are taken into account. This can have a significant improvement in the optimisation by improving the accuracy of the results.

7.2.4 Experimental validation

In this thesis, we used computational experimentation in order to validate the mathematical models developed. The ideal methodology would be to actually run the experiments for the examples we are using, by running them though the specific chromatographic columns that have been selected and compare the purities and recoveries achieved. These are straightforward experiments using a liquid chromatography method that is available.

7.2.5 Mathematical correlation predictions

The input of the developed model is the mathematical correlations that have been experimentally derived, by running liquid chromatography to determine the retention time and by relating that to charge, molecular weight and hydrophobicity. These correlations have been derived mainly by the use of partial least square methods. Given that new experimental data can become available more sophisticated methods such as support vector regression or neural networks can be applied to create a database of mathematical correlations that can predict retention times given the parameters responsible for separation and possibly the column specifics.

7.3 Summary and main contributions

This thesis has developed and presented a number of optimisation-based models for the synthesis and operation of chromatographic processes. Three illustrative examples have been used to verify the models. The main contributions from this thesis are:

- a mixed integer non-linear programming mathematical model for minimising the number of chromatographic steps and determining the timeline at which the product is collected;
- three mixed integer linear programming mathematical models solving the same problem; and
- validation of the models through computational experimentation using *gPROMS*.

Appendix A

Calculated KD_{ip} and DF_{ip} for MINLP model

Below, six tables follow, containing all the calculations for dimensionless retention times KD_{ip} and deviation factors DF_{ip}, for all three examples. KD_{ip} and DF_{ip} were calculated based on equations 3.2-3.6 and 3.7 respectively, as presented in section 3.3.

Table A.1: Dimensionless retention times in example 1

KD_{ip}	dp	p_1	p_2	p_3
AE4	0	0	0	0
AE5	0.015	0.1	0.154	0
AE6	0.1	0.174	0.233	0
AE7	0.132	0.206	0.272	0
AE8	0.152	0.215	0.270	0
CE4	0.073	0.124	0.161	0.209
CE5	0	0	0	0.208
CE6	0	0	0	0.211
CE7	0	0	0	0.206
CE8	0	0	0	0.144
HI	0.427	0.64	0.4	0.407

TABLE A.2: Deviation factors in example 1

DF_{ip}	dp	p_1	p_2	p_3
AE4	0	0.085	0.139	0
AE5	0	0.074	0.133	-0.015
AE6	0	0.074	0.140	-0.100
AE7	0	0.063	0.118	-0.132
AE8	0	0.051	0.088	-0.152
CE4	0	0	0.161	0.136
CE5	0	0	0	0.208
CE6	0	0	0	0.211
CE7	0	0	0	0.206
CE8	0	0	0	0.144
HI	0	0.213	-0.027	-0.020

TABLE A.3: Dimensionless retention times in example 2

KD_{ip}	dp	p1	p2	p3	p4	p5	p6	p7	p8
AE40	0	0	0	0	0	0	0	0	0
AE45	0	0	0	0	0	0	0	0	0
AE50	0.112	0.099	0.082	0.052	0	0	0	0	0.092
AE55	0.118	0.093	0.037	0.022	0	0	0.056	0.210	0.042
AE60	0.160	0.107	0.037	0.022	0.072	0.045	0.117	0.263	0.042
AE65	0.225	0.141	0.043	0.026	0.120	0.079	0.157	0.272	0.048
AE70	0.253	0.193	0.103	0.066	0.136	0.091	0.181	0.293	0.115
AE75	0.262	0.220	0.154	0.104	0.138	0.092	0.197	0.293	0.168
AE80	0.262	0.213	0.194	0.137	0.135	0.089	0.205	0.293	0.209
AE85	0.299	0.213	0.269	0.207	0.132	0.087	0.207	0.293	0.284
CE40	0.156	0.100	0.133	0.092	0.133	0.092	0.132	0.151	0.144
CE45	0.017	0.008	0.013	0.008	0.199	0.152	0.098	0.016	0.015
CE50	0	0	0	0	0.133	0.092	0.034	0	0
CE55	0	0	0	0	0.037	0.022	0	0	0
CE60	0	0	0	0	0	0	0	0	0
CE65	0	0	0	0	0	0	0	0	0
CE70	0	0	0	0	0	0	0	0	0
CE75	0	0	0	0	0	0	0	0	0
CE80	0	0	0	0	0	0	0	0	0
CE85	0	0	0	0	0	0	0	0	0
HI	1	1	1	1	1	1	0.020	0.020	0.317

Table A.4: Deviation factors in example 2

KD_{ip}	dp	p1	p2	p3	p4	p5	p6	p7	p8
AE40	0	0	0	0	0	0	0	0	0
AE45	0	0	0	0	0	0	0	0	0
AE50	0	-0.013	-0.03	-0.06	-0.112	-0.112	-0.112	-0.112	-0.020
AE55	0	-0.025	-0.081	-0.096	-0.118	-0.118	-0.062	0.092	-0.076
AE60	0	-0.053	-0.123	-0.138	-0.088	-0.115	-0.043	0.103	-0.118
AE65	0	-0.084	-0.182	-0.199	-0.105	-0.146	-0.068	0.047	-0.177
AE70	0	-0.06	-0.150	-0.187	-0.117	-0.162	-0.072	0.040	-0.138
AE75	0	-0.042	-0.108	-0.158	-0.124	-0.170	-0.065	0.031	-0.094
AE80	0	-0.049	-0.068	-0.125	-0.127	-0.173	-0.057	0.031	-0.053
AE85	0	-0.086	-0.03	-0.092	-0.167	-0.212	-0.092	-0.006	-0.015
CE40	0	-0.056	-0.023	-0.064	-0.023	-0.064	-0.024	-0.005	-0.012
CE45	0	-0.009	-0.004	-0.009	0.182	0.135	0.081	-0.001	-0.002
CE50	0	0	0	0	0.133	0.092	-0.034	0	0
CE55	0	0	0	0	0.037	0.022	0	0	0
CE60	0	0	0	0	0	0	0	0	0
CE65	0	0	0	0	0	0	0	0	0
CE70	0	0	0	0	0	0	0	0	0
CE75	0	0	0	0	0	0	0	0	0
CE80	0	0	0	0	0	0	0	0	0
CE85	0	0	0	0	0	0	0	0	0
HI	0	0	0	0	0	0	-0.98	-0.98	-0.683

TABLE A.5: Dimensionless retention times in example 3

KD_{ip}	dp	p1	p2	p3	p4	p5	p6	p7	p8	p9	p10	p11	p12
AE40	0	0	0	0	0	0	0.176	0	0.020	0	0	0	0
AE50	0	0	0	0	0.100	0	0.178	0.188	0.050	0	0.149	0	0
AE60	0.039	0	0	0	0.173	0	0.212	0.215	0.104	0.287	0.227	0	0.048
AE70	0.077	0	0	0.102	0.206	0	0.287	0.270	0.120	0.316	0.253	0	0.114
AE80	0.101	0	0	0.148	0.214	0	0.291	0.303	0.132	0.329	0.265	0	0.150
CE40	0.128	0.218	0.238	0.269	0.128	0.289	0.000	0.126	0	0.260	0.163	0.256	0.178
CE50	0.080	0.216	0.204	0.181	0	0.287	0	0	0	0.187	0	0.182	0.092
CE60	0	0.215	0.184	0.103	0	0.287	0	0	0	0	0	0.153	0
CE70	0	0.215	0.147	0	0	0.283	0	0	0	0	0	0.109	0
CE80	0	0.149	0.090	0	0	0.266	0	0	0	0	0	0.003	0
HI	0.702	0.629	0.818	0.392	0.701	0.655	0.871	0.290	0.649	0.075	0.780	0.682	0.503

TABLE A.6: Deviation factors in example 3

DF_{ip}	dp	p1	p2	p3	p4	p5	p6	p7	p8	p9	p10	p11	p12
AE40	0	0	0	0	0	0	0.176	0	0.020	0	0	0	0
AE50	0	0	0	0	0.100	0	0.178	0.188	0.050	0	0.149	0	0
AE60	0	-0.039	-0.039	-0.039	0.134	-0.039	0.173	0.176	0.065	0.248	0.188	-0.039	0.009
AE70	0	-0.077	-0.077	0.025	0.129	-0.077	0.210	0.193	0.043	0.239	0.176	-0.077	0.037
AE80	0	-0.101	-0.101	0.047	0.113	-0.101	0.190	0.202	0.031	0.228	0.164	-0.101	0.049
CE40	0	0.090	0.110	0.141	0	0.161	-0.128	-0.002	-0.128	0.132	0.035	0.128	0.050
CE50	0	0.136	0.124	0.101	-0.080	0.207	-0.080	-0.080	-0.080	0.107	-0.080	0.102	0.012
CE60	0	0.215	0.184	0.103	0	0.287	0	0	0	0	0	0.153	0
CE70	0	0.215	0.147	0	0	0.283	0	0	0	0	0	0.109	0
CE80	0	0.149	0.090	0	0	0.266	0	0	0	0	0	0.003	0
HI	0	-0.073	0.116	-0.310	-0.001	-0.047	0.169	-0.412	-0.053	-0.627	0.078	-0.020	-0.199

Appendix B

Piecewise linear approximation

Below there is a description of the optimal approximations of single-dimensional nonlinear functions by piecewise linear functions as described by [96]. The approach uses a discrete representation of the non-linear function described by pairs (x_i, f_i), $i \in Q = 1, 2, ...n_Q$, where Q is the predefined sampling set. Binary variable W_{ij} is equal to 1 if $i \in Q$ and $j \in Q$ are two consecutive points, otherwise is 0. N is the number of knots given *a priori*.

At most one one polynomial piece of the approximating function may begin and one piece may end in each of the points in Q.

$$\sum_{\substack{j \in Q \\ j > i}} W_{ij} \leq 1 \qquad \forall i \in Q | i > 1 \tag{B.1}$$

$$\sum_{\substack{i \in Q \\ j > i}} W_{ij} \leq 1 \qquad \forall j \in Q | j > n_Q \tag{B.2}$$

The first and last points of Q are necessarily part of the knots.

$$\sum_{\substack{j\in Q\\ j>i}} W_{ij} = 1 \qquad \forall i = 1 \tag{B.3}$$

$$\sum_{\substack{i\in Q\\ j>i}} W_{ij} = 1 \qquad \forall j = n_Q \tag{B.4}$$

Any knot has to be both the start and the end of a polynomial piece of the approximating function and the end of another (except of the first and last ones).

$$\sum_{\substack{i\in Q\\ k>i}} W_{ik} = \sum_{\substack{i\in Q\\ j>k}} W_{kj} \qquad \forall k > 2...n_Q - 1 \tag{B.5}$$

The approximating function is predefined to have N internal knots.

$$\sum_{i\in Q} \sum_{\substack{j\in Q\\ j>i}} W_{ij} = N - 1 \tag{B.6}$$

The values of the approximating function are defined by the following set of constraints.

$$f_k^P = \sum_{\substack{i\in Q\\ i<k}} \sum_{\substack{j\in Q\\ j>k}} \frac{[(x_k - x_i)\cdot f_j + (x_j - x_k)\cdot f_i]}{(x_j - x_i)} \cdot W_{ij} \qquad \forall k \in Q \tag{B.7}$$

To measure the quality of the approximation, the 1-norm of distance between the vectors describing the original function and the piecewise linear approximation. The objective function is to minimise this norm and is given by the following constraints.

$$Z = \sum_{i \in Q} z_i \tag{B.8}$$

$$z_i \geq (f_i - f_i^P) \forall i \in Q \tag{B.9}$$

$$z_i \geq -(f_i - f_i^P) \forall i \in Q \tag{B.10}$$

Appendix C

Calculation of concentration factors

STEP 1: Generation of cut-points, $xs_{i,dp}$, $xf_{i,dp}$

STEP 2: Calculation of shifted cut-points $\bar{x}s_{ip}$.

$$\bar{xs}_{ip} = xs_{i,dp} - DF_{ip} \qquad \forall i, p \neq dp \qquad \text{(C.1)}$$

$$\bar{xf}_{ip} = xf_{i,dp} - DF_{ip} \qquad \forall i, p \neq dp \qquad \text{(C.2)}$$

STEP 3: Correction of shifted cut points $\bar{x}s_{ip}$.

- If $\bar{x}s_{ip} < 0 \rightarrow \Delta s_{ip} = 0$ & $\bar{x}f_{ip} < 0 \rightarrow \Delta f_{ip} = 0$
- If $\bar{x}s_{ip} > \sigma_i \rightarrow \Delta s_{ip} = \sigma_i$ & $\bar{x}f_{ip} > \sigma_i \rightarrow \Delta f_{ip} = \sigma_i$
- If $0 \leq \bar{x}s_{ip} \leq \sigma_i$ & $0 \leq \bar{x}f_{ip} \leq \sigma_i \rightarrow \Delta f_{ip} = \bar{x}f_{ip}$

STEP 4: Calculation of concentration factors CF_{ip}.

Model 1

$$\Delta s_{ip}, \Delta f_{ip} < \frac{\sigma_i}{2} \qquad CF_{ip} = \frac{2 \cdot \left(\Delta f_{ip}^2 - \Delta s_{ip}^2\right)}{\sigma_i^2} \tag{C.3}$$

$$\Delta s_{ip} < \frac{\sigma_i}{2}, Delta f_{ip} > \frac{\sigma_i}{2} \qquad CF_{ip} = 1 - \frac{2 \cdot [(\Delta s_{ip})^2 + (\sigma_i - \Delta f_{ip})^2]}{\sigma_i^2} \tag{C.4}$$

$$\Delta s_{ip}, \Delta f_{ip} > \frac{\sigma_i}{2} \qquad CF_{ip} = \frac{2 \cdot [(\sigma_i - \Delta s_{ip})^2 + (\sigma_i - \Delta f_{ip})^2]}{\sigma_i^2} \tag{C.5}$$

Model 2

$$CF_{ip} = Af_{ip} - As_{ip} \tag{C.6}$$

$$\Delta s_{ip}, \Delta f_{ip} < \frac{\sigma_i}{2} \qquad Af_{ip} = 2 \cdot \frac{\Delta f_{ip}^2}{\sigma_i^2} \qquad \& \qquad As_{ip} = 2 \cdot \frac{\Delta s_{ip}^2}{\sigma_i^2} \tag{C.7}$$

$$\Delta s_{ip}, \Delta f_{ip} > \frac{\sigma_i}{2} \qquad Af_{ip} = 1 - \frac{(\sigma_i - \Delta f_{ip})^2}{\sigma_i^2} \qquad \& \qquad As_{ip} = 1 - \frac{(\sigma_i - \Delta s_{ip})^2}{\sigma_i^2} \tag{C.8}$$

C.1 Discretisation of peak width

In Figure C.1, C.2 the discretisation of peak width for bot starting and finishing cut point is presented. Given the values above and the procedure described in the previous page the concentration factors can be calculated.

Table C.1: Discretisation of peak width using 5 integrals

	IEX	HIC
1	0	0
2	0.004	0.006
3	0.008	0.011
4	0.011	0.017
5	0.015	0.022

	IEX	HIC
1	0.075	0.110
2	0.094	0.138
3	0.112	0.165
4	0.131	0.193
5	0.150	0.220

Table C.2: Discretisation of peak width using 10 integrals

	IEX	HIC
1	0	0
2	0.002	0.002
3	0.003	0.005
4	0.005	0.007
5	0.007	0.010
6	0.008	0.012
7	0.010	0.015
8	0.012	0.017
9	0.013	0.020
10	0.015	0.022

	IEX	HIC
1	0.075	0.110
2	0.083	0.122
3	0.092	0.134
4	0.100	0.147
5	0.108	0.159
6	0.117	0.171
7	0.125	0.183
8	0.133	0.196
9	0.142	0.208
10	0.150	0.220

Appendix D

Simulation results from *gPROMS*

The following figures, show the simulation results from *gPROMS*. In all cases the curve with the red colour is the target protein and the rest are the contaminants. The *x axis* is the time in seconds and the *y axis* is the concentration of each component p in g/l.

To obtain these figures we used the parameters presented in Table 6.2.

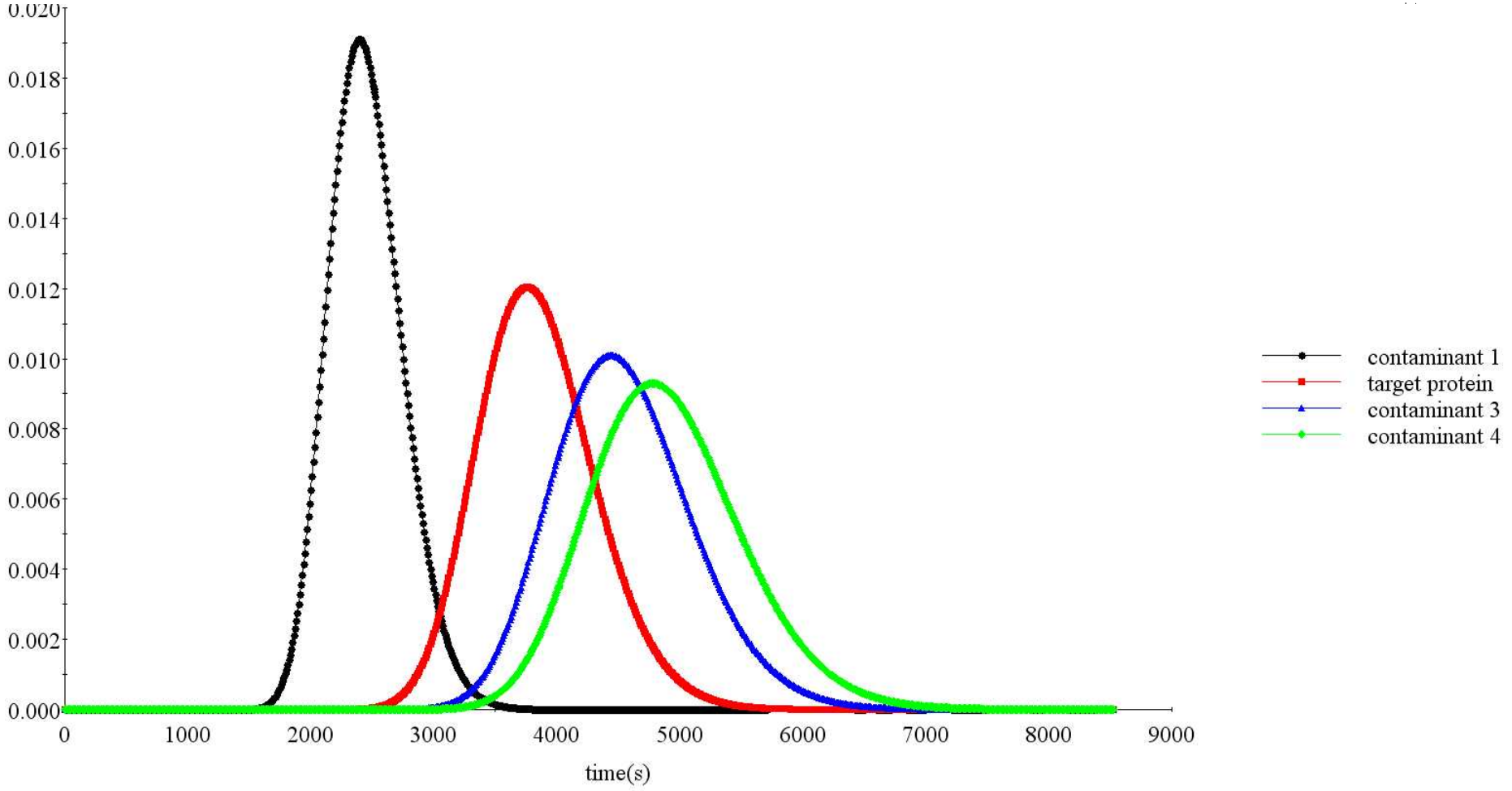

FIGURE D.1: Elution profiles in bed 1

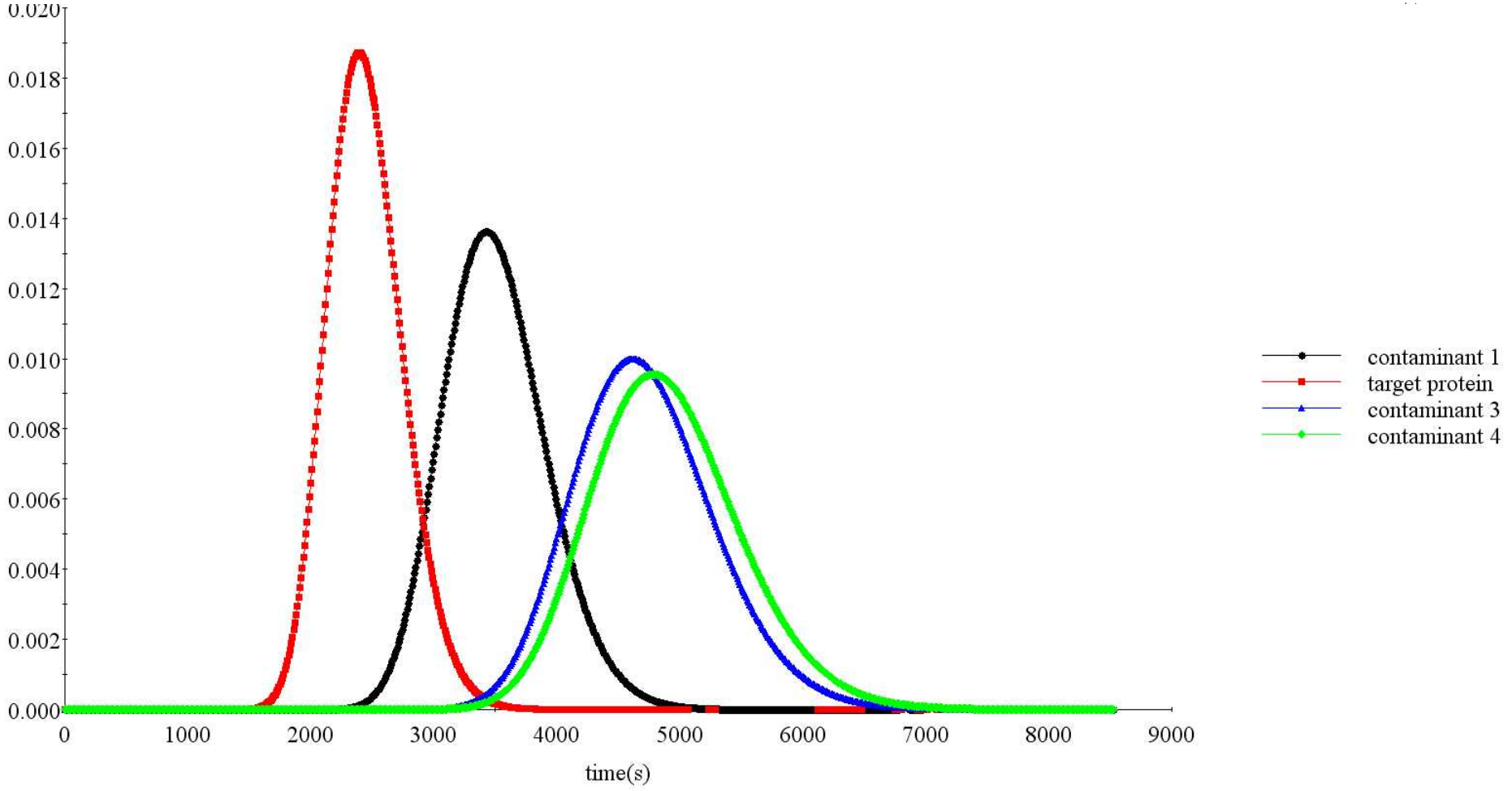

FIGURE D.2: Elution profiles in bed 2

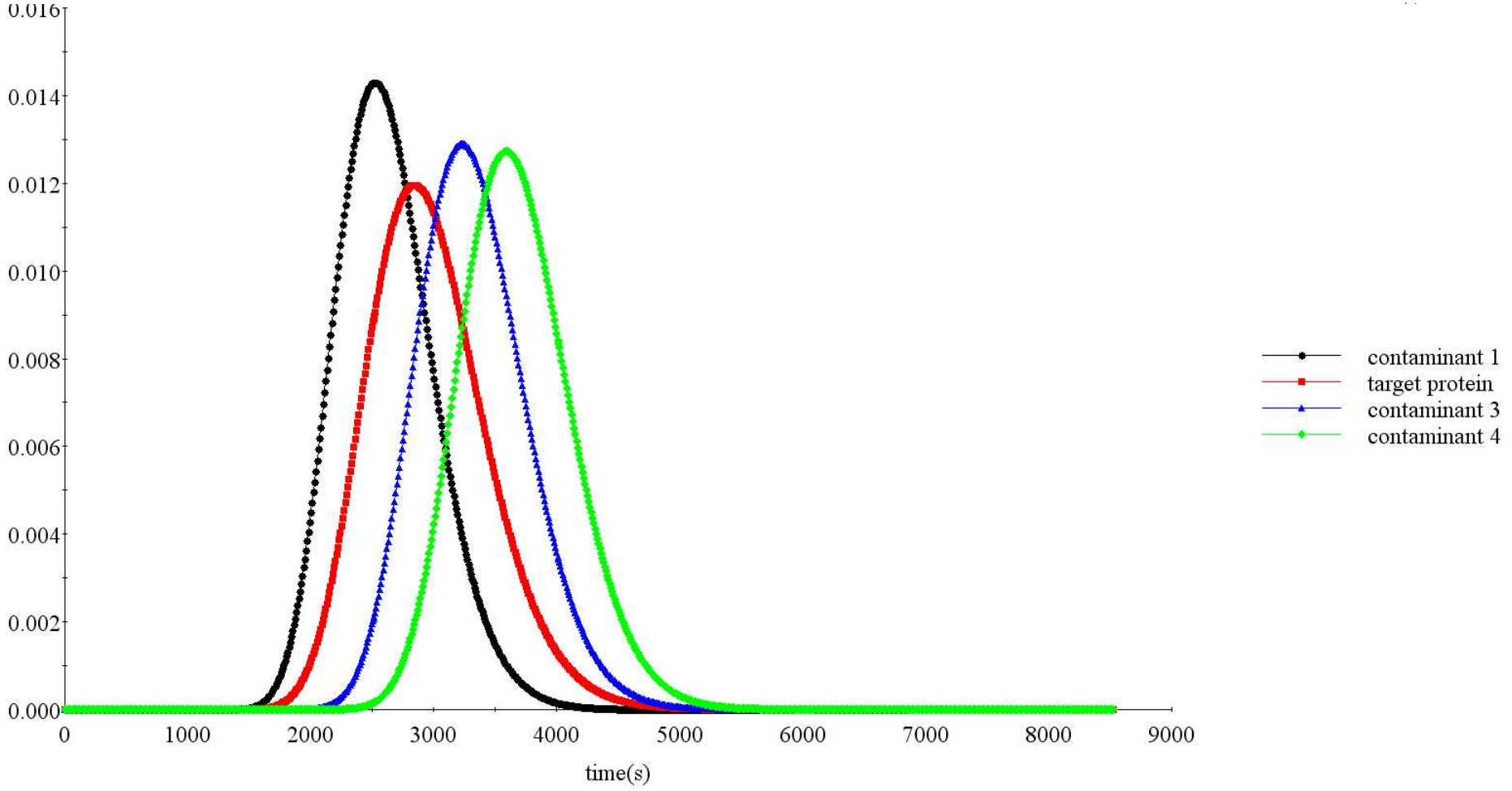

FIGURE D.3: Elution profiles in bed 3

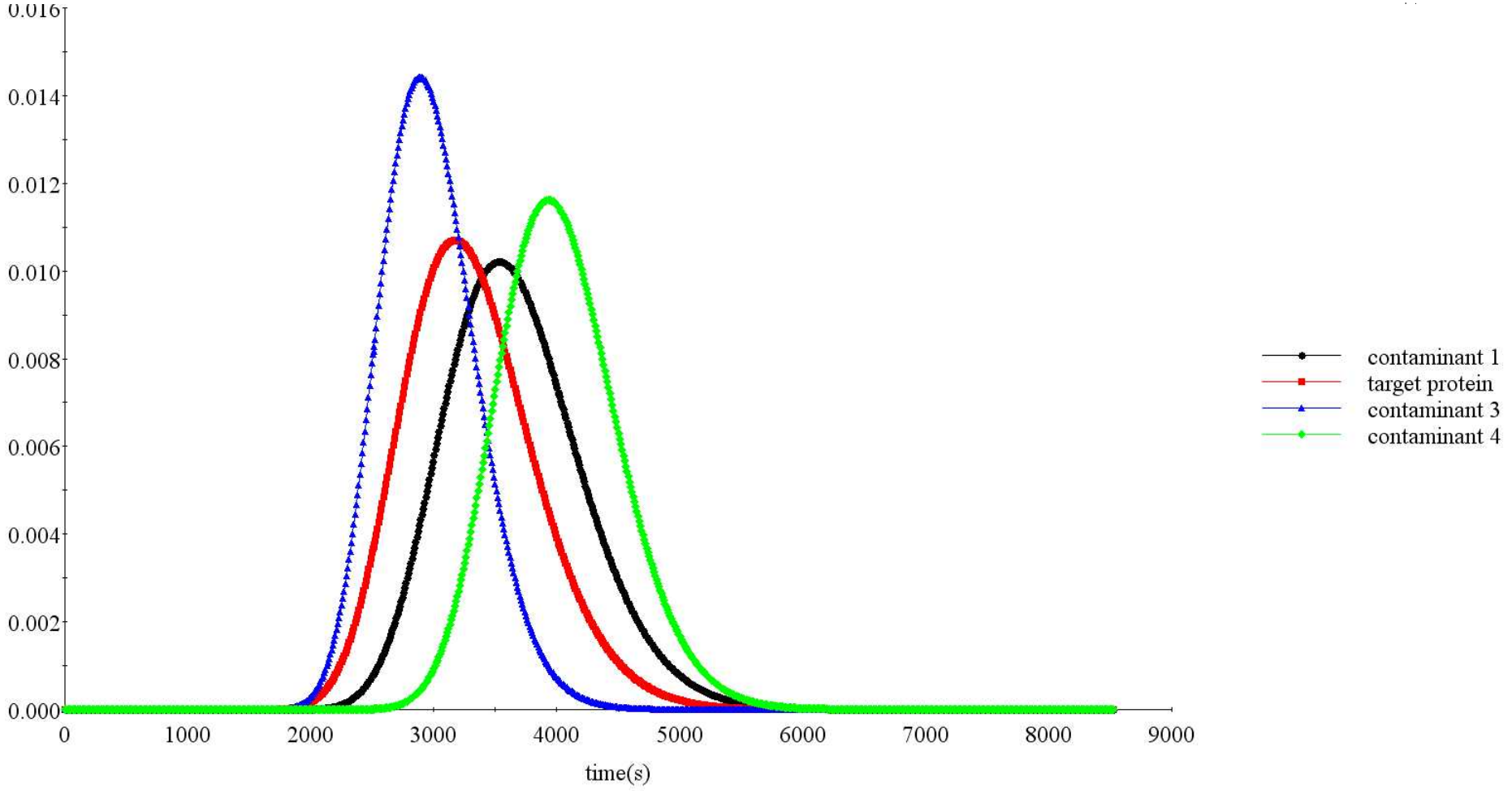

FIGURE D.4: Elution profiles in bed 4

Bibliography

[1] IMS Health. The global pharmaceurical market, 2011. URL `http://www.vfa.de/en/statistics/pharmaceuticalmarket/`.

[2] E. Vasquez-Alvarez, M. E. Lienqueo, and J. M. Pinto. Optimal synthesis of protein purification processes. *Biotechnology Progress*, 17:685–696, 2001.

[3] E. M. Polykarpou, P. A. Dalby, and L. G. L. G. Papageorgiou. An MINLP Formulation for the Synthesis of Chromatographic Protein Purification Processes with Product Loss. In *European Symposium on Computer Aided Process Engineering-19*, volume 26 of *Computer-Aided Chemical Engineering*, pages 1057–1062, 2009.

[4] G. Jagschies. Process-scale chromatography, 2000.

[5] G. Walsh. Biopharmaceutical benchmarks 2010. *Nature biotechnology*, 28(9):917 – 924, 2010.

[6] IMS Health. Ims health forecasts global pharmaceutical market growth of 5-7 percent in 2011, 2010. URL `http://www.imshealth.com/portal/site/imshealth/`.

[7] B. Munos. Lessons from 60 years of pharmaceutical innovation. *Nature Reviews Drug Discovery*, 8:959–968, 2009.

[8] Steven J Projan, Davinder Gill, Zhijian Lu, and Steven H Hermann. Small molecules for small minds? The case for biologic pharmaceuticals. *Expert Opinion on Biological Therapy*, 4:1345–1350, 2004.

[9] S. Ahuja. *Handbook of BioSeparations.* Academic Press, 2000.

[10] L. S. Ettre. Nomenclature for Chromatography. *Pure and Applied Chemistry*, 65(4):819–872, 1993.

[11] Kirk-Othmer. *Encyclopedia of Chemical Technology, volume 2.* John Wiley and Sons, Inc., 5th edition, 2007.

[12] H. M. McNair and J. M. Miller. *Basic Gas Chromatography.* John Wiley and Sons, Inc., 1998.

[13] J. P. Martin and R. L. M. Synge. A new form of Chromatogram employing two liquid phases 1. A theory of Chromatography 2. Application to the micro-determination of the higher monoamino-acids in proteins. *Biochemical Journal*, 35:1358–1368, 1941.

[14] A. T. James and J. P. Martin. Gas liquid partition chromatography: the separation and micro-estimation of volatile fatty acids from formic acid to dodecanoic acid. *Biochemical Journal*, 50: 679–690, 1952.

[15] R. P. W. Scott. *Contemporary Liquid Chromatography.* John Wiley and Sons, Inc., 1976.

[16] P. A. Schweitzer. *Handbook of Separation for Chemical Engineers.* McGraw-Hill, Inc., 1996.

[17] J. J. McKetta. *Encyclopedia of Chemical Processing and Design, volume 8.* Marcel Dekker, Inc., 1976.

[18] J. M. Coulson and J. F. Richardson. *Chemical Engineering Volume 2: Particle Technology and Separation Processes.* Butterworth-Heinemann, 4th edition, 1991.

[19] A. Tiselius. Displacement development in adsorption analysis. *Stockholm Almqvist Wiksell Berlin Natura*, 16A(18):1–18, 1943.

[20] R. Freitag and J. Breier. Displacement chromatography in biotechnological downstream processing. *Journal of chromatography A*, 691:101 – 112, 1995.

[21] A. Jungbauer. Chromatographic media for bioseparation. *Journal of Chromatography A*, 1065(1):3–12, 2005.

[22] Pall Corporation. Mixed-mode chromatography selection guide, 2011. URL `http://www.pall.com/`.

[23] S. H. Ngiam, D. G. Bracewell, Y. Zhou, and N. J. Titchener-Hooker. Quantifying process tradeoffs in the operation of chromatographic sequences. *Biotechnology Progress*, 19(4):1315–1322, 2003.

[24] C. R. Lowe, A. R. Lowe, and G. Gupta. New developments in affinity chromatography with potential application in the production of biopharmaceuticals. *Journal of Biochemical and Biophysical methods*, 49:561–574, 2001.

[25] J. Curling. Process chromatography: Five decades of innovation. *Biopharm International*, 20:10–19, 2007.

[26] T. M. Przybycien, N. S. Pujar, and L. M Steele. Alternative bioseparation operations: life beyond packed-bed chromatography. *Current Opinion in Biotechnology*, 15:469–478, 2004.

[27] G. Larsson, S. B. Jorgensen, M. N. Pons, B. Sonnleitner, A. Tijsterman, and N. J. Titchener-Hooker. Minireview: Biochemical engineering science. *Journal of Biotechnology*, 59(1-2):3–9, 1997.

[28] J. Thommes and M. Etzel. Alternatives to chromatographic separations. *Biotechnology Progress*, 23(1):42–45, 2007.

[29] B. Kelley. Industrialization of mab production technology the bioprocessing industry at a crossroads. *mAbs*, 1(5):443–452, 2009.

[30] D. Low, R. O'Leary, and N. S. Pujar. Future of antibody purification. *Journal of Chromatography B*, 848(1):48 – 63, 2007. Polyclonal and Monoclonal Antibody Production, Purification, Process and Product Analytics.

[31] J. A. Asenjo and B. A. Andrews. Challenges and trends in bioseparations. *Journal of Chemical Technology and Biotechnology*, 83 (2):117–120, 2008.

[32] B. K. Nfor, T. Ahamed, G. W. K. van Dedem, L. A. M. van der Wielen, E. J. A. X. van de Sandt, M. H. M. Eppink, and M. Ottens. Design strategies for integrated protein purification processes: challenges, progress and outlook. *Journal of Chemical Technology and Biotechnology*, 83(2):124–132, 2008.

[33] FDA. *International Committee on Harmonization Q8: Pharmaceutical Development FDA*, 2009.

[34] A. Jungbauer and O. Kaltenbrunner. Fundamental questions in optimizing ion-exchange chromatography of proteins using computer-aided process design. *Biotechnology and Bioengineering*, 52(2):223–236, 1996.

[35] A. Mahn, M. E. Lienqueo, and J. C. Salgado. Methods of calculating protein hydrophobicity and their application in developing correlations to predict hydrophobic interaction chromatography retention. *Journal of Chromatography A*, 1216(10):1838–1844, 2009.

[36] J. Bonnerjea, S. Oh, M. Hoare, and P. Dunnill. Protein purification: The right step at the right time. *Biotechnology*, 4:954–958, 1986.

[37] J. C. Salgado, I. Rapaport, and J. A. Asenjo. Predicting the behaviour of proteins in hydrophobic interaction chromatography 2. using a statistical description of their surface amino acid distribution. *Journal of Chromatography A*, 1107:120–129, 2006.

[38] F. Dismer and J. Hubbuch. A novel approach to characterize the binding orientation of lysozyme on ion-exchange resins. *Journal of Chromatography A*, 1149(2):312 – 320, 2007.

[39] F. Dismer, M. Petzold, and J. Hubbuch. Effects of ionic strength and mobile phase ph on the binding orientation of lysozyme on different ion-exchange adsorbents. *Journal of Chromatography A*, 1194(1):11–21, 2008. 27th International Symposium on the Separation of Proteins, Peptides and Polynucleotides.

[40] F. Dismer and J. Hubbuch. 3d structure-based protein retention prediction for ion-exchange chromatography. *Journal of Chromatography A*, 1217(8):1343–1353, 2010.

[41] D. Karlsson, N. Jakobsson, A. Axelsson, and B. Nilsson. Model-based optimization of a preparative ion-exchange step for antibody purification. *Journal of Chromatography A*, 1055(1-2):29 – 39, 2004.

[42] H. Weiqiang, Z. Xiangmin, and H. Fengli. Analysis of the ideal model for a single component in preparative gradient elution chromatography. *Analytical Chemistry*, 79(6):2507–2517, 2007.

[43] J. M. Mollerup, T. B. Hansen, Steffen Kidal, Lars Sejergaard, and Arne Staby. Development, modelling, optimisation and scale-up of chromatographic purification of a therapeutic protein. *Fluid Phase Equilibria*, 261(1-2):133 – 139, 2007.

[44] S. Chan, N. Titchener-Hooker, D. G. Bracewell, and E. Sorensen. A systematic approach for modeling chromatographic processesapplication to protein purification. *AIChE Journal*, 54(4):965–977, 2008.

[45] C. Shene, A. Lucero, B. A. Andrews, and J. A. Asenjo. Mathematical modeling of elution curves for a protein mixture in ion exchange chromatography and for the optimal selection of operational conditions. *Biotechnology and Bioengineering*, 95(4): 704–713, 2006.

[46] O. Kaltenbrunner, O. Giaverini, D. Woehle, and J. A. Asenjo. Application of chromatographic theory for process characterization

towards validation of an ion-exchange operation. *Biotechnology and Bioengineering*, 98(1):201–210, 2007.

[47] H. K. Teoh, M. Turner, N. Titchener-Hooker, and E. Sorensen. Experimental verification and optimisation of a detailed dynamic high performance liquid chromatography column model. *Computers and Chemical Engineering*, 25(4-6):893 – 903, 2001.

[48] C. A. Orellana, C. Shene, and J. A. Asenjo. Mathematical modeling of elution curves for a protein mixture in ion exchange chromatography applied to high protein concentration. *Biotechnology and Bioengineering*, 104(3):572–581, 2009.

[49] M. Degerman, N. Jakobsson, and B. Nilsson. Designing robust preparative purification processes with high performance. *Chemical Engineering and Technology*, 31(6), 2008.

[50] N. Jakobsson, M. Degerman, E. Stenborg, and B. Nilsson. Model based robustness analysis of an ion-exchange chromatography step. *Journal of Chromatography A*, 1138(1-2):109 – 119, 2007.

[51] S. H. Ngiam, Y. H. Zhou, M. K. Turner, and N. J. Titchener-Hooker. Graphical method for the calculation of chromatographic performance in representing the trade-off between purity and recovery. *Journal of Chromatography A*, 937(1-2):1–11, 2001.

[52] S. Edwards-Parton, N. F. Thornhill, D. G. Bracewell, J. M. Liddell, and N. J. Titchener-Hooker. Principal component score modeling for the rapid description of chromatographic separations. *Biotechnology Progress*, 24(1):202–208, 2008.

[53] R. S. Salisbury, D. G Bracewell, and N. J. Titchener-Hooker. A methodology for the graphical determination of operating conditions of chromatographic sequences incorporating the trade-offs between purity and yield. *Journal of Chemical Technology and Biotechnology*, 81(11):1803–1813, 2006.

[54] C. B. Mazza, N. Sukumar, C. M. Breneman, and S. M. Cramer. Prediction of protein retention in ion-exchange systems using molecular descriptors obtained from crystal structure. *Analytical Chemistry*, 73(22):5457–5461, 2001.

[55] M. Song, C. M. Breneman, J. Bi, N. Sukumar, K. P. Bennett, S. M. Cramer, and N. Tugcu. Prediction of protein retention times in anion-exchange chromatography systems using support vector regression. *Journal of Chemical Information and Computer Sciences*, 42(6):1347–1357, 2002.

[56] A. Ladiwala, K. Rege, C. M. Breneman, and S. M. Cramer. Investigation of mobile phase salt type effects on protein retention and selectivity in cation-exchange systems using quantitative structure retention relationship models. *Langmuir*, 19(20):8443–8454, 2003.

[57] A. Ladiwala, F. Xia, Q. Luo, C. M. Breneman, and S. M. Cramer. Investigation of protein retention and selectivity in hic systems using quantitative structure retention relationship models. *Biotechnology and Bioengineering*, 93(5):836–850, 2006.

[58] J. Chen, T. Yang, Q. Luo, C. M. Breneman, and S. M. Cramer. Investigation of protein retention in hydrophobic interaction chromatographic (hic) systems using the preferential interaction theory and quantitative structure property relationship models. *Reactive and Functional Polymers*, 67(12):1561–1569, 2007.

[59] J. Chen, T. Yang, and S. M. Cramer. Prediction of protein retention times in gradient hydrophobic interaction chromatographic systems. *Journal of Chromatography A*, 1177(2):207–214, 2008.

[60] M. Wiendahl, P. S. Wierling, J. Nielsen, D. F. Christensen, J. Krarup, A. Staby, and J. Hubbuch. High throughput screening for the design and optimization of chromatographic processes miniaturization, automation and parallelization of breakthrough

and elution studies. *Chemical Engineering and Technology*, 31(6): 893–903, 2008.

[61] S. Chhatre and N. J. Titchener-Hooker. Review: Microscale methods for high-throughput chromatography development in the pharmaceutical industry. *Journal of Chemical Technology and Biotechnology*, 84(7):927–940, 2009.

[62] A. Jungbauer. Insights into the chromatography of proteins provided by mathematical modeling. *Current Opinion in Biotechnology*, 7(2):210–218, 1996.

[63] C. Ostlund. Large-scale purification of monoclonal antibodies. *Trends Biotechnology*, 4:288–293, 1986.

[64] J. A. Asenjo, L. Herrera, and B. Byrne. Development of an expert system for selection and synthesis of protein purification processes. *Journal of Biotechnology*, 11:275–298, 1989.

[65] S. M. Wheelwright. The design of downstream processes for large-scale protein purification. *Journal of Biotechnology*, 11:89–102, 1989.

[66] J. A. Asenjo. Selection of operations in separation processes. *Bioprocess Technology*, 9:3–16, 1990.

[67] H. Eriksson, K. Sandahl, G. Forslund, and B. Gsterlund. Knowledge-based planning for protein purification. *Chemometrics and Intelligent Laboratory Systems: Laboratory Information Management*, 13:173–184, 1991.

[68] E. W. Leser and J. A. Asenjo. Rational design of purification processes for recombinant proteins. *Journal of Chromatography B: Biomedical Sciences and Applications*, 584(1):43 – 57, 1992.

[69] E. Watanabe, S. Tsoka J. A., and Asenjo. Selection of chromatographic protein purification operations based on physicochemical propertiesa. *Annals of the New York Academy of Sciences*, 721 (1):348–364, 1994.

[70] E. W. Leser and J. A. Asenjo. The rational selection of purification processes for proteins: An expert system for downstream processing designa. *Annals of the New York Academy of Sciences*, 721(1):337–347, 1994.

[71] N. Nishida, G. Stephanopoulos, and A. W. Westerberg. A review of process synthesis. *AIChE Journal*, 27:321–351, 1981.

[72] M. E. Lienqueo. *Desarollo de un sistema experto para la selection racional de processos de purification de proteinas:optimizacion de criterios se seleccion de sequenciase*. PhD thesis, Universidad De Chile Facultad de Ciencias Fisicas y matematicas departamento de Ingeniera Quimica, 1999.

[73] M. E. Lienqueo, E. W. Leser, and J. A. Asenjo. An expert system for the selection and synthesis of multi-step protein separation processes. *Computers Chemical Engineering*, 20:189–194, 1996.

[74] M. E. Lienqueo and J. A. Asenjo. Use of expert systems for the synthesis of downstream protein processes. *Computers and Chemical Engineering*, 24:2339–2350, 2000.

[75] J. A. Asenjo and B. A. Andrews. Is there a rational method to purify proteins? from expert systems to proteomics. *Journal of Molecular Recognition*, 17(3):236–247, 2004.

[76] M. A. Steffens, E. S. Fraga, and I. D. L. Bogle. Synthesis of bioprocesses using physical propertie data. *Biotechnology and Bioengineering*, 68(2):218–230, 1999.

[77] M. A. Steffens, E. S. Fraga, and I. D. L. Bogle. Synthesis of purification tags for optimal downstream processing. *Computers and Chemical Engineering*, 24:717–720, 2000.

[78] E. Vasquez-Alvarez and J. M. Pinto. Efficient milp formulation for the optimal synthesis of chromatographic protein purification processes. *Journal of Biotechnology*, 110:295–311, 2004.

[79] E. Simeonidis, J. M. Pinto, M. E. Lienqueo, S. Tsoka, and L. G. Papageorgiou. Minlp models for the synthesis of optimal peptide tags and downstream protein processing. *Biotechnology Progress*, 21:875–884, 2005.

[80] M. E. Lienqueo, J. C. Salgado, O. Giaverini, and J. A. Asenjo. Computer-aided design to select optimal polypeptide tags to assist the purification of recombinant proteins. *Separation and Purification Technology*, 65(1):86–94, 2009.

[81] J. M. Natali, J. M. Pinto, and L. G. Papageorgiou. Efficient milp formulations for the simultaneous optimal peptide tag design and downstream processing synthesis. *AIChE Journal*, 55:2303–2317, 2009.

[82] M. E. Lienqueo, J. C. Salgado, O. Giaverini, and J. A. Asenjo. Computer-aided design to select optimal polypeptide tags to assist the purification of recombinant proteins. *Separation and Purification Technology*, 65(1):86 – 94, 2009. Advances in Biopartitioning and Purification.

[83] B. K. Nfor, P. D. E. M. Verhaert, L. A. M. van der Wielen, J. Hubbuch, and M. Ottens. Rational and systematic protein purification process development: the next generation. *Trends in Biotechnology*, 27(12):673–679, 2009.

[84] E. Vasquez-Alvarez and J. M. Pinto. Mixed integer optimization models for the Synthesis of Protein Purification Processes with product loss. In *European Symposium on Computer Aided Process Engineering-12*, volume 10 of *Computer-Aided Chemical Engineering*, pages 373–378, 2002.

[85] E. Vasquez-Alvarez and J. M. Pinto. A mixed integer linear programming model for the optimal synthesis of protein purification processes with product loss. *Chemical and Biochemical Engineering Quarterly*, 17(1):77–84, 2003.

[86] N. J. Samsatli and N. Shah. Optimal integrated design of biochemical processes. *Computers and Chemical Engineering*, 20(1): 310–320, 1996. European Symposium on Computer Aided Process Engineering-6.

[87] N. J. Samsatli and N. Shah. An optimization based design procedure for biochemical processes: Part i: Preliminary design and operation. *Food and Bioproducts Processing*, 74(4):221–231, 1996.

[88] N. J. Samsatli and N. Shah. An optimization based design procedure for biochemical processes: Part ii: Detailed scheduling. *Food and Bioproducts Processing*, 74(4):232–242, 1996.

[89] J. M. Montagna, A. R. Vecchietti, O. A. Iribarren, J. M. Pinto, and J. A. Asenjo. Optimal design of protein production plants with time and size factor process models. *Biotechnology Progress*, 16(2):228–237, 2000.

[90] J. A. Asenjo, J. M. Montagna, A. R. Vecchietti, O. A. Iribarren, and J. M. Pinto. Strategies for the simultaneous optimization of the structure and the process variables of a protein production plant. *Computers and Chemical Engineering*, 24(9-10):2277–2290, 2000.

[91] J. M. Pinto, J. M. Montagna, A. R. Vecchietti, O. A. Iribarren, and J. A. Asenjo. Process performance models in the optimization of multiproduct protein production plants. *Biotechnology and Bioengineering*, 74(6):451–465, 2001.

[92] J. A. Asenjo and B. A. Andrews. Protein purification using chromatography: selection of type, modelling and optimization of operating conditions. *Journal of Molecular Recognition*, 22(2): 65–76, 2009.

[93] A. A. Shukla and J. Thommes. Recent advances in large-scale production of monoclonal antibodies and related proteins. *Trends in Biotechnology*, 28(5):253 – 261, 2010.

[94] M. E. Lienqueo, A. Mahn, and J. A. Asenjo. Mathematical correlations for predicting protein retention times in hydrophobic interaction chromatography. *Journal of Chromatography A*, 978 (1-2):71 – 79, 2002.

[95] A. Brooke, D. Kendrick, A. Meeraus, and Raman. *GAMS - A User's Guide. GAMS Development Corporation*, 2008.

[96] J. M. Natali and J. M. Pinto. Piecewise polynomial interpolations and approximations of one-dimensional functions through mixed integer linear programming. *Optimization Methods & Software*, 24:783–803, 2009.

[97] M. Tawarmalani and N. V. Sahinidis. A polyhedral branch-and-cut approach to global optimization. *Mathematical Programming*, 103:225–249, 2005.

[98] A. Jungbauer and O. Kaltenbrunner. Fundamental questions in optimizing ion-exchange chromatography of proteins using computer-aided process design. *Biotechnology and Bioengineering*, 52(2):223–236, 1996.

[99] G. Guiochon. Preparative liquid chromatography. *Journal of Chromatography A*, 965(1-2):129 – 161, 2002.

[100] G. Guiochon and S. G. Shirazi. *Fundamentals of Preparative and Nonlinear Chromatography*. Academic Press, Boston, 4th edition, 1994.

[101] F. Gritti and G. Guiochon. The ultimate band compression factor in gradient elution chromatography. *Journal of Chromatography A*, 1178(1-2):79 – 91, 2008.

[102] E. Vasquez-Alvarez and J. M. Pinto. Dynamic liquid chromatography column models in protein separation processes. *In 4th Mercosur Congress on Process Systems Engineering*, pages 1–10, 2005.

[103] M. Almqvist. Modeling and calibration of preparative chromatography in gproms separations of protein monomers from dimers, 2009.

[104] J. C. Bellot and J. S. Condoret. Modelling of liquid chromatography equilibria. *Process Biochemistry*, 28(6):365 – 376, 1993.

[105] J. C. Bellot and J. S. Condoret. Liquid chromatography modelling: a review. *Process Biochemistry*, 26(6):363 – 376, 1991.

[106] Process Systems Enterprise. gproms, 1997-2001. URL `http://www.psenterprise.com/gproms`.

List of Communications

1. Eleftheria M. Polykarpou, Paul Dalby, Lazaros G. Papageorgiou
   Optimisation of Chromatography for the purification of Mutant Proteins, **IMRC Meeting 2009**, London, UK (05/2009)

2. Eleftheria M. Polykarpou, Paul Dalby, Lazaros G. Papageorgiou
   An MINLP Formulation for the Synthesis of Chromatographic Protein Purification Processes with Product Loss
   Computer Aided Chemical Engineering, **ESCAPE19**, Volume 26, 2009, Pages 1057-1062

3. Eleftheria M. Polykarpou, Paul Dalby, Lazaros G. Papageorgiou
   Synthesis of chromatographic protein purification processes using optimisation techniques, **EURO XXIV**, Lisbon, Portugal (06/2010)

4. Eleftheria M. Polykarpou, Paul Dalby, Lazaros G. Papageorgiou
   Synthesis of Downstream Processes: Optimal selection of Chromatographic Sequences, **Recovery of Biological Products XIV**, Lake Tahoe, CA, USA (08/2010)

5. Eleftheria M. Polykarpou, Paul Dalby, Lazaros G. Papageorgiou
   Synthesis of Downstream Processes: Optimal Selection of Chromatographic Sequences, **CPSE Consortium**, London, UK (12/2010)

6. Eleftheria M. Polykarpou, Paul Dalby, Lazaros G. Papageorgiou
   Optimal Synthesis of Chromatographic Trains for Downstream Protein Processing, **Biotechnology Progress Journal** (Accepted)

7. Eleftheria M. Polykarpou, Paul Dalby, Lazaros G. Papageorgiou An MILP formulation for the synthesis of protein purification processes, **Chemical Engineering Research and Design Journal** (Under review)

8. Eleftheria M. Polykarpou, Paul Dalby, Lazaros G. Papageorgiou Novel efficient optimisation systems for purification process synthesis, **Biochemical Engineering Journal** (Under review)